Safety of Lithium Nickel Cobalt Aluminum Oxide Battery Packs in Transit Bus Applications

MNTRC MINETA NATIONAL TRANSIT RESEARCH CONSORTIUM

PENN**STATE** 1855

MINETA TRANSPORTATION INSTITUTE
LEAD UNIVERSITY OF MNTRC

The Mineta Transportation Institute (MTI) was established by Congress in 1991 as part of the Intermodal Surface Transportation Equity Act (ISTEA) and was reauthorized under the Transportation Equity Act for the 21st century (TEA-21). MTI then successfully competed to be named a Tier 1 Center in 2002 and 2006 in the Safe, Accountable, Flexible, Efficient Transportation Equity Act: A Legacy for Users (SAFETEA-LU). Most recently, MTI successfully competed in the Surface Transportation Extension Act of 2011 to be named a Tier 1 Transit-Focused University Transportation Center. The Institute is funded by Congress through the United States Department of Transportation's Office of the Assistant Secretary for Research and Technology (OST-R), University Transportation Centers Program, the California Department of Transportation (Caltrans), and by private grants and donations.

The Institute receives oversight from an internationally respected Board of Trustees whose members represent all major surface transportation modes. MTI's focus on policy and management resulted from a Board assessment of the industry's unmet needs and led directly to the choice of the San José State University College of Business as the Institute's home. The Board provides policy direction, assists with needs assessment, and connects the Institute and its programs with the international transportation community.

MTI's transportation policy work is centered on three primary responsibilities:

Research

MTI works to provide policy-oriented research for all levels of government and the private sector to foster the development of optimum surface transportation systems. Research areas include: transportation security; planning and policy development; interrelationships among transportation, land use, and the environment; transportation finance; and collaborative labor-management relations. Certified Research Associates conduct the research. Certification requires an advanced degree, generally a Ph.D., a record of academic publications, and professional references. Research projects culminate in a peer-reviewed publication, available both in hardcopy and on TransWeb, the MTI website (http://transweb.sjsu.edu).

Education

The educational goal of the Institute is to provide graduate-level education to students seeking a career in the development and operation of surface transportation programs. MTI, through San José State University, offers an AACSB-accredited Master of Science in Transportation Management and a graduate Certificate in Transportation Management that serve to prepare the nation's transportation managers for the 21st century. The master's degree is the highest conferred by the California State University system. With the active assistance of the California Department of Transportation, MTI delivers its classes over a state-of-the-art videoconference network throughout the state of California and via webcasting beyond, allowing working transportation professionals to pursue an advanced degree regardless of their location. To meet the needs of employers seeking a diverse workforce, MTI's education program promotes enrollment to under-represented groups.

Information and Technology Transfer

MTI promotes the availability of completed research to professional organizations and journals and works to integrate the research findings into the graduate education program. In addition to publishing the studies, the Institute also sponsors symposia to disseminate research results to transportation professionals and encourages Research Associates to present their findings at conferences. The World in Motion, MTI's quarterly newsletter, covers innovation in the Institute's research and education programs. MTI's extensive collection of transportation-related publications is integrated into San José State University's world-class Martin Luther King, Jr. Library.

REPORT 12-61

SAFETY OF LITHIUM NICKEL COBALT ALUMINUM OXIDE BATTERY PACKS IN TRANSIT BUS APPLICATIONS

Timothy Cleary, MS
Marc Serra Bosch
Jim Kreibick
Joel Anstrom, Ph.D.

October 2016

TECHNICAL REPORT DOCUMENTATION PAGE

1. Report No. CA-MNTRC-16-1247	2. Government Accession No.	3. Recipient's Catalog No.
4. Title and Subtitle Safety of Lithium Nickel Cobalt Aluminum Oxide Battery Packs in Transit Bus Applications		5. Report Date October 2016
		6. Performing Organization Code
7. Authors Timothy Cleary, MS, Marc Serra Bosch, Jim Kreibick, and Joel Anstrom, Ph.D.		8. Performing Organization Report MTI Report 12-61
9. Performing Organization Name and Address Mineta National Transit Research Consortium College of Business San José State University San José, CA 95192-0219		10. Work Unit No.
		11. Contract or Grant No. DTRT12-G-UTC21
12. Sponsoring Agency Name and Address U.S. Department of Transportation Office of the Assistant Secretary for Research and Technology University Transportation Centers Program 1200 New Jersey Avenue, SE Washington, DC 20590	The Thomas D. Larson Pennsylvania Transportation Institute Pennsylvania State University 201 Transportation Research Building University Park, PA 16802-4710	13. Type of Report and Period Covered Final Report
		14. Sponsoring Agency Code

15. Supplemental Notes

16. Abstract

The future of mass transportation is clearly moving toward the increased efficiency and greenhouse gas reduction of hybrid and electric vehicles. With the introduction of high-power/high-energy storage devices such as lithium ion battery systems serving as a key element in the system, valid safety and security concerns emerge. This is especially true when the attractive high-specific-energy and power-chemistry lithium nickel cobalt aluminum oxide (NCA) is used. This chemistry provides great performance but presents a safety and security risk when used in large quantities, such as for a large passenger bus. If triggered, the cell can completely fuel its own fire, and this triggering event occurs more easily than one may think.

To assist engineers and technicians in this transfer from the use of primarily fossil fuels to battery energy storage on passenger buses, the Battery Application Technology Testing and Energy Research Laboratory (BATTERY) of the Thomas D. Larson Pennsylvania Transportation Institute (LTI) in the College of Engineering at The Pennsylvania State University partnered with advanced chemistry battery and material manufacturers to study the safety concerns of an NCA battery chemistry for use in transit buses. The research team ran various experiments on cells and modules, studying rarely considered thermal events or venting events. Special considerations were made to gather supporting information to help better understand what happens, and most importantly how to best mitigate these events and/or manage them when they occur on a passenger bus.

The research team found that the greatest safety concern when using such a high-energy chemistry is ensuring passenger safety when a cell's electrolyte boils and causes the ventilation of high-temperature toxic material. A cell-venting event can be triggered by a variety of scenarios with differing levels of likelihood. Also, though the duration of a venting event is relatively short, on the order of just a few seconds, the temperature of the venting material and cell is extremely high. During a venting event, the high-pressure, burning gases tend to burn holes in nearby packaging materials. Most interestingly, the team discovered that following a venting event the large-format cells tested immediately reached and remained at extremely high external skin temperatures for very long periods, on the order of hours. The majority of this report covers the testing designed to better understand how high-energy cells of this chemistry fail and what materials can be used to manage these failures in a way that increases passenger survivability.

17. Key Words NCA battery fire; nail puncture; overcharge; package materials; battery design	18. Distribution Statement No restrictions. This document is available to the public through The National Technical Information Service, Springfield, VA 22161		
19. Security Classif. (of this report) Unclassified	20. Security Classif. (of this page) Unclassified	21. No. of Pages 128	22. Price $15.00

Form DOT F 1700.7 (8-72)

To order this publication, please contact:

102016

ACKNOWLEDGMENTS

TABLE OF CONTENTS

LIST OF FIGURES

List of Figures

LIST OF TABLES

EXECUTIVE SUMMARY

Electrical energy storage is a key component in many of today's advanced vehicles. Lithium nickel cobalt aluminum oxide (NCA) offers great energy and power density but also presents a safety and security risk when used on passenger buses. To assist engineers and technicians in the process of implementing NCA battery systems in heavy vehicles, the Penn State research team, with support from MNTRC and research sponsors, tested large-format NCA cells and modules under several scenarios and explored various materials and methods to improve passenger and vehicle survivability.

Following a literature review and study of current hybrid electric and/or electric bus manufacturers' high-voltage battery design and fabrication methods, the research team developed a plan to study the results of NCA battery failures at both cell and module levels. This plan included various stresses applied to cells and modules such as overcharge, short-circuit, nail puncture, and crash testing. An investigation into packaging materials was also performed during these tests to help determine the response of a full battery system. The research team considered all likely system failures and vehicle impact scenarios as well as other maintenance issues resulting in protection system failure or damage to cell casing.

Initial testing was only commissioned after a detailed safety analysis and after the development of a series of standard operating procedures, including an analysis of required personal protective equipment, test procedures, and cleanup practices. This testing is extremely dangerous and should only be performed by properly prepared experts. The research team utilized an open-air site within their vehicle testing area and set up a control center at a distance of several hundred feet to ensure that all personnel on site were always safe and clear of any flying debris. This control center is capable of starting, stopping, and recording all sensor data while remote cameras record audio and video of the element under test.

The first tests were intended to understand how currently used materials handle the worst-case scenario, an overcharge event. Healthy 45Ah NCA cylindrical cells were fully charged, then introduced to the test site. The first test evaluated the performance of acetal material, commonly used to package cells in a module. The second test was used to evaluate the metal materials typically used in battery pack enclosures, a 6061 aluminum alloy and a low-carbon steel. These fully charged cells were then overcharged, one at a time, at approximately a C/2 rate or 22.5 A. Cell voltage climbed less than one volt before venting and also experienced an interesting 0.25 to 0.5 dip in voltage just before the cell vented. External cell temperatures during this overcharge event slowly climbed until just before the venting event with the rate increasing to about 10°C per minute. During the venting event, fire and electrolyte shot out of the cell under test, reaching distances upward of six feet in two directions and lasting about 10 seconds.

Regardless of the cause, each venting event showed similar results in violent venting of electrolyte and extreme temperature increases. Most cell exteriors exceeded 600°C and remained at relatively high temperatures for several hours.

The results of just about any test using acetal material concluded in the complete failure of structural support or thermal insulation. Immediately following a venting event, the acetal material would start burning and in only a few minutes deteriorate to a puddle of liquid, and then continue to burn until the majority of the material was gone. Any testing using aluminum in direct contact with venting gases resulted in melting, creating a large opening ranging from the size of a quarter to about 6 inches, depending on the proximity of the material to the opening in the cell.

Understanding these results, the team modified the test plans to select a reliable material to both sustain the heat and flames of a venting event as well as support thermal insulation, limiting nearby cells from excessive heat exposure. Materials such as Teflon and an intumescent phase-changing material produced by Pyrophobic showed promise.

Finally, module-level testing and metal materials analysis resulted in the following conclusions. First, a check valve to release the hot gases of a large-format cell venting, even if only one cell is venting, is not feasible. Commercially available check valves do not allow the high flow rate necessary to utilize a check valve. Only large blowout walls or sections are feasible based on the high flow rate. This led the team down the path of designing a ducting system to evaluate the electrolyte as quickly and safely as possible utilizing the dynamics learned in single-cell testing. Also, aluminum alloys are not capable of sustaining the initial impact of high-pressure venting gases and flames because of the excessive temperature. Finally, a modular, thin, lightweight steel skin is recommended to absorb the initial blast of cell venting as well as to direct the gases out of the battery system. While aluminum can be used as exterior packaging or for the pack level enclosure, steel must absorb and guide the impact of the gases and direct to a common exit point large enough to handle a relatively high flow rate such as a blowout panel or ducting to a safe exterior location.

The team showed, through testing, that it is possible to have all the cells in a 20-cell module vent and not burn down the entire enclosure if the venting electrolyte gases are directed properly. If Teflon packaging material is used, the structural integrity will also remain intact even in the high heat environment, allowing for high survivability rates and longer evacuation times on passenger buses.

I. INTRODUCTION

This report was written for a broad audience and covers safety and security concerns when using lithium nickel cobalt aluminum oxide (NCA) cell systems; other research regarding current regulations; and the setup, execution, and results of testing performed by this research group.

After a presentation of the literature review and introduction to the test setup, the report primarily covers the various tests performed and results obtained, specifically the cell and material performance during an overcharge, nail puncture, short circuit, or impact test. This entailed simulating some of the most likely scenarios to which a passenger bus battery system would likely be exposed during its service life on the road, while charging, or during maintenance.

To safely perform these tests, experts were consulted to determine all the necessary personal-protective equipment, operating distances, preparation, and disposal procedures. This information was made available to all researchers and support personnel. It is not recommended that these tests be performed without properly preparing for the worst-case scenario. Please do not try to repeat these tests without all necessary safety measures in place.

To safely operate a vehicle with large, onboard electrical energy storage, including hundreds of cells, a battery management system with a design capable of handling thermal events for a reasonable amount of time is necessary. Educating the workforce responsible for the safe and secure design, integration, and maintenance of these high-power/high-energy systems is necessary for the long-term success of electric and hybrid electric vehicles using this chemistry. This work strives to support the education effort.

The goal of this report is to expose design engineers and technicians who maintain hybrid electric or electric-only passenger buses to the dangers of the high power and high energy of a large-format NCA cell. Many of the groups designing battery systems or working in or around such systems are not able to perform this level of investigation. To educate them on the dangers of this chemistry, cells and modules were pushed past their limits and their responses were studied. The surrounding materials used to package and enclose these cells are also studied and the results presented.

The researchers present commonly used methods and materials and investigate others to improve survivability on passenger buses, producing research results that range from avoiding vehicle fires to extending evacuation time.

II. LITERATURE REVIEW

The investigators conducted a literature review to evaluate standards, regulations, and publications; to identify research gaps; and to pursue new innovative safety tests to run on large-format NCA battery cells and packs that are used in bus transit applications.

This section is divided into three subsections. The first contains information necessary to gain familiarity with the cells used in this research. The second goes over the regulations that electrical energy storage manufacturers are facing as well as the problems that transit authorities and firefighters are confronting due to the increase of electric and hybrid vehicles on the road. Finally, the third subsection summarizes the set of test scenarios evaluated by this research group.

CELL INFORMATION

The collection of information started with the cells themselves, including format, chemistry, and properties that inevitably lead to thermal runaway. However, there are not many studies available on large-format cells used in transit applications, presumably due to recent growth in battery technology. Most of the publications are on the smaller-format 18650 cells, which contain much less energy and, as a consequence, exhibit fewer energetic thermal events.

In addition to reviewing publications, the research group contacted cell manufacturers for information regarding how to safely operate their batteries and what conditions should be avoided. According to manufacturers, unsafe conditions occur when any cell is operated outside of published temperature, voltage, and/or current ranges. If NCA cells experience one or more of these conditions, they are assumed to be damaged and could possibly enter thermal runaway. Overcharging one or more cells to the point of failure was determined to be a feasible default test, since this fits the scope of the project and was safely repeatable within lab facilities and capabilities. It is also reasonably affordable, and representative of many likely scenarios on board electric transit buses. This scenario primarily simulates the failure of a battery management system (BMS) to accurately measure cell voltage and/or to act on a voltage fault resulting in a cell overcharge.

The data sheet for the cells selected as part of this work, GAIA NCA 45 Ah, provided a well-defined range of operating conditions for voltage, current, and temperature. Failures generally occur when a cell is operated outside its manufacture rating. According to manufacturer's information, the safe cell voltage range is 2 to 4.2V. This is the primary safety limitation. The safe range of operating temperatures is strictly defined as -30ºC to 60ºC. This work will show, however, that thermal/venting events occur even within this range. As far as the current limitations, values for continuous and peak charge and discharge are detailed within the attached specification sheet. They range from 270 A (charge) to 1250 A (discharge) but are condition and state dependent. A full specification sheet for the large-format cell selected for this research can be found in Appendix A – Specification Sheets.

Generally, when cells are overcharged or mechanically damaged, cell failures are followed by thermal runaway as a result of a cell internal fault, which is one of the most severe failure conditions for this chemistry.

In general, whenever a charged Li-ion cell is exposed to temperatures above 60°C, there is a risk of initiating a strong exothermic reaction within the cell. The heat generated by these reactions will result in a rise in the cell temperature, which in turn activates heat generation amplitude or additional exothermic reactions that build up pressure in the cell. The cells used in this research are equipped with a safety/pressure burst disc at each terminal side rated at 144-200 psi at room temperature. Figure 1 shows a cell that was overcharged until its burst discs were opened and the cell vented.

Open Burst Disc

Figure 1. Cell after Venting Event

The venting process implies release of flammable electrolyte, generation of gases, or even rupture of the cell casing. In most cases, all three happen almost simultaneously. Figure 2 demonstrates the intensity of the venting process, as exhibited by flames and gases energetically flowing out over approximately five seconds.

Figure 2. Single Cell Nail Puncture Test

Figure 2 only shows what can happen to one cell, but in heavy buses, battery packs consist of hundreds of cells wired in a series/parallel configuration. In a high-quantity, multi-cell pack, such as an electric bus, the venting of just one cell can propagate its thermal energy to neighboring cells causing a chain reaction until all cells rupture due to extreme thermal conditions.

GAIA, the manufacturer of the cells used in this testing, shared the following data found in Figure 3 and Figure 4 through their United States company Lithium Technology Corporation. Figure 3 presents voltage, current, and temperature from an overcharge test performed by the cell manufacturer GAIA. As seen in this figure, a fully charged cell (4.2 V at no load) was continuously charged at 100 A until the battery vented. During the test, the constant current increased voltage to approximately 5.2 V. This high potential between terminals and/or other internal phenomena likely caused internal shorts, dropping the cell voltage to below 5 V. Once internal shorts or other energy-releasing reactions occur, there is an abrupt increase in the rate of temperature rise.
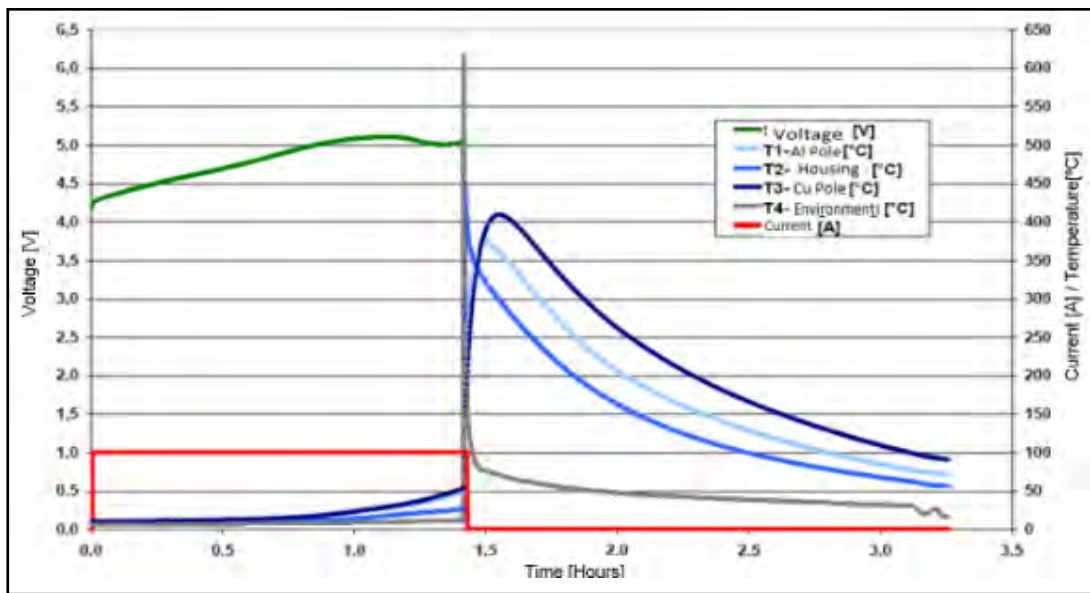
Figure 3. Data from Manufacturer Overcharge

As a result, when the cell vented, the temperature in the surrounding environment rose immediately to 600ºC for a short period of time. Temperature sensors placed on the battery rose to 400-450ºC and remained warm, taking several hours to cool down to ambient temperature.
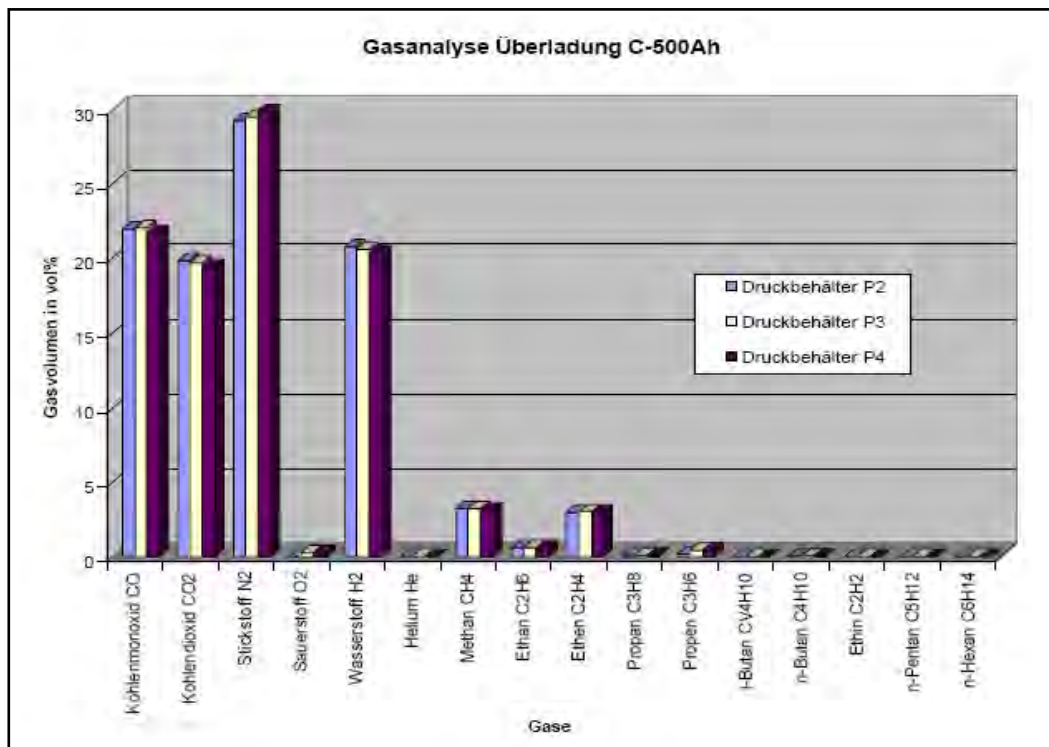
Figure 4. Molecules Present in Venting Gas

Figure 4 shows the molecules present in the venting gases by percentage of total volume. Carbon monoxide, carbon dioxide, nitrogen and hydrogen are the principal gases released during venting of the cell. Nitrogen, hydrogen, and carbon dioxide represent minimal threats to the atmosphere and humans. Carbon monoxide, however, is toxic.

BATTERY FAILURES AND REGULATIONS

The most common failures in automotive battery systems were researched by contacting car insurance companies and consulting the Pennsylvania Department of Transportation reports. However, significant information was not found, so other publications were examined to determine the forces batteries experience during a crash event, how to reproduce them, and what level of hazard they would represent.

During the process of going over the standards and regulations for electric vehicles (EV), hybrid electric vehicles (HEV), and Plug-In Hybrid Electric Vehicles (PHEV), it became apparent that many associations such as the Society of Automotive Engineers (SAE), National Fire Protective Association (NFPA), and Federal Motor Vehicle Safety Standards (FMVSS) have developed standards. Information is scattered, however, and varies between associations. The researched information was divided into the following topics:

1. Regulation of electrical energy storage in buses

2. First responder strategies/tactics to respond to EV/HEV/PHEV incidents

3. Commercial battery pack characteristics

4. Fire-suppression systems

5. Electric vehicle crashes

Government Regulations

The authors review here the statistics of the proportion of vehicles involved in traffic accidents in US. The data is obtained from the 2013 Traffic Safety Facts[1] report, which is an annual compilation of motor vehicle crash data presented by the National Highway Traffic Safety Administration (NHTSA).[2]

.
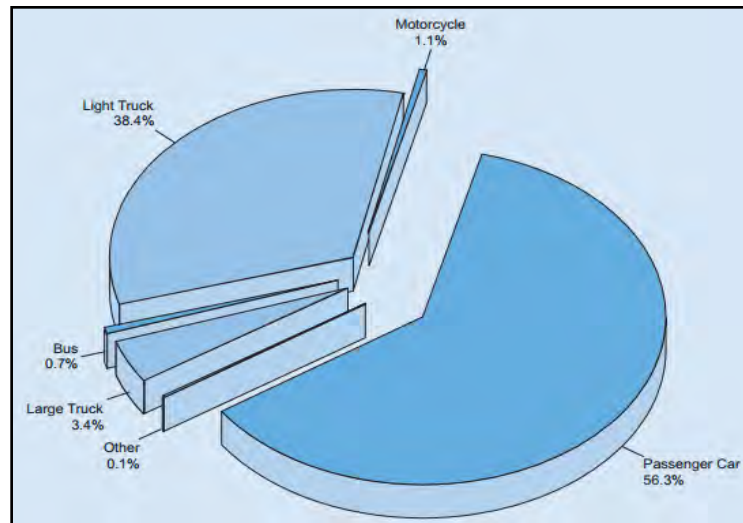
Figure 5. Proportion of Vehicles Involved in Traffic Crashes in US[2]

Figure 5 shows that buses are involved in less than 1% of accidents compared to passenger cars and light trucks, which are the most common vehicles on the road. Figure 6 illustrates the percentage of bus accident fatalities in 2013 based on the initial point of impact.
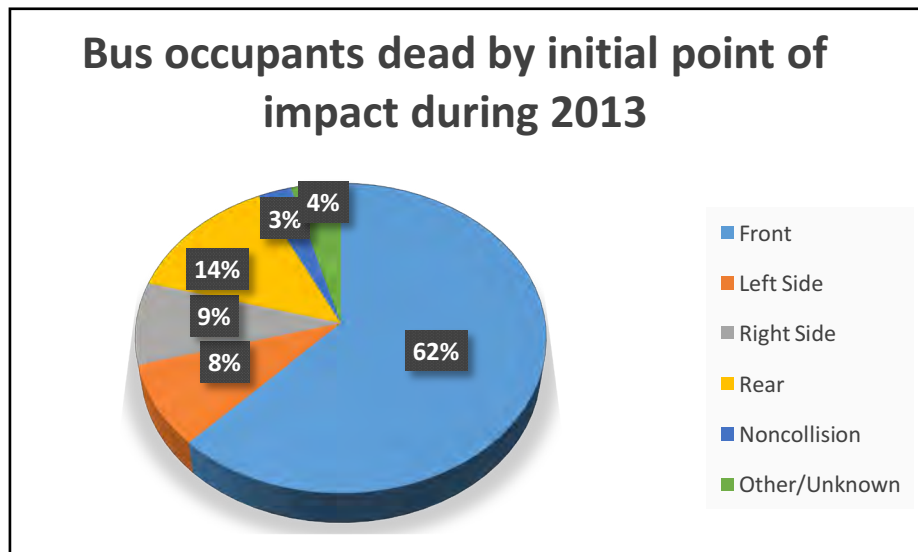
Figure 6. Bus Occupants Dead by Initial Point of Impact[2]

Figure 6 also indicates that frontal impacts are the worst-case scenario with the highest percentage of fatalities. In 62% of fatal accidents, the impact came from the front. Lower fatality rates occur during rear (14%), right-side (9%), and left-side (8%) accidents. In Figure 7, the same data are presented for injuries, and it is observed that the percentages are more equally distributed among each side of the vehicle.

Bus occupants injured by initial point of impact during 2013

37% Front
21% Left Side
21% Right Side
21% Rear
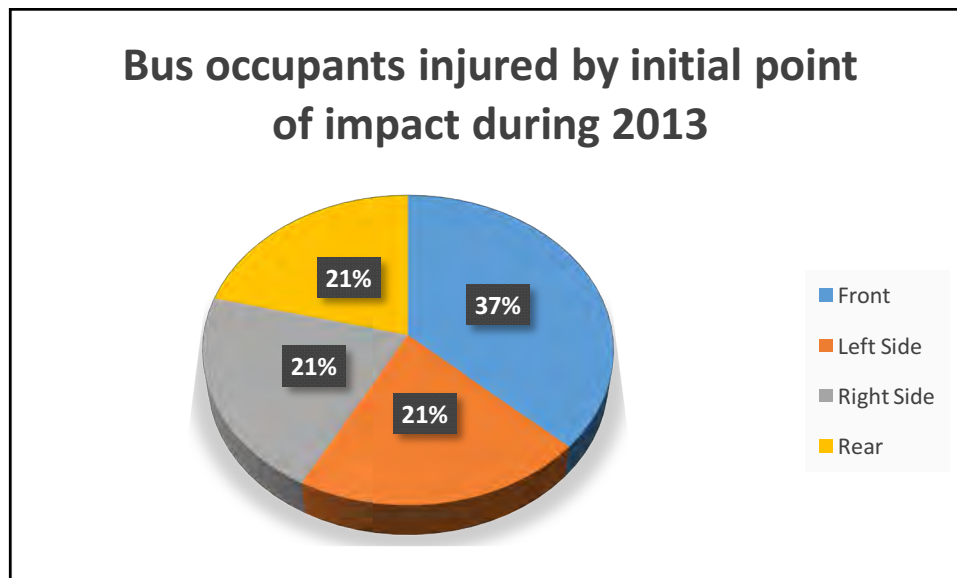
Figure 7. Bus Occupants Injured by Initial Point of Impact[2]

In a frontal crash, the most common mechanisms of injury for passengers seated in a seat-to-seat configuration are neck flexion or extension. These injuries are due to the combination of unrestrained passengers and the low back seat designs.[3] The Federal Motor Vehicle Safety Standard (FMVSS) No. 207 establishes requirements for seats, attachment assemblies, and installation, to minimize the possibility of failure as a result of forces acting on the seat in vehicle impact. The standard FMVSS No. 208 regulates the "Occupant Crash Protection" to reduce the number of fatalities and the number and severity of injuries to occupants involved in frontal crashes.

The FMVSS are the requirements issued by the US government to qualify vehicles before they enter the market to ensure that vehicles on the road are safe. Compliance with government regulations is analyzed through a set of tests to determine if the vehicle passes or fails. In addition, there are institutes and associations that provide ratings to give clients some guidelines about the safety of the vehicle. Associations and institutes such as the Insurance Institute for Highway Safety (IIHS) have developed different tests and ratings to be able to measure and report the safety response of the vehicle during a crash. These associations are well known and respected by consumers.

Figure 8, which was taken from Safety Companion 2016,[4] illustrates vehicle safety regulations and associations by country. Please, notice that the star indicates "association" while § means "government regulation."
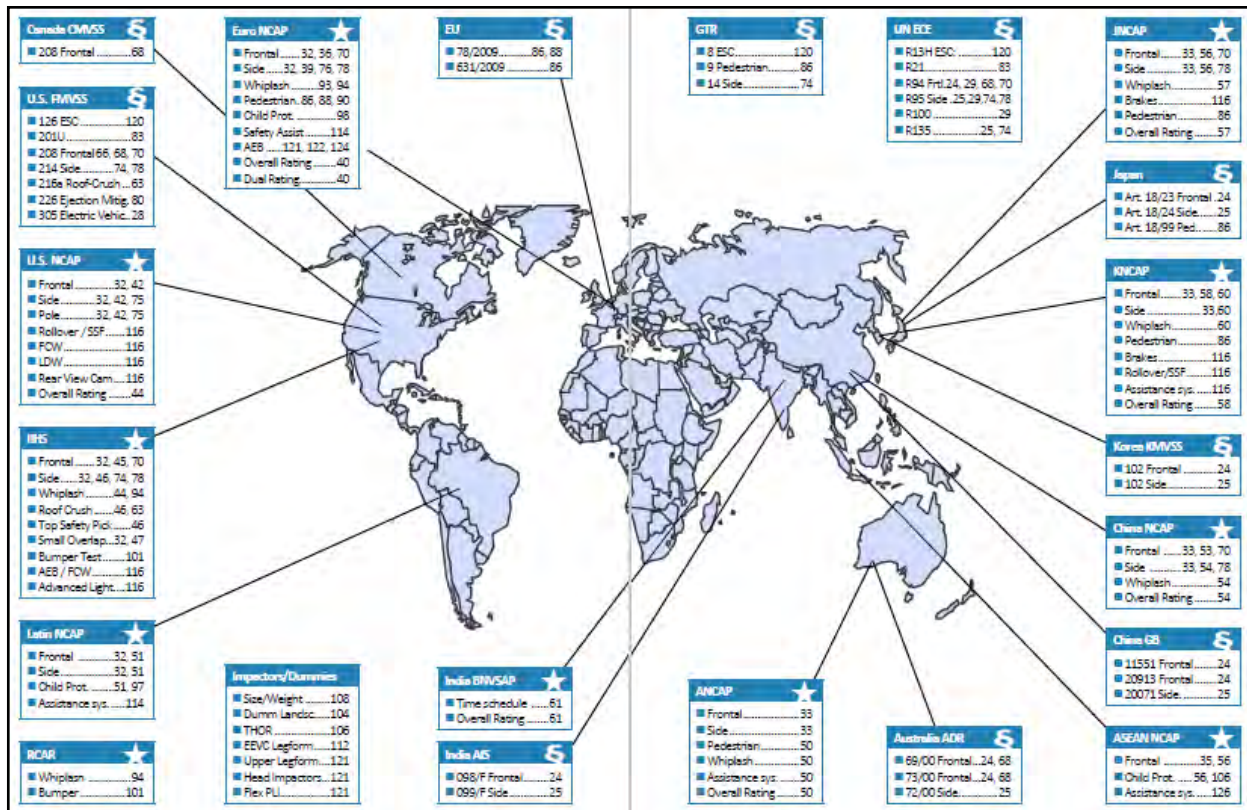
Figure 8. Vehicle Standards Around the World[5]

The U.S. is regulated by the standards under the U.S. FMVSS and several ratings, including the U.S. New Car Assessment Program (NCAP) and IIHS. Moreover, the United Nations Economic Commission for Europe (UNECE) also applies to US.

UNECE:

The UNECE is the forum in which the countries of Western, Central and Eastern Europe, Central Asia and North America (56 countries in all) come together to forge the tools of their economic cooperation. That cooperation concerns economics, statistics, environment, transport, trade, sustainable energy, timber and habitat.[5] The UNECE released the Proposal for an Electric Vehicle Regulatory Reference Guide, which cites, summarizes, compares and analyzes regulations from the countries that form the UNECE.

U.S. NCAP:

The National Highway Traffic Safety Administration's NCAP[6] created the 5-Star Safety Ratings Program to provide consumers with information about crash protection and rollover safety of new vehicles beyond what is required by Federal law. One star is the lowest rating; five stars is the highest.

IIHS:

The IIHS is an independent, nonprofit scientific and educational organization dedicated to reducing losses, deaths, injuries and property damage from crashes on the nation's roads. The Highway Loss Data Institute (HLDI) shares and supports this mission through scientific studies of insurance data representing human and economic losses resulting from ownership and operation of different types of vehicles and by publishing insurance loss results by vehicle make and model.[7]

FMVSS No. 305: SAFETY REQUIRIMENTS FOR ELECTRIC VEHICLES

Scope: Cars, buses, trucks with a GVWR of 4536kg or less that use electrical components with working voltages higher than **60 volts direct current (VDC) or 30 volts alternating current (VAC)**, and whose speed attainable is more than 40km/h.

Requirements:

- Maximum 5 liters of electrolyte may spill from the batteries.

- There shall be no evidence of electrolyte leakage into the passenger compartments.

- All components of the electric energy storage/conversion system must be anchored to the vehicle.

- No battery system component that is located outside the passenger compartment shall enter the passenger compartment. Isolations must be greater than or equal to

    ° 500 ohms/V for all DC high voltage sources without isolation monitoring and for all AC high voltage sources.

    ° 100 ohms/V for all direct current, high voltage sources with continuous monitoring of electrical isolation.

- The voltage of the voltage source (Vb, V1, V2) must be less than or equal to 30 VAC for AC components or 60 VDC for DC components.

Test conditions:
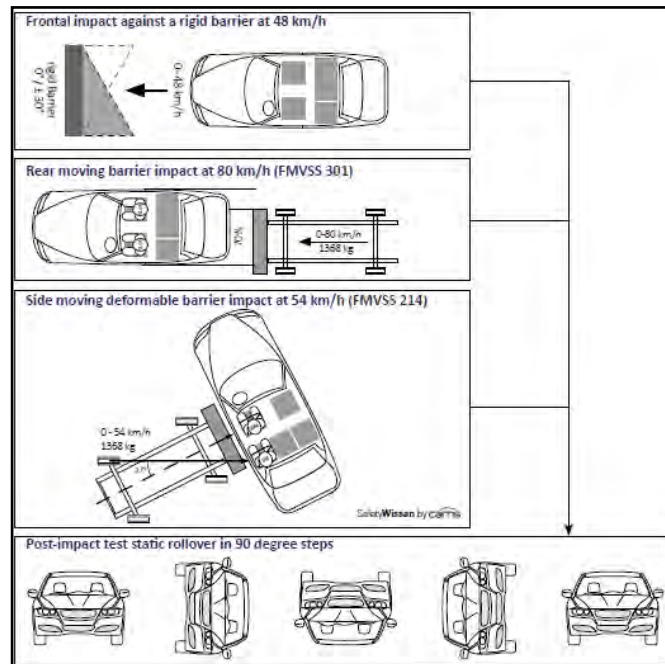
Figure 9.   FMVSS No. 305 Tests Conditions[5]

Figure 9 details the test conditions of FMVSS No. 305. According to the scope, it is assumed that this regulation is not applicable to all kinds of buses. For example, a full-size bus is around 39,000 lbs., exceeding the weight specified in the scope, so the standard does not cover all the buses.

Buses must also comply with state regulations. In the case of New York State, there is the "Bus & Passenger Vehicle Regulations" published by New York State Department of Transportation that establishes a set of requirements, always according to the US Department of transportation (DOT).[8] These include:

• Vehicle inspection

• Motor vehicle identification and markings

• Vehicle safety requirements

• Vehicles for transporting the disabled

• Electrical systems

• Electric-powered motor vehicles

• Identification of electric vehicles

• Equipment requirements for electric and hybrid-electric buses

- Batteries and battery compartment

- Electric propulsion circuit

- Range selectors

- Electrical overload protection

- Regenerative braking systems

- Backup alarm

"Batteries and Battery Compartment" specifies a set of requirements for the battery pack with respect to crash-worthiness including:

- Battery compartment(s) shall be designed and constructed to prevent all battery fluids, such as gel, liquid electrolytes, caustic, reactive or toxic gases or fumes, from entering the passenger compartment when a vehicle is subjected to a moving contoured barrier crash test such that:

  a. The contoured barrier shall weigh 4,000 pounds and be configured as specified in Figure 2 of FMVSS 301[9]

  b. The barrier assembly shall be traveling longitudinally forward at any speed up to and including 30 mph at the time of impact

  c. The barrier assembly may impact the test vehicle at any point and at any angle

Note that that "Batteries and Battery Compartment" refers to FMVSS No. 301 to specify the characteristics of the barrier. State laws therefore also take into account FMVSS standards and adapt them.

Furthermore, the Standard Bus Procurement Guidelines (SBPG) 2013 released by American Public Transit Association (APTA) are a model for solicitation of offers and contracts for the supply of transit buses and also specify crash requirements.[10]

Transit Authorities and First Responders

This section addresses how first responders perform their duties in response to accidents involving battery-powered vehicles. This question is very general and there is no unique answer. However, firefighters are usually the group in charge and manipulate the vehicle to rescue victims if necessary. This understanding directed the research group to investigate procedures for first responders or firefighters to approach battery systems in a bus crash. Some concerns are ensuring the safety of the responders and accident victims from potential high voltage and from exposure to dangerous chemicals.

The investigators reviewed strategies the fire departments adopted for EV and HEV fires and, as a result, the training fire fighters are receiving. Although they are already trained to handle conventional vehicles, fire fighters are taught additional procedures by their department for responding to electric vehicle fires. NFPA published a report that developed the technical basis for best practices in emergency response procedures for electric-drive vehicle battery incidents. A major conclusion of the study was that EV fires should be treated differently from conventional vehicle fires, because more water is required to cool down the battery completely in EV fires. Usually an additional engine has to act as an extra water supply since the water is applied for a relatively longer period after the flames are no longer visible. This is because battery cells may reignite after hours of rest. Unless the battery pack has been cooled down sufficiently, reigniting is a potential risk. For this reason, NFPA guidelines also recommended that burned vehicles be kept at least 50 feet away from any combustible material for some time after the event.

Since battery packs are placed in different locations within the vehicle, NFPA published a field guide to determine the location of the high-voltage battery within the vehicle and provide guidance to shut down and disable battery packs and vehicle circuits. NFPA also concluded that the vehicle structure should not be pierced, cut or dismantled, because the first responder has the potential to come in contact with high voltage. Current firefighter personal protective equipment (PPE) does not offer the appropriate level of electrical protection. Field experiments have shown there is no adverse electrical current at the nozzle during the firefighting operations.[11] However, the NFPA field guide does not provide post-crash procedures or a checklist for fire departments and traffic associations to perform after an electric vehicle accident.

Commercial Battery Pack Characteristics

The amount of energy that needs to be stored in an electric bus requires large battery packs that often cannot be located in one specific place. As a consequence, in many cases it has to be distributed throughout the vehicle.

Figure 10. Battery Pack on the Roof of the Bus

The most common locations are the roof and sides. Figure 10, taken from the web site of Power Vehicle Innovation, shows a battery pack on the roof of a bus.[12] Roof mounting is also used in buses running on gaseous fuels like compressed natural gas or hydrogen to protect tanks from side impact.

Figure 11. Battery Packs on the Side of the Bus

Alternatively, Figure 11 taken from the web site of the Life of Guangzhou[13] shows the battery packs mounted on the side. In some cases, cooling systems are also rooftop mounted. The packs also have to be properly enclosed and sealed to avoid any contact with water and prevent damage to any electronic components.

The researchers expected to find guidelines for commercial battery pack design and recommended materials for bus side panels in order to replicate them for testing purposes. The proprietary nature of bus designs, however, made it very difficult to find information on composites and alloys utilized by the bus industry. Most critically, this investigation centered on which plastic material should be used for cell holders within the battery pack, since the material had to have good mechanical, machining, and thermal proprieties at a reasonable price. Fortunately, the investigators had access to several donated commercial vehicle battery packs, which were analyzed in order to design a representative battery pack for testing.

Fire Suppression Systems

According to the NFPA, there is a vehicle fire every two minutes in the United States. With an increase in the number of electric vehicles on the road, the fire suppression systems industry and firefighters and traffic associations have to adopt new procedures to overcome all the challenges posed.

Electric vehicle incidents require development of new products and materials. The industry is considering two main options: material that itself possesses fire-suppressive properties, or a fire suppression system incorporated in or around the battery pack.

No regulation is currently proposed, however, that obligates the addition of fire suppressions systems to Lithium ion cells or packs. In order to control cost, therefore, most electrical energy storage manufacturers are not assembling fire suppression systems into their packs.[14]

Electric Vehicle Crash

Review of battery crash test publications revealed several variants. One consisted of bolting down the battery pack while a crash device was impacted into the battery pack. The other variant was completely the opposite: the battery was moved to impact the crash device. In both variants the vehicle dynamics were neglected.[15]

In regard to crash velocity, our crash tests were conducted near 20 mph, because the literature affirmed that to be a common speed limit in urban environments.

DESIGN OF EXPERIMENTS

The last task was to define a matrix of battery stress tests or destructive test-to-failure tests that would be within the capability of the research facilities and budget and most beneficial to the battery/bus designing and maintenance community. The set of tests was limited by the number of cells, materials, and time to generate pack design and the stressing mechanisms to which the batteries would be subjected. The test matrix included both single cells, ten cell modules, and twenty cell modules to represent sections of a full battery pack found in heavy vehicle systems.

From the literature review, it was understood that during a venting scenario thermal energy is released in the form of visible flames and smoke. Thermal propagation at the pack level is a serious problem, since the thermal energy can propagate to neighboring cells. For this reason, several pack designs were considered to reduce or eliminate thermal propagation by quickly releasing or absorbing heat from the pack to avoid thermal propagation.

Different enclosure designs were tested including aluminum and steel materials with a variety of emergency venting designs to release or contain gases using a check valve. Polyoxymethylene (POM) (commercially known as acetal), Polyethylene terephthalate (PET), Polytetrafluoroethylene (PTFE) (commercially known as Teflon), and a special material donated by a research sponsor were the materials selected to be tested. The batteries were subjected to electrical and mechanical abuse through different tests to induce thermal runaway. To replicate electrical abuse tests, the group subjected the batteries to overcharge and nail puncture tests. As a mechanical abuse test, a 20 mph side impact crash test was performed. The following sections detail each test.

Several primary causes of failure associated with NCA cells have been identified, including overcharge, puncture, thermal runaway, and both external and internal short circuits. More

detail on these failure modes will be provided later in the report. Table 1 summarizes the likely causes, results, countermeasures, test approaches, and likelihood of such events occurring based on the likelihood of each cause. This table represents a simplified Design Failure Mode and Effect Analysis (DFMEA) for NCA battery systems on buses restricted to thermal events. Here the authors will briefly focus on the likelihood of each failure mode. Low likelihoods can normally be assigned to both BMS failure and internal cell shorting due to manufacturing defects, assuming that design and quality control of both are sufficient. These likelihoods could become high, however, if defects manage to escape quality control and test screenings at the factory. Moderate likelihoods should be assigned to cell puncture, thermal runaway, and external shorting, because they are linked to the rate of bus crashes, fires from other causes, and the potential for maintenance issues over the lifespan of a bus, (typically about 12 years). Quality and process control are much more challenging in these environments outside of a factory floor. Reliable data of battery failures in the field should become available soon as more and more electric buses are deployed and begin to age in service.

Table 1.   Likelihood of Cell Events

Thermal Event Cause	Source of Cause	Likely Result	Counter Measures and Mitigation	Test Approach (Chapter)	Likelihood
Overcharge	BMS, charger, sensor, wiring failures	Cell rupture, fire	BMS watchdogs, diagnostics, design, materials	*BMS and charger override (chapter)	Low Linked to electronics reliability
Puncture	Crash, mishandling, projectile	Cell rupture, fire	Pack design, material and pack location	*Nail press, *pendulum impact (chapter)	Moderate Linked to crashes and other accidents
Immediate or Delayed Thermal Runaway	Internal or external heat source	Cell rupture, fire	Pack design, material and pack location	*Exposure to fire (chapter)	Moderate Linked to fire and other heat sources
External Short Circuit	Insulation loss from crash, design, maintenance	Cell rupture, fire	Pack design, material and maintenance standards	*Closed contactor (chapter)	Moderate Linked to crashes and maintenance issues.
Internal Cell Short Circuit	Manufacturing defect	Cell rupture, fire	Manufacturing quality control, design, material	Seed defect (chapter)	Low Cell quality control

* Test approaches performed.

Overcharge

As the cell is overcharged, lithium ions are irreversibly removed from the positive electrode and deposited as lithium metal on the negative electrode. This de-lithiation of the positive electrode continues as the cell voltage increases during overcharge, until eventually the lithium ions are completely depleted from the positive electrode. During the overcharge process, the cell impedance starts to rise, due to an increase in the positive electrode material resistance. At the same time, the electrolyte within the cell begins to decompose,

coating the active materials and further contributing to the increase in cell impedance. The increasing cell impedance results in an increase in resistive losses in the form of thermal energy. The cell temperature starts to rise rapidly as an exothermic reaction between the de-lithiated positive electrode material and the electrolyte occurs. Once cell temperature rises above approximately 60°C, the rate of this reaction accelerates, generating a large amount of carbon dioxide.

Cell temperature continues to rise until the internal temperature reaches approximately 130–135°C. In this temperature range, the cell separator undergoes a phase transition that closes the porosity of the membrane and impedes the transport of ions between the electrodes. This engineered safety feature "shuts down" the separator, terminating the charge current and ending the overcharge process. In some instances, a "shutdown" of the separator is unable to stop the self-heating of the cell, which eventually leads to additional exothermic degradation processes. These additional processes are not well understood but if sufficiently activated can continue to generate heat within the cell and can eventually lead to a thermal runaway.[16]

Nail Puncture

The nail puncture test attempts to simulate a cell internal short circuit condition by using a nail to achieve a short between the cell's positive and negative electrodes. A short between the terminals will generate a very large short-circuit current. Most of this power will be dissipated in the form of heat in the cell, increasing the temperature of the internal materials, boiling electrolyte and increasing pressure inside the cell. The pressure will only reach at most 200 psi, since the burst discs on either terminal of the cell are rated to handle this pressure. A nail puncture test is a standard and was chosen here to replicate damage during a crash event. It was also used to intentionally induce an internal short, dissipating any residual energy. With the purpose of ensuring the cells are safe to handle for disposal after overcharge or any other non-nail puncture testing.

Simulation of Side Impact at 20 MPH

A large impact pendulum located in LTI's facilities was used to simulate a 20 mph side impact. Direct impact of a Sport Utility Vehicle (SUV) bumper was simulated at 20 MPH to replicate the likely scenario of light vehicles crashing into a transit bus on urban streets.

Figure 12.   Safety Discussions Prior to Entering the Test Site

As part of this test, local fire departments and environmental health and safety personnel were invited as part of a workforce development session. Discussions prior to the testing, seen in Figure 12, were centered on the test setup and plan. Following the test, emergency responders acted to suppress the event and educate their firefighters on appropriate response and approach to actual crash situations.

III. MATERIAL STUDY

At the system level, batteries are composed of cell separators to hold each battery in place, and an enclosure to protect the batteries and their BMS components from various environmental conditions. Typically the cell separators and enclosure are not made of the same material due to the different properties a designer looks for from each component. Separators have to be light, be low-cost, have high impedance, and have a high melting point. A thermoplastic polymer accomplishes all these requirements. The material for the enclosure will be responsible for absorbing part of the energy in a crash scenario, so it has to have good mechanical properties, be low in cost, be able to withstand high temperatures, and be as light as possible (since cells make up most of the weight of a battery pack). In this case the material can be conductive, because the cells will not be in contact with the material. Based on these requirements, the ideal material is a metal.

PLASTIC

Acetal is the commercial name of Polyoxymethylene (POM). Graphing all the polymers on the market, it is clear that a linear relation exists between the melting point and the product of price and density. Figure 13 (graph created w/ CES EduPack-Granta Design) shows this relationship between the melting point, cost, and density.
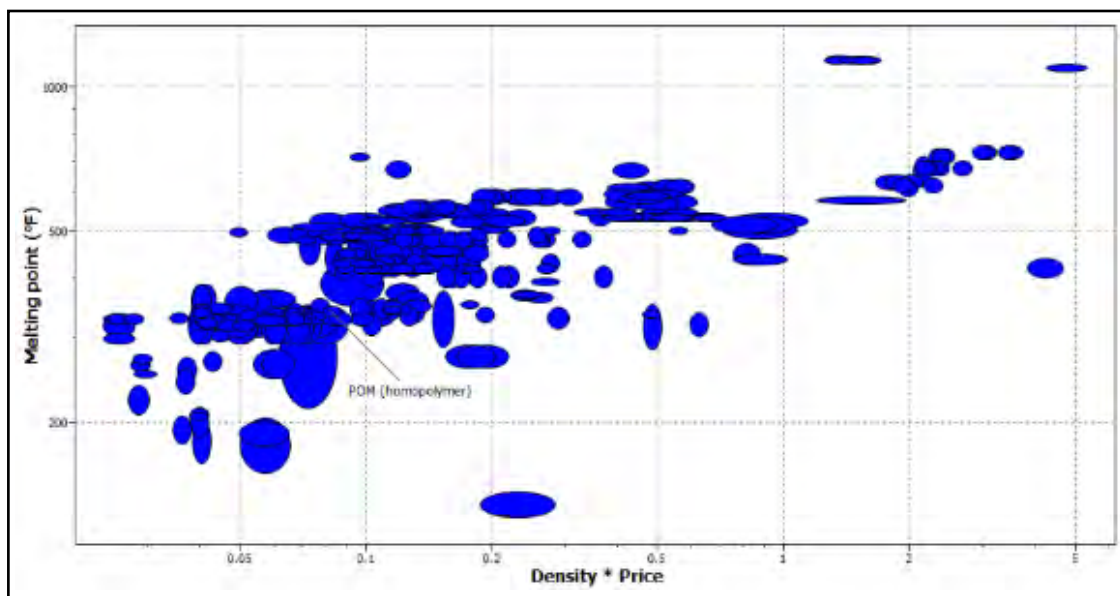
Figure 13. Commercially Available Polymers

In fact, breaking down the product, as seen in Figure 14 (graph created w/ CES EduPack-Granta Design), note the close link between price and melting point.
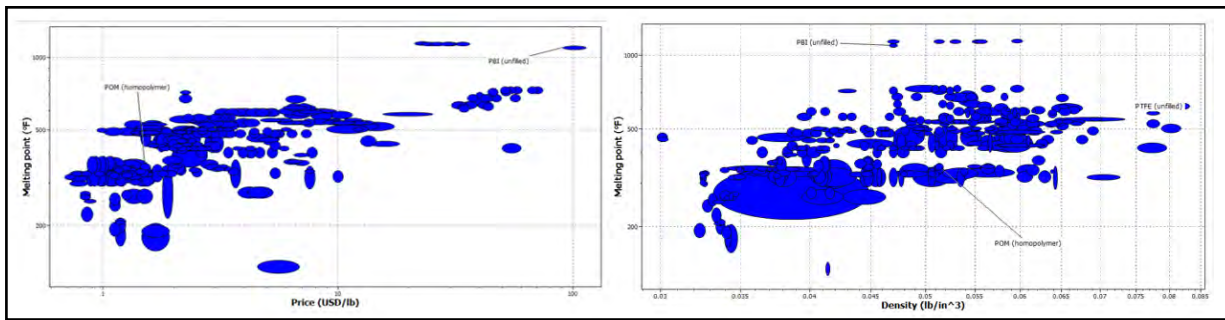
Figure 14. Melting Point v. Price and v. Density

Thus acetal initially looks like a good candidate. Nevertheless, the tests performed showed that the flames coming out the battery and its casing temperature after an event were much higher in temperature than the melting point of acetal (160ºC), so all the acetal melted and ended up burning until it was gone. Different materials with higher melting points were therefore selected. Using the same relationship between price times density versus melting point, the investigators sought the next candidates.

Figure 15 (graph created through CES EduPack-Granta Design) shows materials with a higher melting point than acetal. There are several choices, but none of them is feasible due to excessive price or density. Furthermore, the market does not demand these materials in the thicknesses needed to build the battery systems tested in the research, making it very difficult to get those specific materials with the thickness needed at an affordable price.
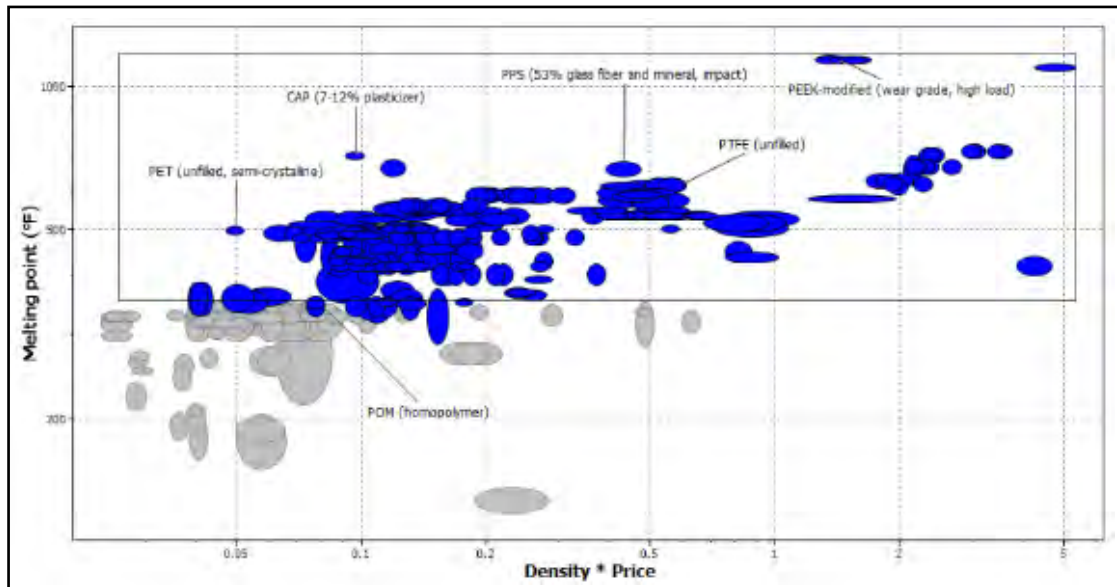
Figure 15. Melting Points Above Acetal

Being more restrictive with the product density x price parameter, Polyphenylene sulfide (PPS) shows up as a possible contender. Again, however, it was hard to find a provider that supplied the thickness needed. Perusing candidates from the same area, Polytetrafluoroethylene (PTFE) then appears, a material often used in the industry because

of its favorable qualities: electrical insulation, inherent flame-resistance, low coefficient of friction and high melting point (338.89ºC).

The fact that Teflon (PTFE) is inherently flame-resistant makes this material very interesting for the worst-case scenario conditions that this research will test. It is expected that this material should not act as a combustible, potentially reducing the length of heat generation and smoke production during an event. Preliminary testing was performed to investigate the real-world performance of some commonly used materials. More detailed tests and test setups are discussed later in this report. Figure 16 shows the results of a single-cell test when acetal was used to hold the cell. The material continued to burn well after the cell vented, producing smoke for approximately 30 minutes after the event and concluding in a complete lack of structural support, mechanical separation, or electrical isolation.

Figure 16. Results of a Single-Cell Acetal Test
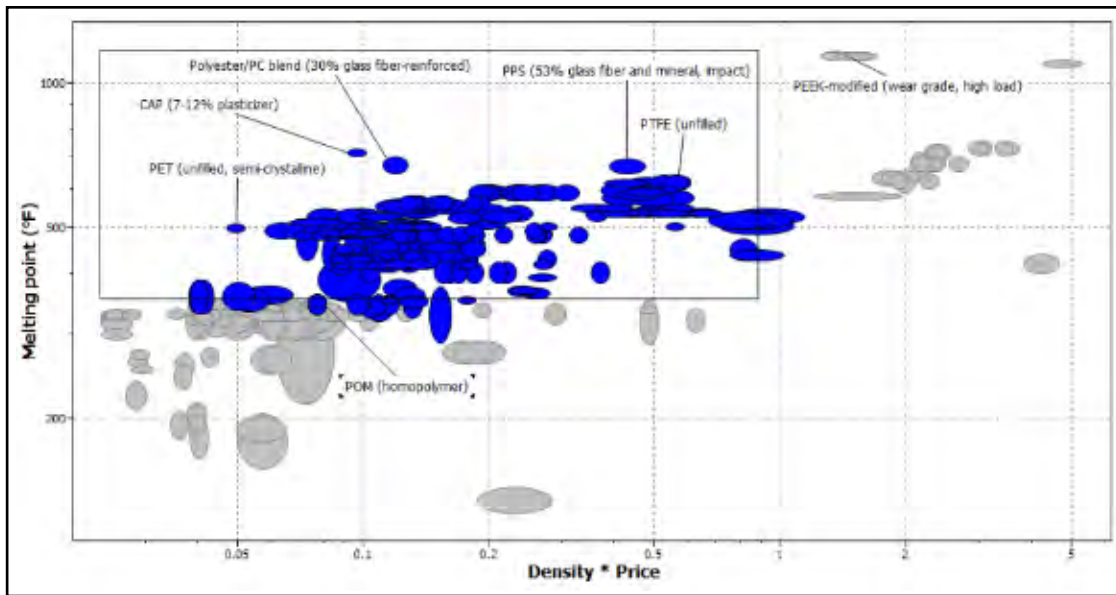
Figure 17. Narrowed Material Search

Polyethylene Terephthalate (PET), as seen in Figure 17 (graph created through CES EduPack-Granta Design) is also selected based on its high melting point relative to acetal. It also has a better price/density relationship than the acetal.

Price				
Price	* 1.44	-	1.58	USD/lb
Physical properties				
Density	0.0509	-	0.0517	lb/in^3
Mechanical properties				
Young's modulus	0.4	-	0.521	10^6 psi
Yield strength (elastic limit)	9.5	-	10	ksi
Tensile strength	9.7	-	10	ksi
Elongation	10	-	75	% strain
Compressive modulus	0.651	-	0.685	10^6 psi
Compressive strength	* 15.7	-	18	ksi
Flexural modulus	0.379	-	0.489	10^6 psi
Flexural strength (modulus of rupture)	13.6	-	16	ksi
Shear modulus	* 0.149	-	0.194	10^6 psi
Bulk modulus	* 0.464	-	0.487	10^6 psi
Poisson's ratio	0.33	-	0.35	
Shape factor	5.1			
Hardness - Vickers	* 19.7	-	24.8	HV
Hardness - Rockwell M	92	-	94	
Hardness - Rockwell R	114	-	126	
Fatigue strength at 10^7 cycles	* 3.46	-	4.49	ksi
Mechanical loss coefficient (tan delta)	* 0.0111	-	0.0145	

Figure 18. Mechanical Properties of POM

Price			
Price	* 0.939 -	1.03	USD/lb
Physical properties			
Density	0.0495 -	0.0506	lb/in^3
Mechanical properties			
Young's modulus	0.4 -	0.45	10^6 psi
Yield strength (elastic limit)	* 9.43 -	10.2	ksi
Tensile strength	10.2 -	10.9	ksi
Elongation	65 -	75	% strain
Compressive modulus	* 0.4 -	0.6	10^6 psi
Compressive strength	* 11 -	14.9	ksi
Flexural modulus	0.434 -	0.448	10^6 psi
Flexural strength (modulus of rupture)	* 10.2 -	10.9	ksi
Shear modulus	* 0.144 -	0.216	10^6 psi
Bulk modulus	* 0.717 -	0.753	10^6 psi
Poisson's ratio	* 0.381 -	0.396	
Shape factor	5.7		
Hardness - Vickers	* 17 -	20	HV
Hardness - Rockwell M	82 -	87	
Hardness - Rockwell R	120 -	125	
Fatigue strength at 10^7 cycles	* 2.8 -	4.2	ksi
Mechanical loss coefficient (tan delta)	* 0.00966 -	0.0145	

Figure 19. Mechanical Properties of PET

As seen in Figure 18 and Figure 19, PET has acceptable mechanical properties for cell separation and structural support as well as similar machining properties to acetal. Another proprietary plastic material manufactured by Pyrophobic Systems was also experimentally analyzed during this work. The results of all materials are presented in each of the test sections to follow.

METAL

Battery packs made for transit-bus applications are typically enclosed in a thin sheeting of plastic, composite, steel or aluminum. There has not yet been a mass acceptance of any one material. This section addresses the question of why special considerations should be made for the material selection of the enclosure material.

First, the objective of this material is to possibly supply structural support, if necessary. It should otherwise at least limit smoke, heat or other materials from leaving the battery system in the event of a cell thermal run away. Second, this material needs to be capable of withstanding the environment, as most battery systems on passenger buses are located outside the cabin and exposed to moisture and debris. Finally, the material shouldn't melt down during a battery thermal event or other fire on board the vehicle.

A preliminary test was performed to evaluate the thermal performance of metals by positioning a sheet of common 6061 aluminum alloy and mild steel at either end of a cell undergoing an overcharge. As Figure 20 shows, the flames that came out from the cell during the venting event melted the aluminum. This proves that the flames/gases are hotter than the melting point of the aluminum, which is approximately 600ºC. On the

other hand, the steel plate was able to withstand the hot gases and remain intact. A mark, indicated by a red circle, where the gases met the steel can also be seen on the far side of the cell in Figure 20.

Figure 20. Results from a Metal Test

This test validated the use of a relatively thin, 1/8" thick, mild steel with approximate melting point of 1300ºC when considering materials for exposure to direct venting. For a ducting system or isolation within a pack, steel is recommended. For small packs with no isolation, steel should also be used to contain the event for as long as possible, giving passengers time to evacuate the bus. Otherwise, materials such as aluminum or even plastic will allow the hot gases to escape immediately and potentially cause more fire damage at a faster rate, thus making evacuation much harder for passengers and allowing less time to exit safely. Also, less time would be available for first responders to contain the event by cooling the pack with water.

IV. TESTING PREPARATION

UNDERSTANDING CELL CONSTRUCTION

To prepare for this destructive battery testing, an investigation into the particular cell construction and internal configurations was performed.
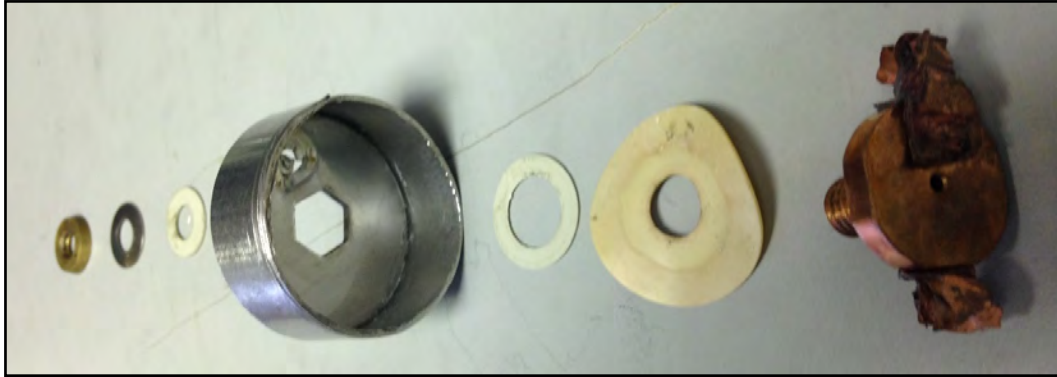
Figure 21. Cell Internals – Negative Terminal Disassembled

To understand the mechanisms inside a cell, the research team, partnered with Pennsylvania College of Technology, safely discharged and disassembled a cell. Figure 21 shows the negative terminal of the GAIA cell and inside view of the pressure release and electrical isolators.

MACHINING

All machining was performed by students and faculty supported on the project. This section details the work performed to prepare for the various battery system destructive tests presented in this report.

During fabrication of battery pack parts, several processes and machining techniques were used. Cell separators were machined using a Computer Numerical Control (CNC) mill; covers and enclosure parts were cut using a water jet; and finally enclosure parts were welded together using Tungsten Inert Gas (TIG) welding. These are processes commonly used in building prototype battery systems and typically available to those designing and building these systems for low-volume transit buses.

To speed series production and at the same time get accurate dimensions, CNC technology was used to machine the complicated cell separators. Programming for CNC machining was done using MasterCAM software. Figure 22 shows the cut profile as planned prior to machining.
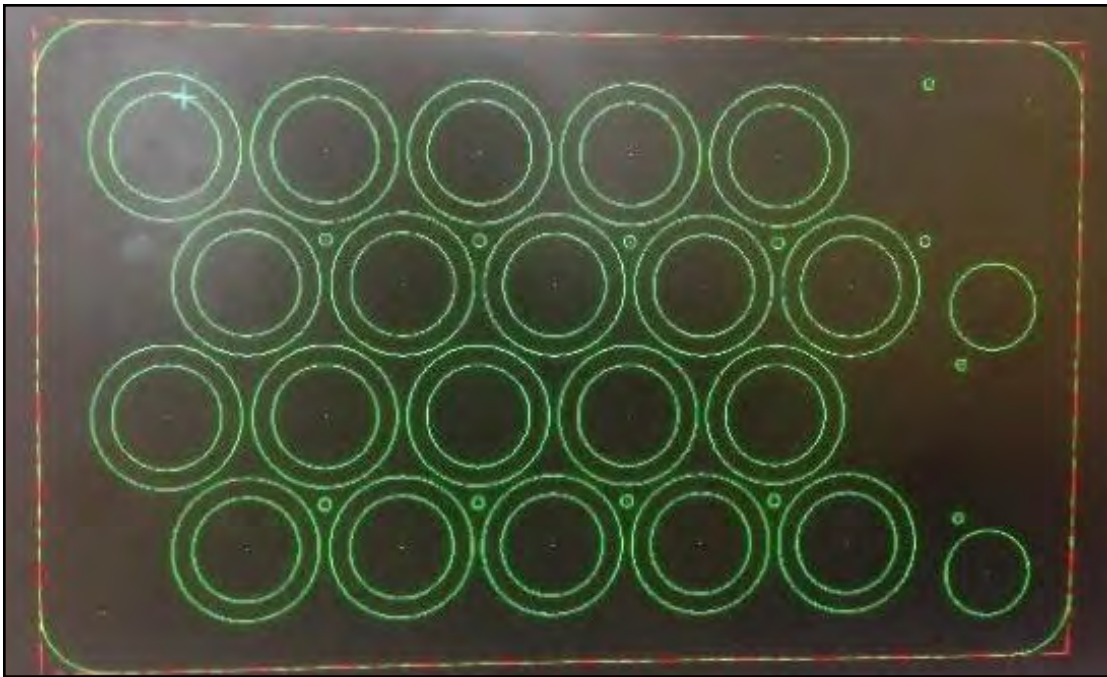
Figure 22. Machining Preparation

An aluminum plate was used below the cell separator so that through-holes could be machined without bottoming out onto the end mill table. Figure 23 shows the aluminum plate and preparations made on the machines prior to any cutting steps.
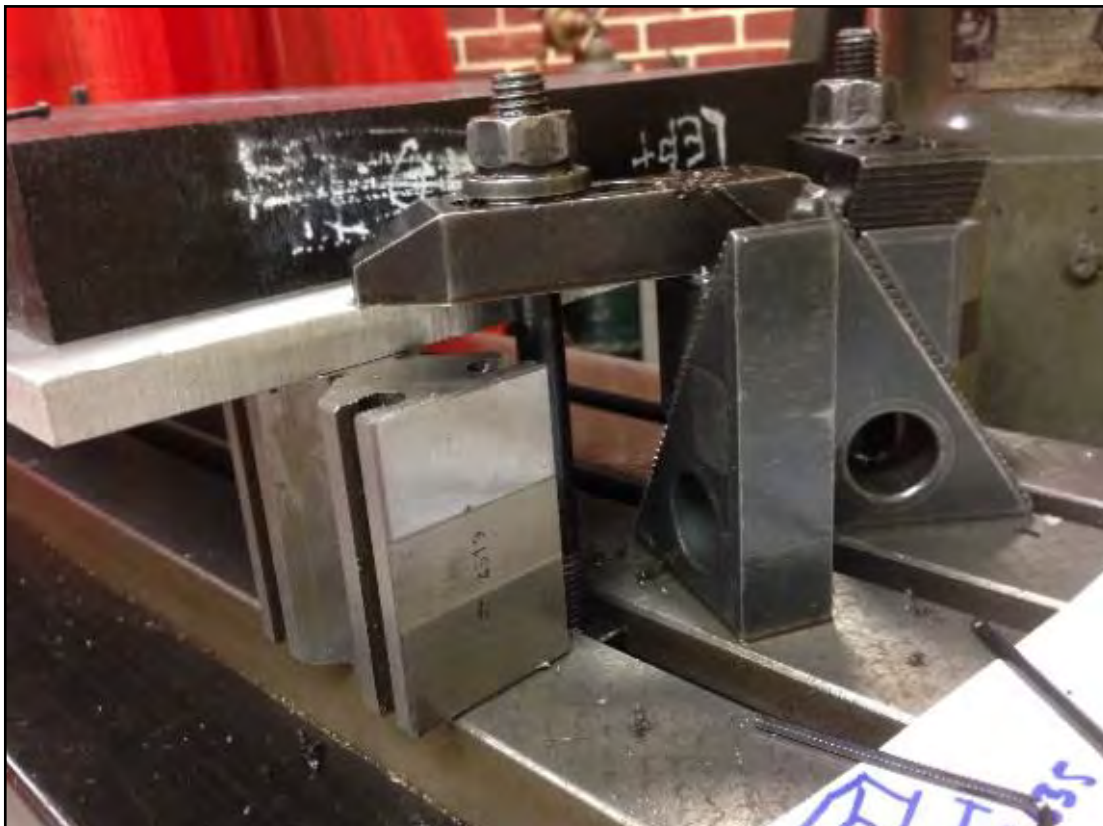
Figure 23. Material Hold-Down for Separator Machining

Figure 24 and Figure 25 show some of the intermediate phases in the machine process while Figure 26 represents the final completed part.

The same steps were followed for all three materials selected for testing. Figure 27 shows the PET material during separator machining. Figure 28 shows a researcher preparing a battery enclosure for module testing while Figure 29 shows the completely machined internal module assembly: top and bottom cell separators and isolation walls.

The parts machined as part of this research were consumed by the battery-destructive testing presented in other sections of this report.

Figure 24. Cell Pockets

Figure 25. Facing Step

Figure 26. Completed Separator

Figure 27. PET Machining

Figure 28. Welding

Figure 29. Complete Assembly

DATA ACQUISITION SETUP

Data from voltage, current, temperature, and pressure sensors are vital to understanding the processes a cell undergoes during a destructive test. To gather all this information at a high rate and over long distances, a Controller Area Network (CAN) bus was setup. All sensors were tied to the CAN bus via custom-built embedded devices including necessary signal conditioning and calibration. Each message broadcast from a CAN node was logged using Vector CANtech hardware and software to monitor and capture the data in real time. This data allowed researchers to quantify batteries' response under extreme conditions of voltage, current, temperature, and (in some cases) pressure.

Figure 30 shows a typical CAN interface setup that logged data from the cells during a test that in this case included voltage, current, and temperature. Notice that the screen is split into three main windows. The window on the top left graphs the temperature of each sensor versus the test time. The window on the bottom left graphs the voltage and the current. In the case of this nail puncture test, no current is flowing; therefore, the current value is zero. The window on the right displays raw data variables and current values available on the CAN network which are available for graphing.
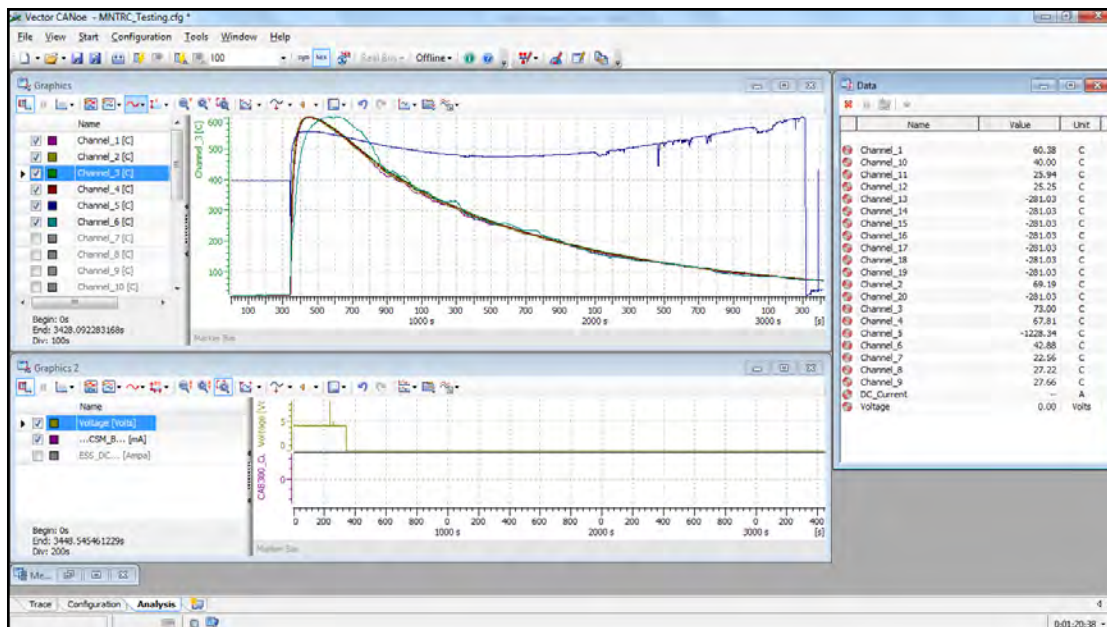
Figure 30. Monitoring the Data through Vector CANoe

After a test, data was post-processed and exported into a MATLAB format to clean up erroneous signals and apply any necessary scaling. Because of the various bus speeds and conflicting CAN IDs, several channels were required to record all test data.

Table 2.   Data CAN Bus Channels

Channel	Bus Speed	Equipment
1	500 kbps	Current sensor (CAB300)
1	500 kbps	Temperature sensor (18B20 and Thermocouples)
2	250 kbps	Pressure sensor (Honeywell MLH150PGB06A)
2	250 kbps	Voltage

Table 2 lists the channels and the bus speeds for each signal. A LEM CAB 300 current sensor was used to measure current with high resolution and accuracy. This current sensor is the same type used in battery monitoring applications where high accuracy and very low offset are required. By collecting accurate current and voltage data during testing, it was possible to integrate the amount of energy each battery consumed during a test.

Thermocouples and single wire digital sensors were placed in various locations along both the cell and packaging materials. In early testing, 18B20 digital temperature sensors were employed, but these have a limited temperature range of -55°C to 125°C. The 18B20 sensor communicated directly with a single board microprocessor system via a digital I/O port, and this system relayed signals with a built-in CAN node. These sensors were destroyed once the cell vented, and data afterwards could not be recorded. The second type of temperature sensor used was a J-type thermocouple connected to a CAN-based scanner from Axiomatic. J-type thermocouples were used for the majority of the testing,

except for the instrumented nail test for which K-type thermocouples were needed to measure higher temperature values.

Table 3.   Thermocouple Ranges

Calibration	Temp Range	Std.Limits of Error	Spec. Limits of error
J	0ºC to 750ºC (32º F to 13382º F)	Greater of 2.2ºC or 0.75%	Greater of 1.1ºC or 0.4%
K	-200ºC to 1250ºC (-328º F to 2282º F)	Greater of 2.2ºC or 0.75%	Greater of 1.1ºC or 0.4%
E	-200ºC to 900ºC (-328º F to 1652º ºF)	Greater of 1.7ºC or 0.5%	Greater of 1.0ºC or 0.4%
T	-250ºC to 350ºC (-328º F to 662 º F)	Greater of 1.0ºC or 0.75%	Greater of 0.5ºC or 0.4%

Table 3 summarizes the temperature ranges for various thermocouples.

There is no guarantee that our sensors are always reading accurately from test to test, so the research team built, replaced and tested just about every temperature sensor between each test to ensure the most accurate data.

Cell voltage measurements were obtained in three different ways:

1. Single cell level: single board computer A/D with CAN conversion and node

2. Pack level: I+ME BMS with CAN node

3. Pack level: single board computer A/D with CAN conversion and node

First Setup

The first setup measured cell voltage analog signal at terminals with single board A/D. Values were converted to CAN format and broadcast to the network using a CAN chip add-on board. Calibration was checked using a factory-calibrated multi-meter.

Second Setup

The second setup was used when the test required 10 cell voltages or more in a battery pack. An I+ME BMS system employed a master/slave communication network. Each slave reported up to 10 voltages back to the master using an RS485 bus. Two slaves were used to collect 20 voltages in our final tests. The Master unit sent out the reported voltage measurements over CAN for logging/monitoring by the Vector CANoe setup.

Third Setup

The third setup was necessary because the I+ME BMS hardware is limited to 4.5V per channel/cell and is inadequate for pack-overcharge tests. The team therefore developed its own switching and isolation circuitry to measure each module cell's voltage independently, sending one cell voltage at a time to a Single Board Computer (SBC) for A/D input.
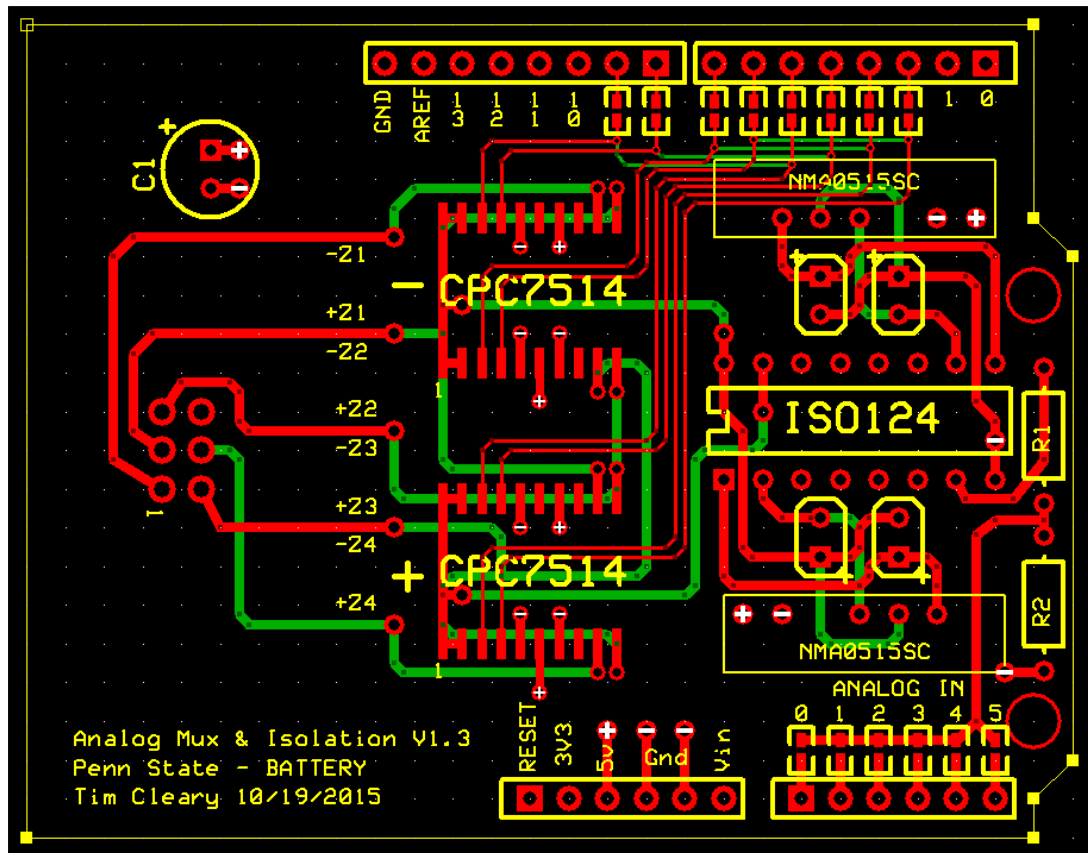
Figure 31. Arduino-Based Isolated Voltage Measurement PCB

The custom Arduino-Based board, seen in Figure 31, allowed for high-voltage isolation and scalable voltage dividers so that peak voltages during overcharge could be captured. The SBC with isolate voltage measurement Printed Circuit Board (PCB) converted data to CAN messages for network broadcast, and these messages were captured by CANoe. Calibration of this device was completed prior to each test.

A pressure sensor was used, when sealed packs were tested, to record how pressure changed inside a battery enclosure before and during an overcharge event. A voltage output single was read by SBC A/D and broadcast via the high speed CAN bus, similar to all other sensors. A curve fit calibration was performed to ascertain pressures prior to any testing.

V. SINGLE-CELL TESTING

Before larger, module-level tests were performed, simpler single-cell testing was needed to provide baseline data such as temperatures and material responses. This section details the testing procedures and results of all single-cell tests performed on the GAIA 45Ah NCA cell. Prior to all tests, cell capacity was verified to be within 80% of its original manufacture specification, as all the used cells in these experiments were donated with unknown State of Health (SOH).

SINGLE-CELL TESTING DESIGN

A set of single-cell tests were planned prior to module-level testing to allow for any information learned to be used in module designs. These tests were used to determine the response of the batteries in accordance with the failure mode to which they were submitted and also to discover the performance of the materials tested.

These goals had to be accomplished without compromising safety. This meant the test setup had to be able to secure the cell during venting processes generating unknown forces. Strong battery tie-downs were used in early testing. Throughout early testing, experience was gained which fed directly into future designs of the single-cell test setup. The first design was a control. The intent was to overcharge a cell to understand the duration of the venting process and the magnitude of the resulting forces to ensure all tests could be performed safely.

Two acetal separators and a base were used to hold the cell. Then two metal straps were also installed to make sure the cell could not escape the test stand. These separators were either bolted down to the platform of an air press or bolted directly to studs in a concrete base.

The majority of the single-cell tests were performed on an air press, which gave the researchers the ability to push a nail through the cell and release the cell energy in the cases where the initial test failed. This made approaching the cell after a test much safer, as researchers could be confident there was no residual energy remaining. Also, researchers could see the energy escape via a severe venting event.

Figure 32 shows a solid model of the early concept for a single-cell test stand.
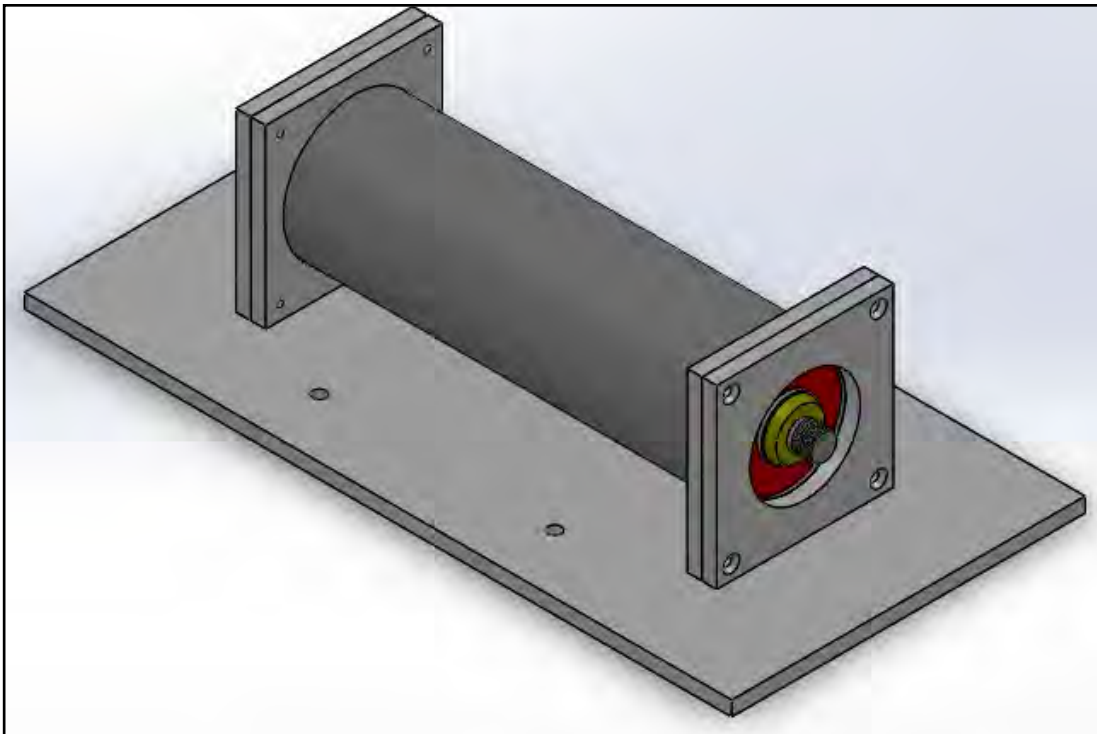
Figure 32. Initial Single-Cell Test Stand Design

The results of initial testing showed that the acetal parts used to hold the cell were strong enough, but shortly after an event they melted and burned until there was little material remaining.
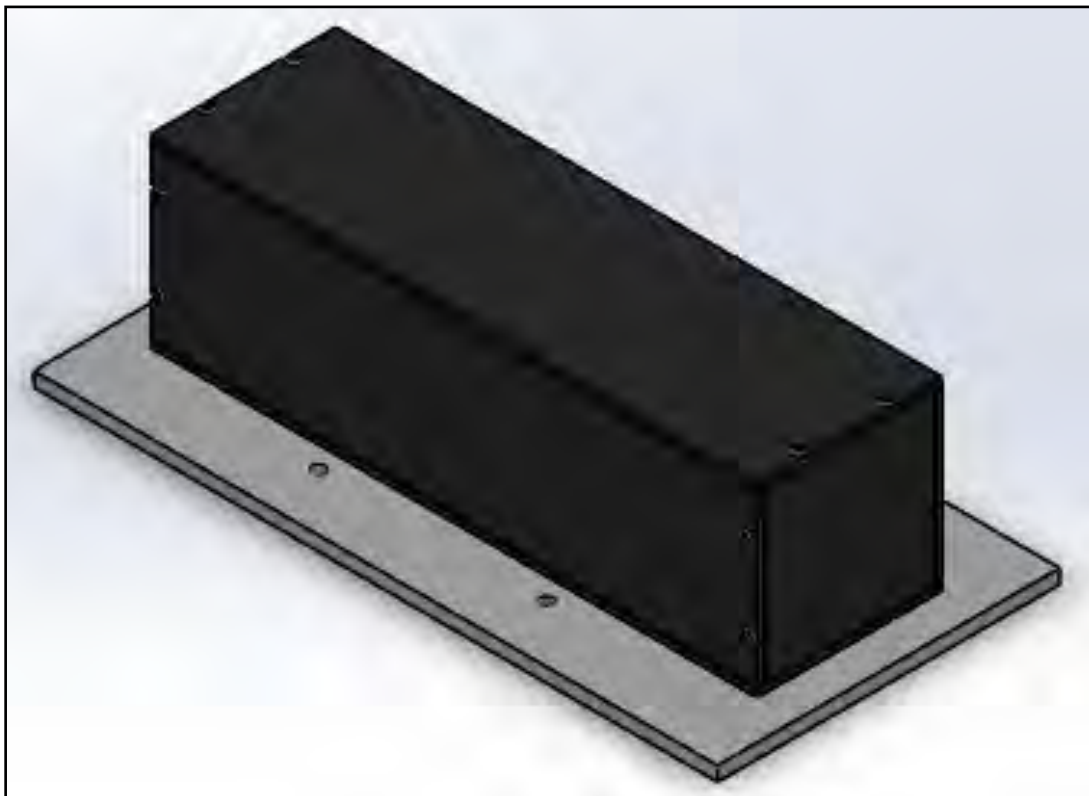
Figure 33. Cell Enclosure

Following the initial testing, a cover was designed to enclose a cell and allow for thermal propagation testing. Figure 33 shows the cell enclosure. This enclosure was slightly larger than the cell and was secured to the testing platform using the same methodology as the previous test stand. Figure 34 shows a top-down view of the inside of this cell enclosure. Note the minimal clearances to minimize any gas pressure relief.
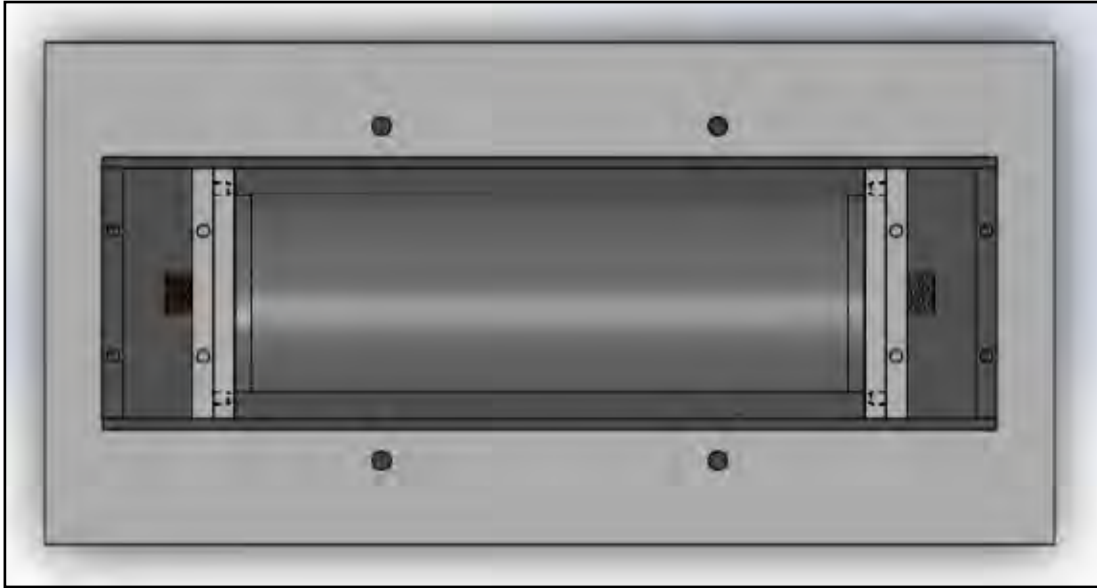
Figure 34. Top-Down View of Cell Enclosure

Holding Cells Down

To be sure that a cell would not escape during a venting or nail puncture test, metal bands (seen in Figure 35) were used to secure the cell.

Figure 35. Metal Straps

Air Press

A Mead AP-122 air press was purchased to be able to perform nail punctures and end all other cell tests safely. The base of the air press was threaded to secure the plastic base of the single cell platform using through bolts.
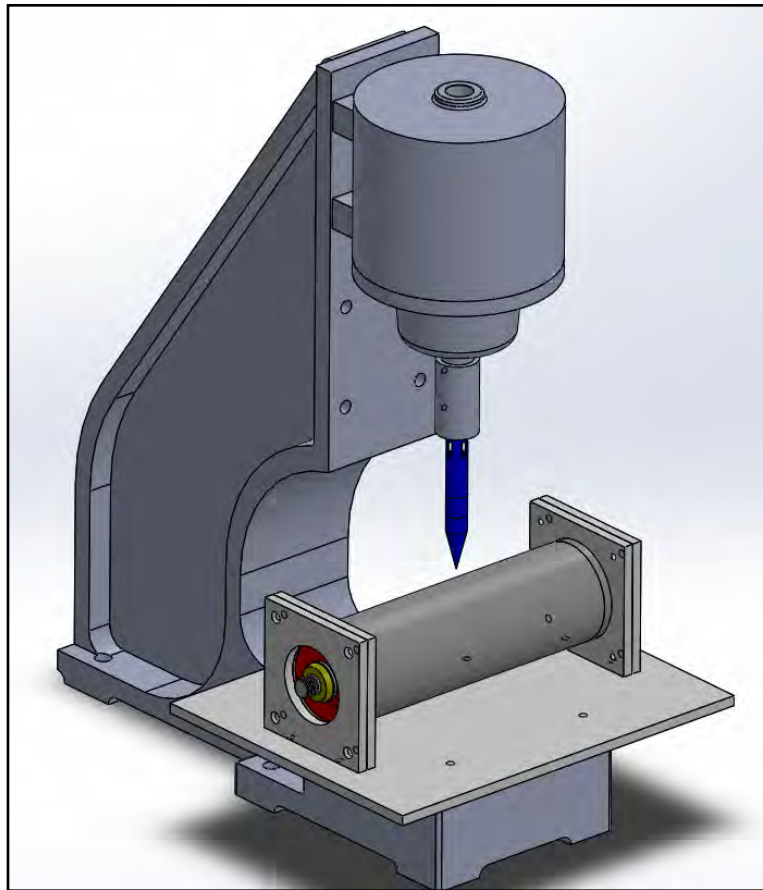
Figure 36. Nail Puncture Air Press

Figure 36 shows the air press system Computer Aided Design (CAD) model including a cell and nail. The air press was bolted to a concrete pad and was operated through a system of valves with air pressure supplied by a typical tool compressor.

ACETAL – OVERCHARGE

In this first test, a 20-Ampere (A) load was applied in an overcharge scenario to replicate a hypothetical undetected voltage measurement error during a constant-current charge mode. If a BMS (specifically its analog-to-digital converter measuring cell voltage) is not accurate, a dangerous charge load may remain active. More intelligent charging systems may measure energy to protect against this, but it is a difficult task to balance the accuracy of an energy measurement; possible human error in the programming and setup of this feature; hardware failure; and the assurance that a battery is fully charged. Despite the attention given to this topic, overcharging of cells continues to occur.

Prior to testing, a single cell was fully charged to 100% State of Charge SOC and/or an open circuit voltage of 4.2 V as specified by the manufacturer. Upon initial electrical loading, the cell entered an overcharged state because it was already fully charged. The cell was allowed to continue charging at a constant current of 20 A until cell pressure discs burst. Immediately following the pressure release, charge current reduced to nothing due to the cell becoming an open circuit, likely because of internal damage to electrodes. All the data and setup of this test are presented in this section.

The single-cell acetal test stand was bolted to a large concrete pad with metal straps as previously described. Figure 37 shows the concrete pad and single-cell test stand, with charge cables, prior to the start of the first overcharge event.

Figure 37.   Single-Cell Overcharge Test

Data was collected during testing, including seven temperature sensors attached to various areas on the surface of the cell, voltage measured between positive and negative terminals of the cell, and current. All this information was gathered by sensors and broadcasted via the CAN while simultaneously being logged by a CAN bus data logger, as discussed in the data acquisition section of this report. Besides recording CAN data, the investigators also recorded video of the test with two stationary high-resolution cameras.

Maxwell DS1820 single-wire digital temperature sensors were used to capture temperature data during this test. It was not until after this test that it was discovered that these sensors would be insufficient due to their range from -55ºC to 125ºC. As a consequence, the sensors were damaged and peak temperatures achieved during venting were not captured. However, the temperatures leading up to this venting event were recorded as they were within range of the sensors.

Figure 38 shows the data recorded via the CAN bus. Cell voltage, temperatures, and cell current until the venting event were logged.
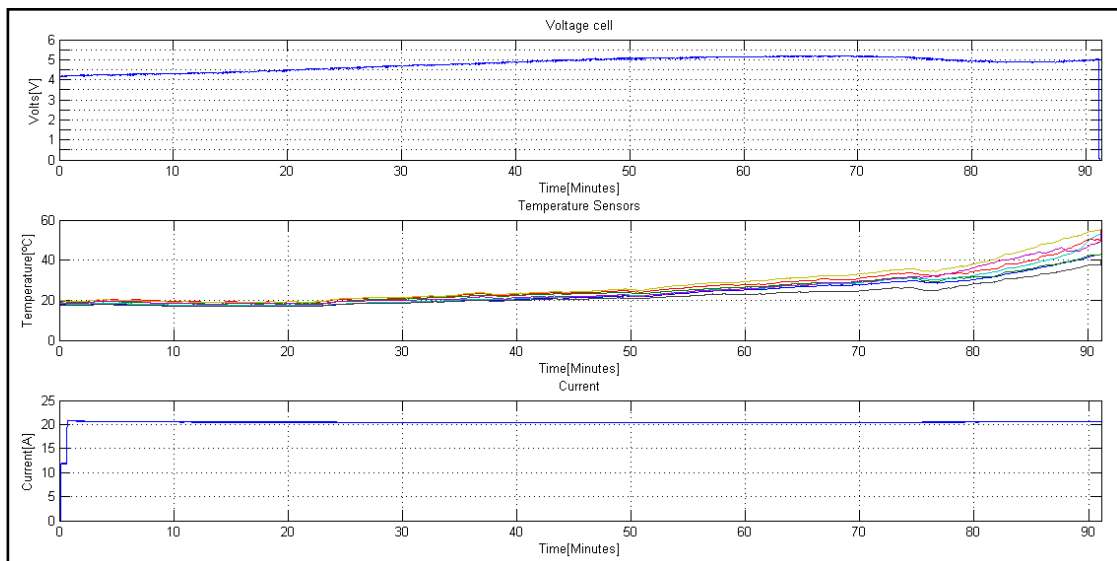
Figure 38. Data from Initial Overcharge Test

Note the dip in voltage (top chart) just prior to the venting event. This is a pattern that was repeatedly observed through all tests and that the research team is confident indicates the onset of thermal runaway, due to the correlation between dip in voltage and the sharp increase in temperature rate. As the voltage dips and temperatures rates increase, the cell experiences an increase in internal pressure right up until the cells' burst discs break open and the cell vents. At this point the cell becomes an open circuit and current stops flowing. Due to internal damage, the electrodes are no longer connected. Note that the temperatures seen on the external surfaces of the cell (middle chart) never exceed 60ºC before venting. These particular cells are rated to operate up to 60ºC, so a BMS that uses temperature data would not have triggered a fault condition since the battery is operating within specifications. Note that a potential solution to this problem would be modeling internal cell temperature based on surface and ambient temperature readings as well as current throughput over a recent time period.

The battery venting lasted roughly five seconds as indicated by flames and huge clouds of smoke. The magnitude of the event is displayed in Figure 39.

Figure 39. Venting Cell – First Test

The single cell was held down to the concrete test pad through an acetal cell holder and plate. The flames and high temperature associated with the venting ignited the acetal plastic, which acted as a combustible and burned out until it was completely gone, as seen in Figure 40.

Figure 40. Cell, Hours After Venting Event

The cell is also visibly swollen after this test. It is clear to the researchers that if not for its large stainless steel cell casing, the cell's casing itself would also likely be completely destroyed. Note that the cell's threaded terminals and terminal nuts are intact following this test. The cell burst discs broke as the design intended, with the casing ends bulged outward slightly.

ACETAL – NAIL PUNCTURE

Based on the previous test of an overcharge, it was important to transition to initiating an internal short circuit on the cell to simulate a crash event with battery system penetration.

This early test also served a dual role in testing battery enclosure materials by testing their thermal capabilities and the appropriate thickness of material needed to withstand a direct venting event. As a starting point, sheets of 1/8-inch-thick aluminum alloy (6061) and a general low-carbon steel material were used.

This test also marked the initial use of the air press system designed to press a nail through a cell. For this particular test, only temperature was recorded, and Type J thermocouples were used. These sensors were located in various areas through the surface of the cell including the top of the cell by the positive terminal; the positive terminal; the negative terminal; the top of the cell in the center; the top of the cell by the negative terminal; the surrounding air (ambient); the aluminum sheet by the negative terminal; the steel sheet by the positive terminal; and the aluminum base.

Figure 41 shows cell temperature measurements in two charts. The top is scaled to the highest temperatures while the bottom is scaled to the lower values. The highest values were measured on the top of the cell by the positive and negative terminals, peaking at about 273 ºC and 175 ºC respectively. The bottom chart shows little rise in temperature. Note that this test was performed in -3 ºC ambient conditions.
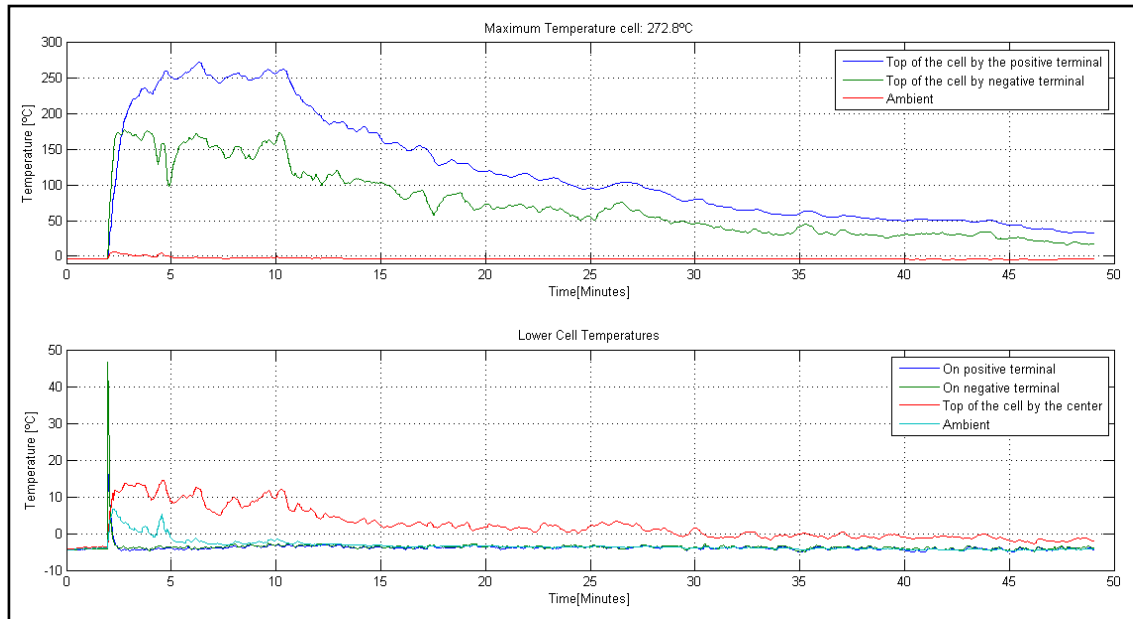
Figure 41. Acetal Nail Puncture – Cell Temperatures

Temperature data was also gathered from the surfaces of the aluminum and steel sheets. These sensors are on the opposite side of that which took the direct blast from the cell through the vent discs. The maximum material temperature was measured to be 32.7ºC. Note that these sensors were not directly opposing the point of impact, but instead a few inches away. Material temperatures did not exceed their respective melting points and did not exceed 12ºC.

ACETAL – OVERCHARGE AND MATERIAL TEST

The nail puncture testing causing a dramatic internal short circuit did not provide the heat necessary to melt nearby metals. The objective of this test, therefore, was to determine if an overcharge would melt the aluminum or steel used to deflect and/or redirect the venting, burning electrolyte. An overcharge event is likely to release much more energy than a nail puncture at 100% SOC. As in the previous test, aluminum and steel were placed on either side of the cells, normal to the pressure release discs, in direct line with the venting gases. These sheets of material were placed at 1.5 inches from the cell terminal (approximately where they would be in a pack design for a large bus application to direct venting electrolyte away from other cells).

Figure 42 shows the setup of the cell and blast shield material. Two acetal separators that were bolted down on an aluminum base held the cell. The aluminum base was mounted on the air press, and the blast shield sheets were attached to the base through L type brackets.

Figure 42. Acetal Overcharge with Blast Shield Material Test Setup

Temperature sensor location was identical to previous tests. As before, only temperature data was logged during this test. These temperature readings are presented through the next few charts. Figure 43 shows two charts with the same data but at different time scales. The top chart shows the entire test from the start, through the venting event, and until the end of the cells' cool-down. The bottom chart highlights the temperature profile immediately following the event.
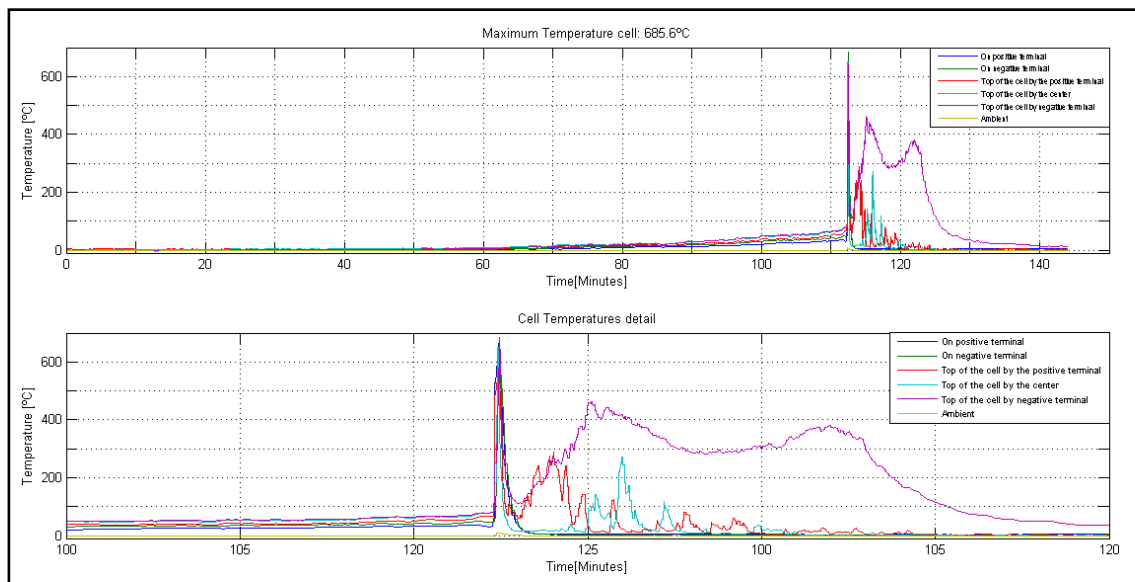
Figure 43. Acetal Overcharge w/ Material – Cell Temperatures

Note the spikes in temperature: some sensors reach in excess of 600ºC, then are followed immediately by an aggressive cool-down. The second climb in temperature and sustained 300ºC readings are from the combustion of the cell holders made of acetal material. If acetal did not burn, then the time during this event in which temperatures exceeded common vehicle material combustion temperatures would be greatly reduced. This in turn would reduce the chance of a vehicle fire, or at least limit the damage and increase time to evacuate and for emergency responders to cool the pack with water.

The response of the metal is summarized in Figure 44. The first noteworthy point is that the metal's temperature exceeds temperature measurements from the cell itself. This is likely a result of the metal blast shields being in direct contact with the venting gases while the cell surface temperature sensors are likely limited by the insulation properties of the cell casing. These material temperatures are assumed to be much closer to internal cell temperatures than the surface measurements captured from the cell's exterior. The aluminum sheet experiences a temperature 100ºC warmer than the steel sheet. One of the causes of this response could be that the cell did not vent uniformly. Also, the thermal distribution proprieties of each material are substantially different. If the sensors were directly on the opposite side of the impact area, more accurate readings would be possible. In reality, the sensors were at different distances from the impact point of the gases, which also contributed to this difference.
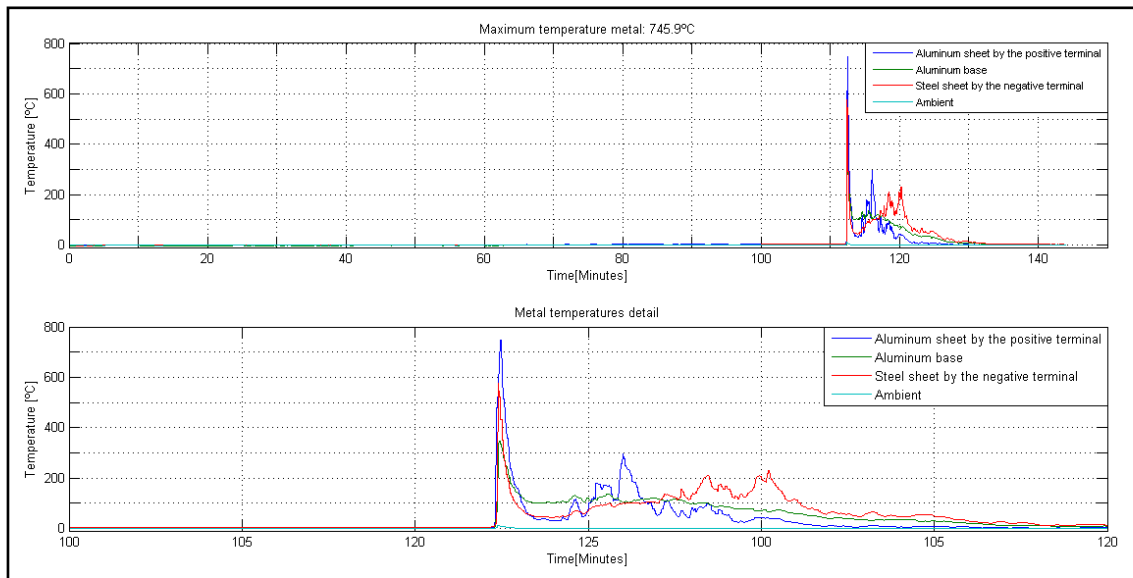
Figure 44. Acetal Overcharge w/ Material – Material Temperatures

According to the measured temperatures and melting point of the aluminum and steel, it is not surprising that a two-inch diameter hole was burned through the aluminum while the steel remained intact.

The venting process for this test was very intense, as Figure 45 demonstrates. Although the testing was completed in non-ideal environmental conditions (very cold, windy weather), it did unexpectedly provide a valuable measurement. The black smoke escaping the cell stained the snow, providing a radius for measuring the effective distance debris can be expected to travel. Upon visual inspection, the smoke and flames traveled approximately 125 inches from each side of the cell, or in a radius of the same dimension.

Figure 45. Acetal – Overcharge with Material Test

This test resulted in valuable information useful in understanding the magnitude of temperature and burning electrolyte that a single 45Ah NCA cell is capable of releasing. The finding raises concerns of safety and security when using this type of energy storage system, as well as reason to have redundant sensors to ensure accurate measurements during charging.

PYROPHOBIC – OVERCHARGE

Part of this research was to investigate fire suppression systems and fire prevention techniques using new materials and design. Pyrophobic Systems produces proprietary compounds that claim to both absorb fires and suppress them from spreading to adjacent areas. This research team formed a partnership with Pyrophobic by receiving donations of their materials in the form of machined components ready for testing in our single-cell scenarios. To thoroughly test this material an overcharge test was commissioned. It is well known from previous tests that the most stressful scenario will occur from an overcharge-venting event. For this test the cell was surrounded by a wall of Pyrophobic material with cell separators holding the cell at each terminal. Again the assembly was bolted down to an aluminum base that was also secured down to the air press just in case the cell failed to vent and a nail had to be put through to induce the discharge.

Figure 46. Pyrophobic – Overcharge Setup

Temperatures of the walls and cell surface were recorded as well as cell voltage and current. Unfortunately, a sensor placed on the cell and another one on the walls were lost due to the intensity of the event, so their data is not available. Other than these two sensors, all others were valid throughout the test. The data gathered from these sensors can be seen in Figure 47.
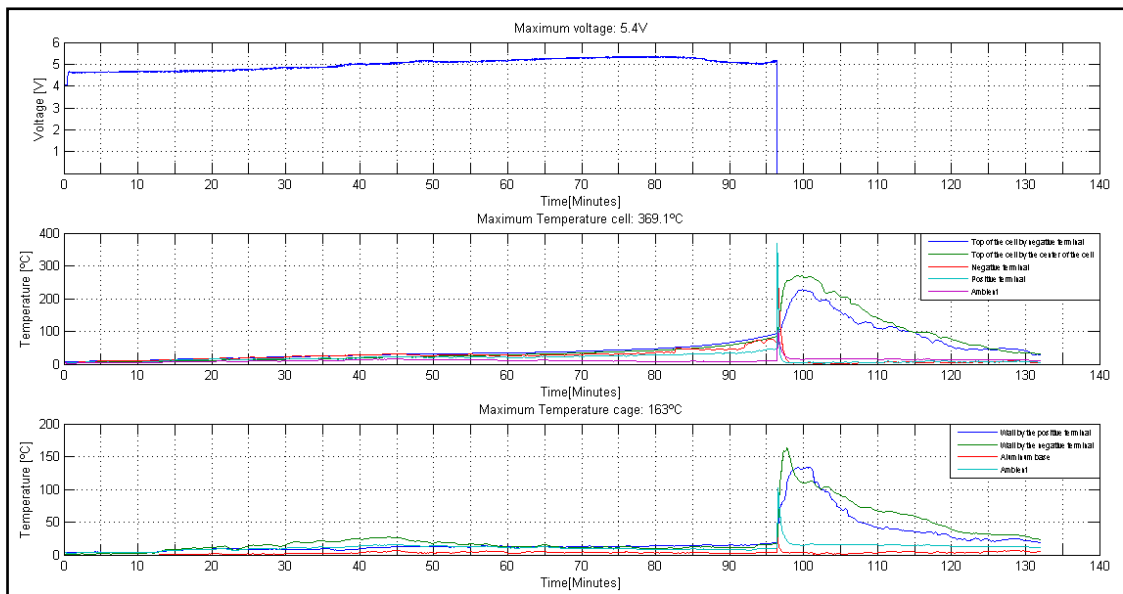
Figure 47. Pyrophobic – Overcharge Data

Analyzing the voltage (top chart), notice that the cell was charged before starting the test and at an open circuit voltage of 4.2. Although current is not shown in the data charts, the cell was charged at the typical 20 A constant current which brought the cell up to approximately 5.4 V just prior to the typical voltage dip. This dip is followed by the increase in temperature rise, then concludes in a powerful overcharge venting event.

It is notable that the venting event resulted in a peak cell surface temperature of approximately 400ºC, which is considerably lower than in the earlier tests.

Figure 48. Pyrophobic – Overcharge Results

This test resulted in confirming this material as a viable candidate for use with NCA cells (see Figure 48.) It is able to maintain structural integrity and not melt or burn during or following an extreme cell-venting event.

PYROPHOBIC – NAIL PUNCTURE

The test detailed in this section is the evaluation of the Pyrophobic brand intumescent thermoplastic material under a nail puncture scenario. Temperature sensors were placed on the cell surface as in previous tests, as well as on all six parts of the cell and wall separators used in this design. To capture the thermal distribution during an event, but also to document how well this material held up to this extreme temperature and force, the temperature sensors were distributed along the cell and the surrounding walls, all made of the same Pyrophobic material. Figure 49 shows the voltage and temperature data recorded during this test.
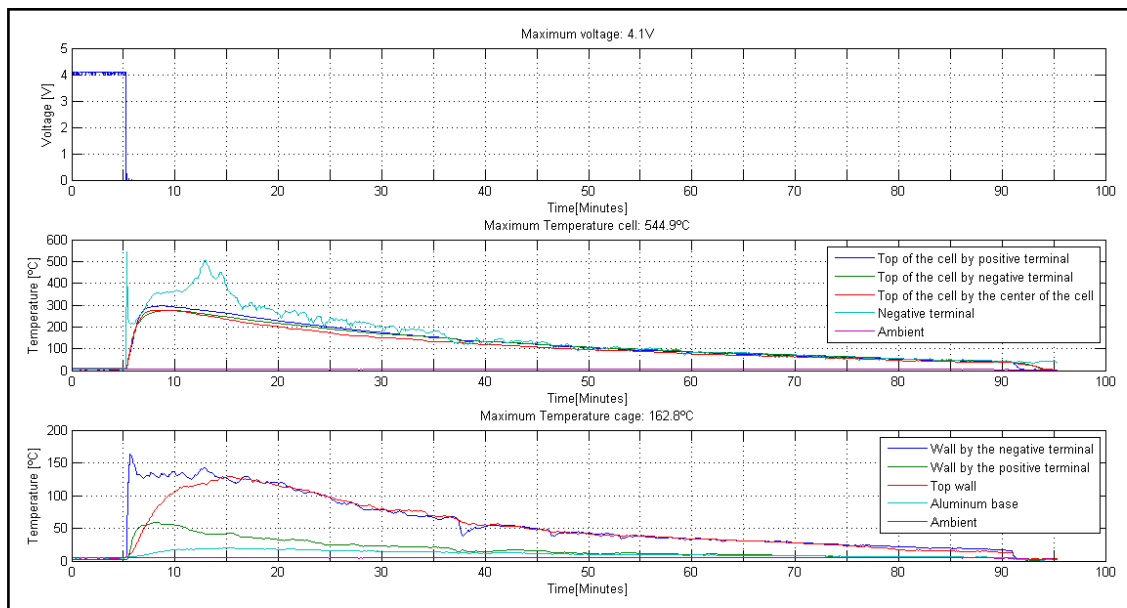
Figure 49. Pyrophobic – Nail Puncture Data

The top chart shows cell voltage readings; the middle chart cell surface temperature readings; and the bottom chart Pyrophobic material temperature readings. The cell had a steady open circuit, unloaded, voltage of 4.1 VDC up until the nail went through to force the cell into an extreme short circuit condition. As typically seen in these tests, this led to an internal open circuit dropping the measured voltage to 0 VDC. Temperature readings from this test are comparable to the previous acetal tests but without the second jump in temperature due to burning materials. Cell surface temperatures rose quickly to approximately 300ºC, then slowly cooled back down to ambient over a 1.5-hour period.

The negative terminal wall heated up as soon as the nail went through the cell. This sensor achieved a peak temperature of 162.8ºC, which is significantly lower than the heat released by the cell. This fact highlights the excellent capabilities of the material to dissipate heat. A sensor on the top of the wall took a bit longer to heat up, although it quickly achieved the same temperature as the wall by the negative terminal.

Another notable result was the measurable difference between positive and negative terminals. It seemed that the majority of the heat during this test came from the negative terminal of the cell, so it was no surprise that this side of the material showed more damage.

Figure 50 shows both the positive (left) and negative (right) terminal walls/covers. This material, just as with the aluminum and steel blast shields, was in the direct path of the venting, burning, electrolyte released during a nail puncture. As presented above, the positive terminal experienced a lower temperature rise compared to the negative terminal. The images of these terminal covers may show why this happened. Venting gases quickly punctured the positive terminal cover, while the negative cover seems to have contained these hot gases and only vented on the side opening of the cell separator.
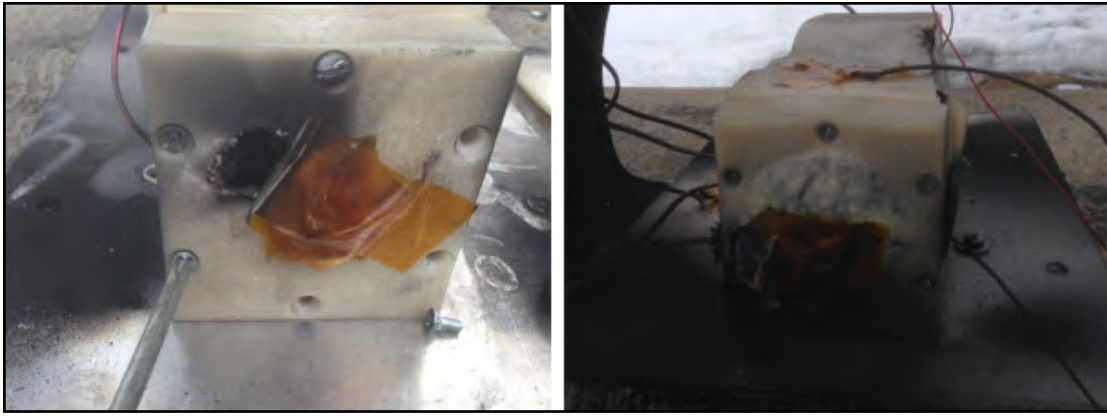
Figure 50. Pyrophobic Material Results

Following a long cool-down period, all the material including each cover and wall plate was removed and analyzed.

Figure 51. Pyrophobic Material After Nail Puncture

Figure 51 shows all the parts used to contain this cell nail puncture event. The material has obviously grown in thickness, yet it clearly hasn't lost integrity. It would likely keep this event from impinging into another area, limiting thermal propagation and maintaining structural integrity.

PYROPHOBIC – OVERCHARGE WITH HOUSING

Based on the previous test results for the Pyrophobic material, the manufacturer recommended compliantly enclosing their product to take full advantage of the intumescent functionality. In hopes of absorbing even more energy, an aluminum housing surrounded the Pyrophobic material and cell to simulate an enclosed battery system. The metal enclosure was made out of aluminum 6061 alloy and welded together to create a sealed enclosure. It was not completely closed, however, as it had openings on the sides by the terminals to release the smoke and the flames, thus limiting the pressure buildup inside the enclosure to prevent an explosion.

The housing was bolted down on the same aluminum base that held all previous assemblies on the air press as seen in Figure 52.

Figure 52. Pyrophobic – Overcharge with Enclosure Setup

The cell was then overcharged as in previous tests. The results are presented in Figure 53. This test started prior to a complete charge. Instead of fully charging, resting, then resuming in an overcharge state, the test started at approximately 50% SOC. This was a mistake on the part of the researchers performing the test but resulted in an overcharge venting event nonetheless. The typical voltage dip at the start of thermal runaway occurred, but the peak voltage prior to venting was much higher than usual at 8.1 VDC. It is also notable that the surface temperatures of the cells reached 100ºC right before the cell vented. This is substantially higher than typical tests, and was probably because of the insulation effect the aluminum enclosure had on the cell and its surface-mounted temperature sensors. Despite having higher values of voltage and temperature relative to other tests, the cell did not get extremely hot during the venting event or thereafter. All the temperatures except the one on the top of the cell by the center remained between 400-500ºC, which is a lower range than typical. The temperature measurements remained in

this range for approximately 10 minutes, at which point the cool-down process started. It took around 1.5 hours to cool down to ambient temperatures, which was about average.

During the cooling-down process, the temperatures captured by each sensor placed on the cell were similar and constituted a very homogenous profile, although after the venting the material caught on fire.
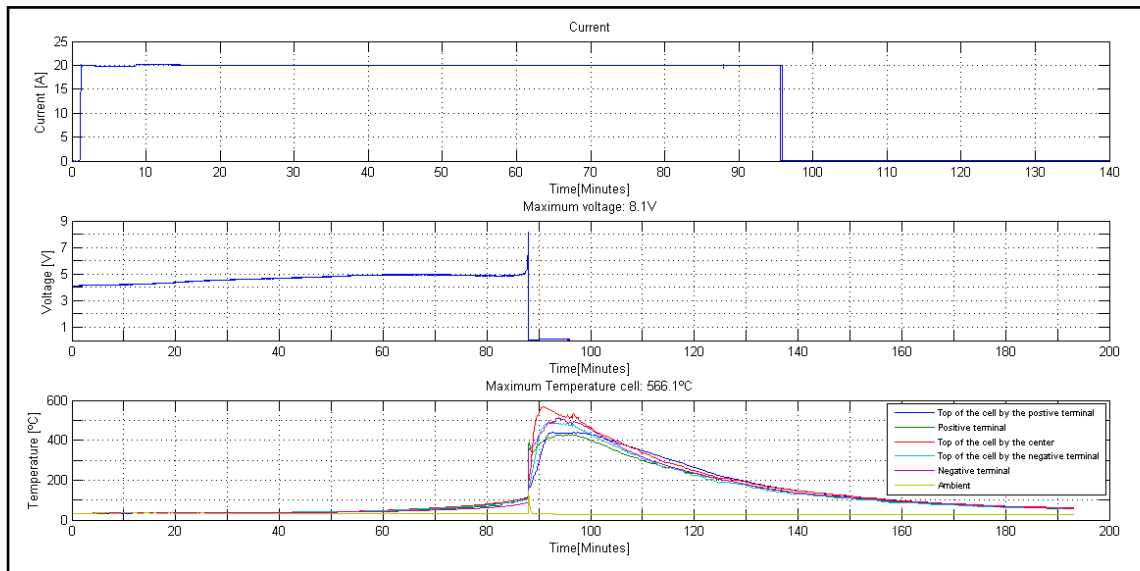
Figure 53. Pyrophobic – Overcharge with Enclosure Data

Figure 54 shows the machined opening, the larger diameter hole, and the smaller opening cut by the venting gases.

Figure 54. Pyrophobic Enclosure Vent Opening

Figure 55 shows the results of using the Pyrophobic materal inside the enclosure. Clearly this material is more charred and not as strong or capable of holding a cell as that in the test perfomed without an enclosure.

Figure 55. Pyrophobic Overcharge with Enclosure Material Results

This test shows the aptitude of Pyrophobic material to absorb substantial amounts of energy, a desirable trait when selecting a material for battery pack designs. **However, it must be noted that the material cannot be used to both absorb energy and maintain structrual integrity.**

PET – OVERCHARGE

The thermal response of a PET material used in a single-cell test stand was also evaluated. This section details the setup and results of an overcharge event using PET to both hold and enclose a single cell. Figure 56 shows the setup for this test. As with previous tests, the cell is securely mounted to the air press and equipped with temperature, voltage and current sensors.
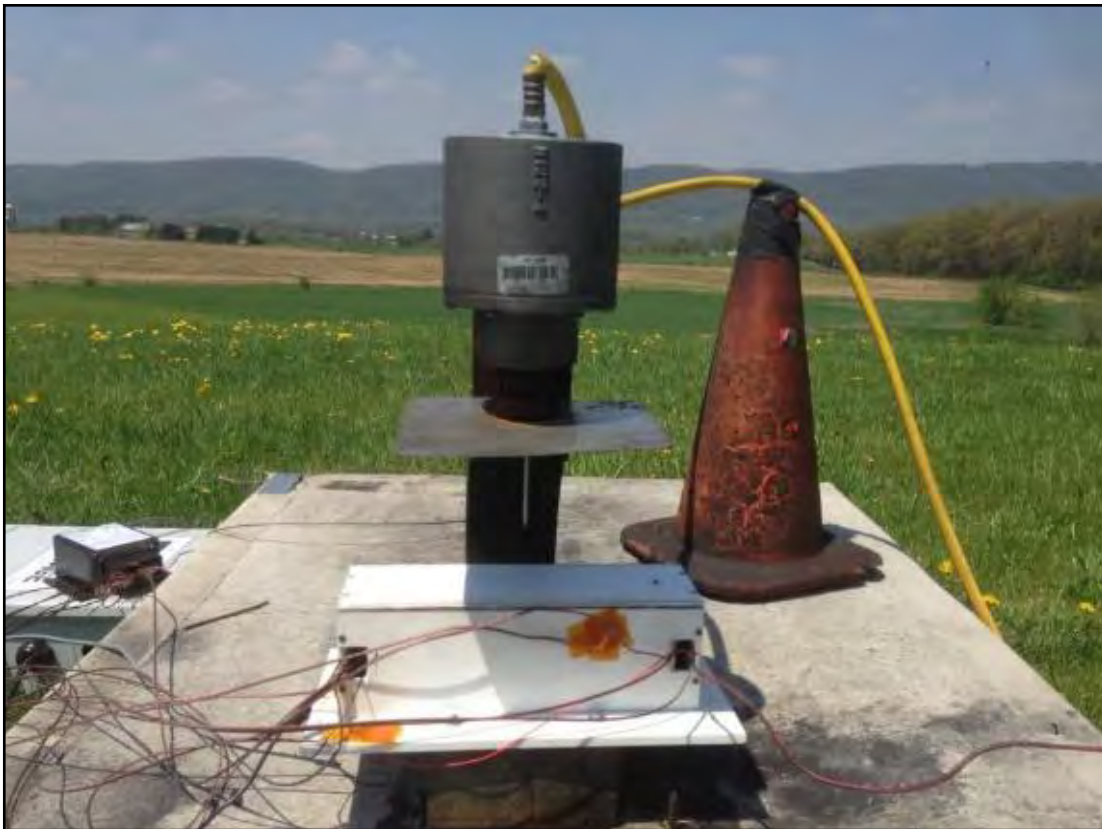
Figure 56. PET – Overcharge Setup

Extreme temperatures were reached during the PET overcharge test, peaking at approximately 750ºC. Figure 57 shows the current, voltage and temperature data recorded during this test. Note that typical current and voltage profiles were seen. Leading up to the vent, a dip in voltages occurred just as temperatures increased to thermal runaway values. An open circuit was realized when the cell began to vent.
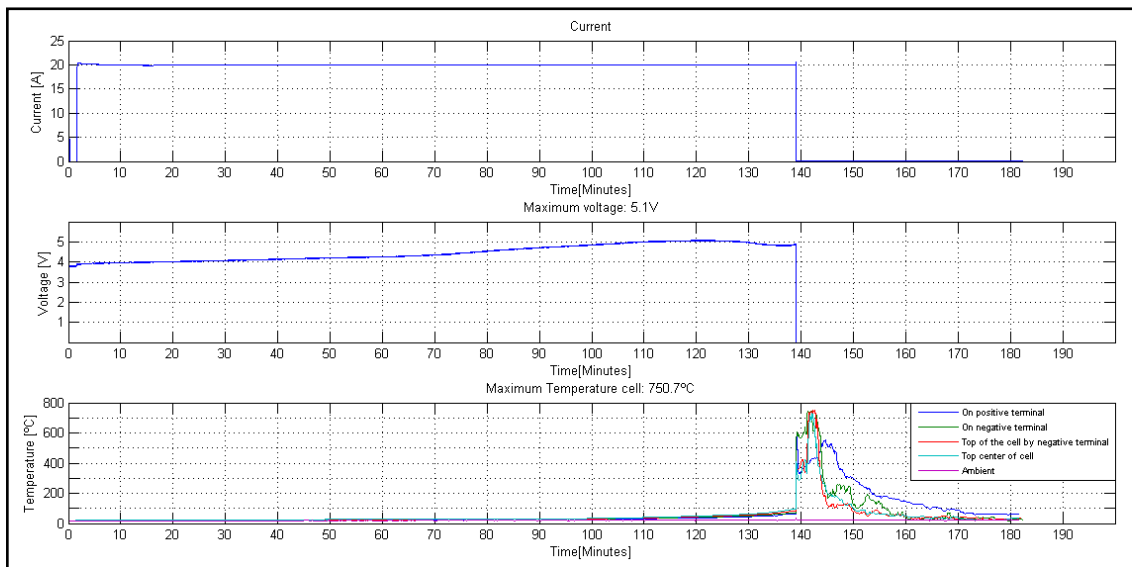
Figure 57. PET – Overcharge Data

Figure 58 shows the temperature data leading up to the venting event. Note the exponential rise in temperature starting around the 110-minute mark, just around the same time as the typical voltage dip.
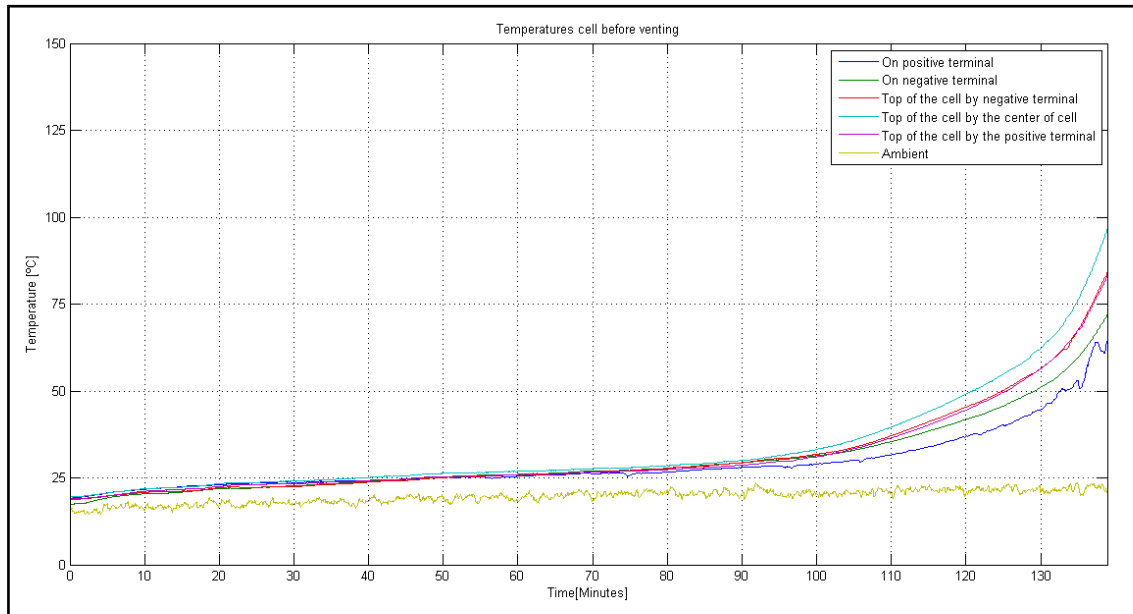
Figure 58. PET – Overcharge Temperature Data

Not all tests result in exactly the same temperature measurement distribution. Some show that the positive terminal is hotter than the negative. In this test, however, because the PET material caught fire (as seen in Figure 59) most sensors detected extremely high and sustained values.

Figure 59. PET – Material Result

In this test, after the violent venting that included flames, the material kept burning until completely gone. In fact, playing back the video recorded during the test, it took around ten minutes to burn the entire cell enclosure down to nothing. After that the enclosure cooled down very quickly, because it basically disappeared after ten minutes and sensors then read ambient temperature. This fire surrounded the cell, heating it. As a consequence, the cell did not cool down as rapidly as the PET enclosure.

Figure 60 shows the remains after the PET enclosure melted down. The only part not damaged was the base, which was made of a substantially thicker, 0.5-inch plate.

Figure 60.   PET – Material Result 2

The conclusions of this test are that the PET material is not capable of handling the temperatures, containing the event or remaining structurally intact.

PET – NAIL PUNCTURE

Given the poor material results of the PET during and following its overcharge test, expectations were low for a nail puncture test using the same material.

Voltage and temperature data were gathered during this test. Figure 61 shows the logged data.
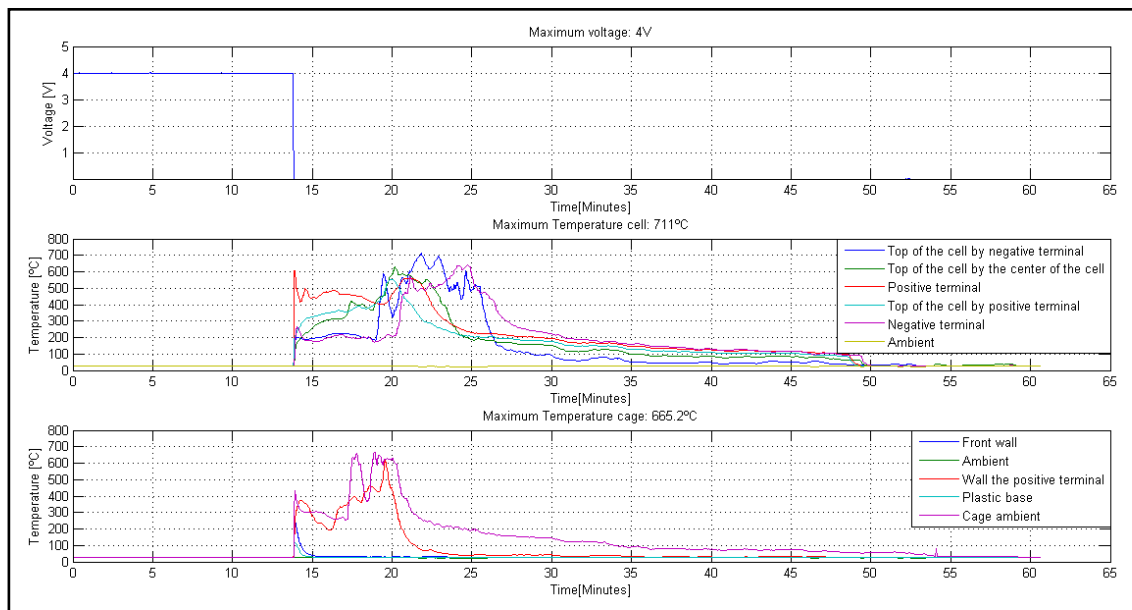
Figure 61. PET – Nail Puncture Data

The top voltage chart indicates that the cell was at an open circuit of four VDC prior to the test. The voltage of the cell stayed stationary until it dropped due to the nail penetrating. The nail caused a short between the positive and the negative electrodes, resulting in the typical cell temperature rise and ultimate fierce venting event.

Analyzing the response of the cell, notice that the positive terminal temperature climbed right after the nail went through the cell. It then remained fairly stationary while the other sensors responded slightly more slowly.

All the sensors except one on the top of the cell by the negative terminal achieved a maximum value between 500ºC and 600ºC and remained there for roughly five minutes until the cool-down process started.

In a review of the recorded video, some notable points stand out. The positive terminal was the first to reach the high temperatures recorded and was also the first side to experience a disc rupture, resulting in hot gases venting and flame. This can be seen in Figure 62. Note that the right side represents the positive terminal.

Figure 62. PET – Positive Venting First

As with the previous PET tests, the material caught fire and burned until completely gone. The fire lasted about ten minutes, which according to the graph corresponded to the period of time between the 15th and 25th minute, when the cooling down profile started. The fire a few minutes after the nail puncture can be seen in Figure 63.

Figure 63. PET – Nail Puncture Material Result

The flames of the venting ignited the material by the terminals, and the fire then propagated throughout the entire enclosure. Figure 64 shows that the enclosure was nonexistent after a few minutes and only the cell case and plastic base remained.

Figure 64. PET – Nail Puncture Results 2

The results of this test were similar to that of the other PET/acetal tests. The material is not capable of handling a thermal event from a large-format 45 Ah NCA cell.

TEFLON – OVERCHARGE

Two Teflon overcharge tests were performed, because the first was not successful. Several tests had to be repeated for various reasons, but the results of this failure were rather interesting and are presented here as they provide valuable insight into the possibility of a failed burst disc.

First Test – End Cap Failure

As with all other tests, a fully charged 45 Ah cell was installed into a test stand made of the candidate material in an overcharge event. The first attempt at a Teflon test resulted in a structural failure because the entire cell end-cap burst instead of the burst disc. Shortly after the venting event started, the end-cap came off and the force of the venting gases projected the cap about seven meters from the test site. Cell casings are made by welding end-caps to each end of a stainless steel tube. This weld failed and as a result ejected a substantial amount of electrode material. Figure 65 shows how far this material spread from the test site.

Figure 65. Blast Radius

The cell also ejected from the base and would have likely gone a great distance but hit a pile of snow, limiting its travel. This event gave the researchers an even greater respect for the power released during an event. It should be noted that each cell overcharge/nail puncture usually results in a violent venting event, but the result of each event affects the cell casing slightly differently. In some cases, the burst disc fails and entire sections of the cell burst. A review of the test plan and setup was performed, resulting in an increased distance between the test site and researchers/visitors.

Second Test

The second attempt of this test resulted in the usual burst disc release and was a valid evaluation of the thermal behavior of the system. Figure 66 shows that the cell was overcharged at a constant 20 A. As a consequence, the voltage rose to 5.1 VDC just prior to the onset of the typical dip in voltage and increase in temperature rise rate.
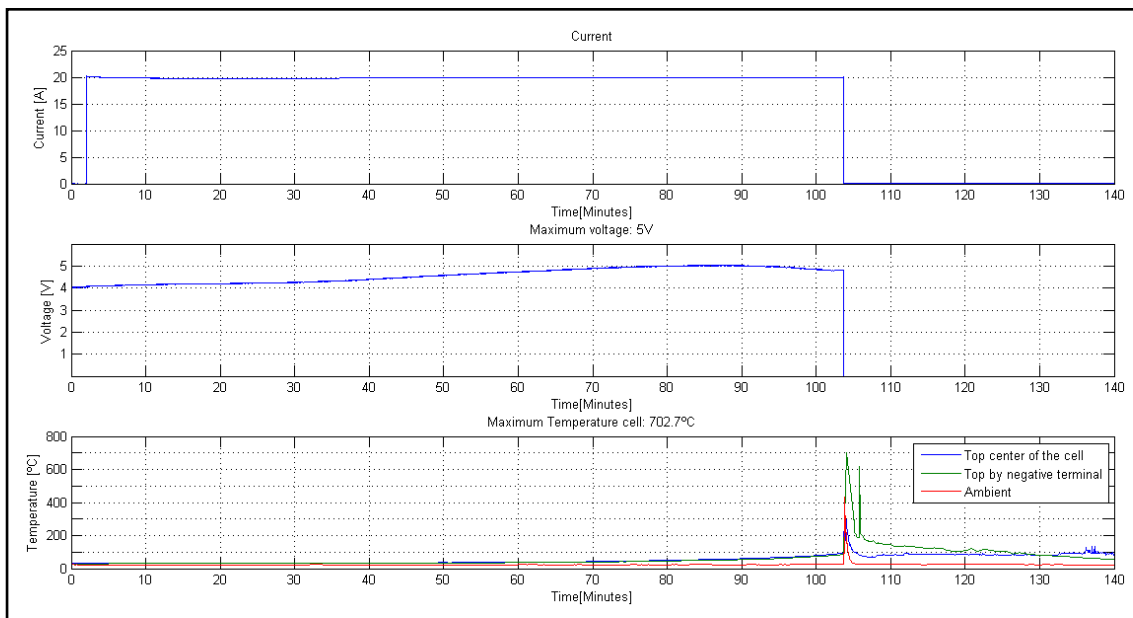
Figure 66. Teflon – Overcharge Data

In this case, venting occurred when the cell surface reached 100ºC. A peak temperature of approximately 700ºC was measured shortly after the event started. It is notable that during this test peak temperature cooled rather quickly. Because the Teflon material didn't burn, there were few sustained temperature readings following the test, unlike all other results.

Figure 67. Teflon Overcharge Material Results

Figure 67 shows the fire resulting from the overcharge event. Note that this fire only lasted about **43 seconds**. Figure 68 shows the temperatures measured by sensors mounted to the walls of the cell enclosure made of Teflon. Note that these temperatures were only above ambient for approximately 2 minutes. This was in contrast to all other tests where high temperatures are typically sustained for at least 10 minutes. Only one signal reported a temperature above 100ºC and is likely due to hot gases venting from the cell.
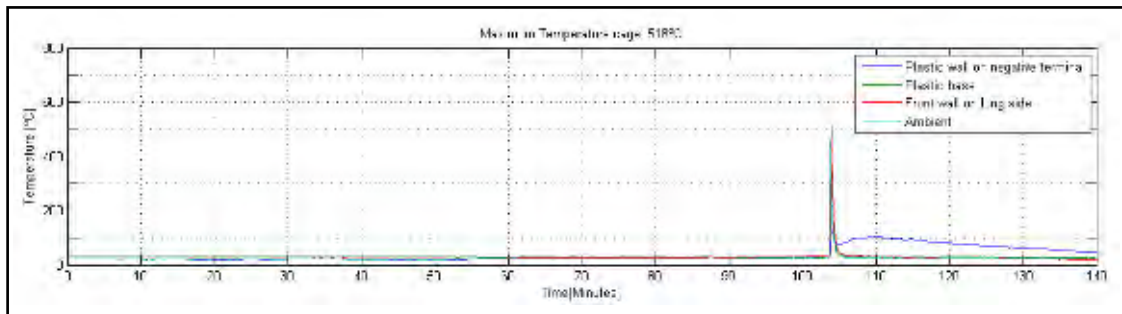
Figure 68. Teflon Overcharge Material Data

Figure 69 shows the results of the Teflon material after the cell and material cooled down to ambient temperature.

Figure 69. Teflon Overcharge Material Results 2

The results of this test show that Teflon is a viable material for use as a cell separator and even thermal barrier as it did not burn during this overcharge event. This single cell test required little material to secure the cell during testing, but it is recommended by the researchers that a substantially thicker stock be used to ensure that the cell remains secure after the event. Thickness should also be carefully considered for structural integrity in normal operation and high impact scenarios.

TEFLON – NAIL PUNCTURE

As with all other nail puncture tests, a cell was fully charged and placed in a test stand made of the material under test. This cell then experienced a nail puncture and resulted in an internal short leading very quickly to a venting event. Figure 70 show the data recorded during this test.
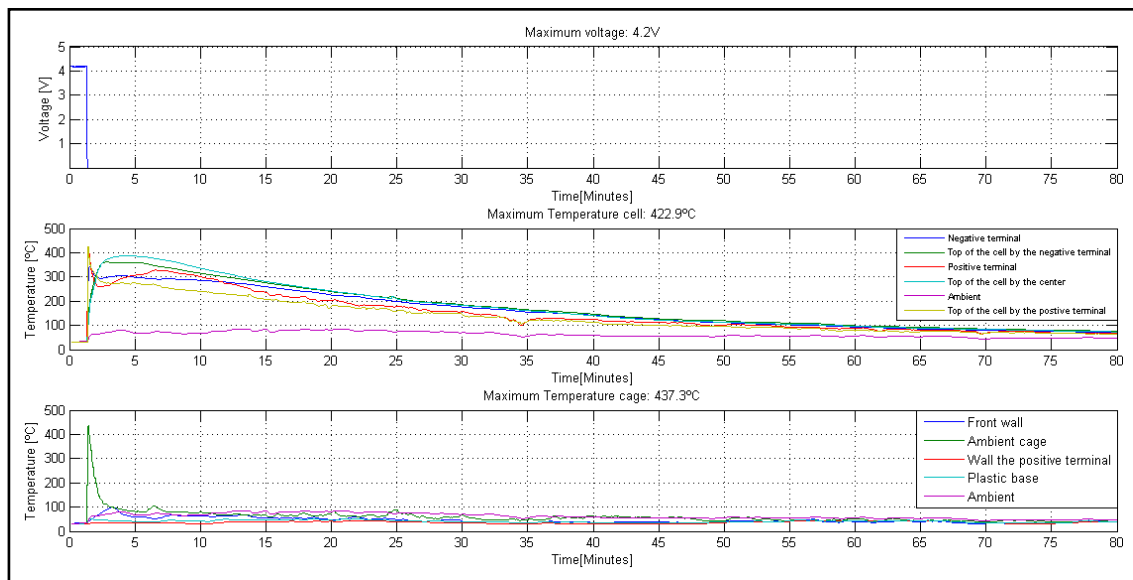
Figure 70. Teflon – Nail Puncture Data

The top chart shows that the cell was fully charged and resting at an open circuit voltage of 4.2 VDC. This voltage dropped to zero once the nail punctured the cell casing, internally shorting the cell. The middle chart shows cell surface temperatures with peaks of approximately 420ºC and a cool-down time of almost one hour. On the bottom chart material wall temperatures can be seen. This chart shows that except for a spike in the air temperature inside the cell enclosure, all measurements remain below 100ºC and mimic the cooling time of the cell.

Figure 71 shows the result of this nail puncture test. Note that the material is intact and shows little signs of damage, only a black coating of burned electrolyte.

Figure 71. Teflon – Nail Puncture Material Results

SINGLE CELL CONCLUSIONS

The researchers conclude that the best packaging material will depend on design scenarios and recommend Teflon for general applications. It is worth considering the Pyrophobic material for designs that require the absorption of energy and possibly using Teflon as a structural and barrier material and Pyrophobic to fill the gaps and absorb energy if necessary. In this case, definitely consider your thermal management, as there may be unintended reactions with the intumescent thermoplastic material. See Appendix C – Tables of Test Setup and Results for a summary of all test setups and results.

NAIL TIP TEMPERATURE MEASUREMENT

To further understand the temperatures experienced inside a large-format NCA cell during a nail puncture, a special nail was fabricated. This nail was much larger in diameter compared to the thin nail used on all other tests. This increase in diameter allowed space

for a thermal pile. Many temperature sensors were packed into the tip of this large nail, and a nail penetration test was performed to capture an internal cell temperature reading during such an event.

To this point, the only temperatures captured from the cell were actually from the casing, which differed from internal temperatures due to the exothermic reactions.

Voltage and case temperature of the cell were also recorded in addition to values recorded by six temperature sensors in the nail with one of them located at the very tip.

Figure 72. Nail Tip Temperature Measurement Test Setup

Figure 72 shows the test setup. Notice that the nail and the cell were lined up symmetrically to get the best approximation of electrolyte temperature.
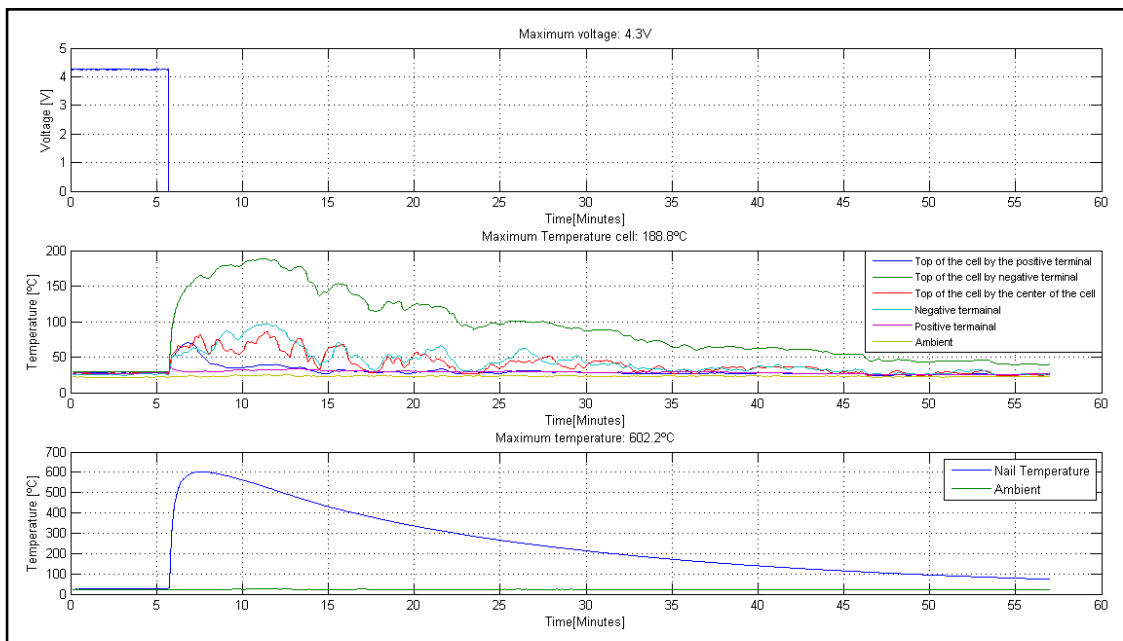
Figure 73. Nail Tip Temperature Measurement Test Data

Figure 73 presents data gathered during this test. As has been mentioned before, six temperature sensors were in the nail. It turns out that all of them captured the same value, so to simplify the graph, just one signal is shown.

The top chart shows voltage recorded during this test. It also indicates when the event started, by displaying a sharp decrease in voltage. The second chart shows cell casing temperature; note that the readings are relatively low compared to other similar tests. The highest temperature reached roughly 200ºC, while the others did not exceed 100ºC. One reason for this may be that the cell had reached very low ambient temperatures beforehand.

The bottom graph showing nail tip temperature demonstrates that the temperature inside the cell was very high in comparison to values captured on the housing, meaning that the majority of heat was released by the evacuation of electrolyte and other solid material through the hole made by the nail.

Figure 74. Cell and Surroundings After Test

This larger diameter instrumented nail caused a more dramatic event relative to the smaller nails used in previous testing. This result indicated that the severity of the puncture and short would change the severity of the venting event. Note that in this test the steel end-cap of the positive terminal broke off and was projected several feet as seen in the Figure 74. The left image shows the internal construction of the cell. Visible are the long strips of foil rolled into a cylindrical jellyroll shape that comprise the different layers of the cell. The same picture also shows how the nail tip broke off in the cell as the air press lifted up. The image on the right demonstrates how savage the event was because the smoke and flames marked the ground.

This concludes single-cell testing.

VI. MODULE-LEVEL TESTING

This section details the design of the 20 cell modules and enclosures used in the test-to-failure scenarios. These high-voltage packs were designed with 10/20 batteries connected in series to produce a 36/72 V nominal pack, 42/84 V fully charged. In the design of a module, the component that held each end of the cell, called the header, was the most critical component in the battery pack because of its structural and isolation requirements. In addition, the headers had to allow series connections between battery terminals. These components are necessary and must meet the high temperature demand set by the exhausting gases if the pack is to remain intact or avoid complete vehicle fire.

SOLIDWORKS, a 3D CAD software package, was used to make mechanical designs and to test feasibility. Later Finite Element Analysis (FEA) and Computational Fluid Dynamics (CFD) analysis were performed on these systems.
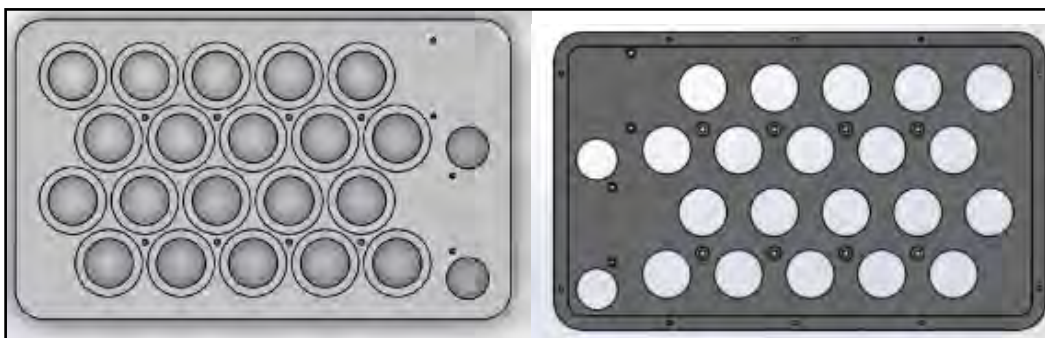
Figure 75. Headers Designed for Module Testing

Figure 75 shows a top and bottom view of the headers. Note that on the side of the second header, 1-inch holes were drilled through the header to pass main positive and main negative cables and to allow for small-gauge cell voltage measurement wires. Finally, to secure down the cover, a set of #6-32 threads were made on the outside lip of the header.

Figure 76 shows the assembled covers, headers and batteries. Two configurations of this module were built, one with and one without cell separators.
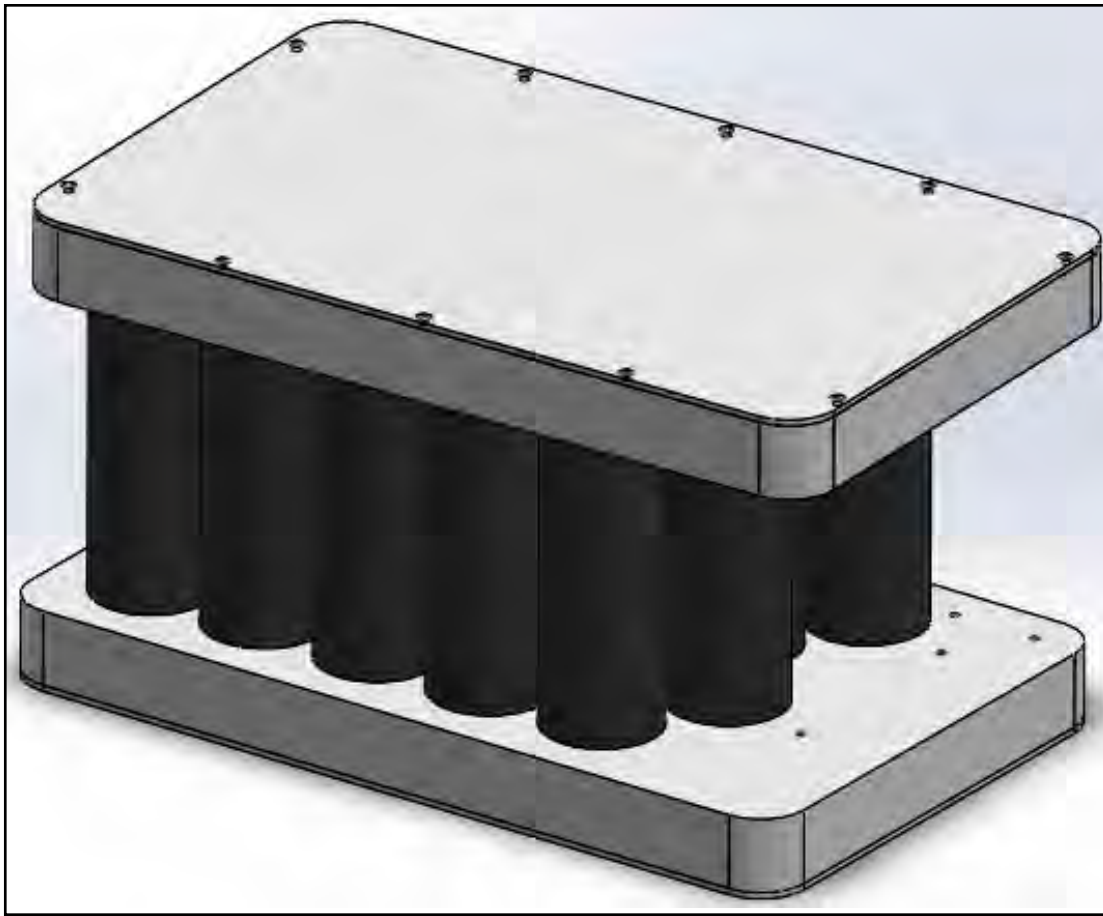
Figure 76. CAD of the Assembled Battery Pack

MANIFOLD DESIGN

The manifold configuration was intended for evaluating the feasibility of evacuating and distributing heat to prevent thermal runaway propagation between cells during a cell vent. To maximize and control the flow of electrolyte bursting out of the cells, four large openings were integrated. These openings, located at each terminal end of the cells, would allow for easy, low-resistance flow of the hot gases.
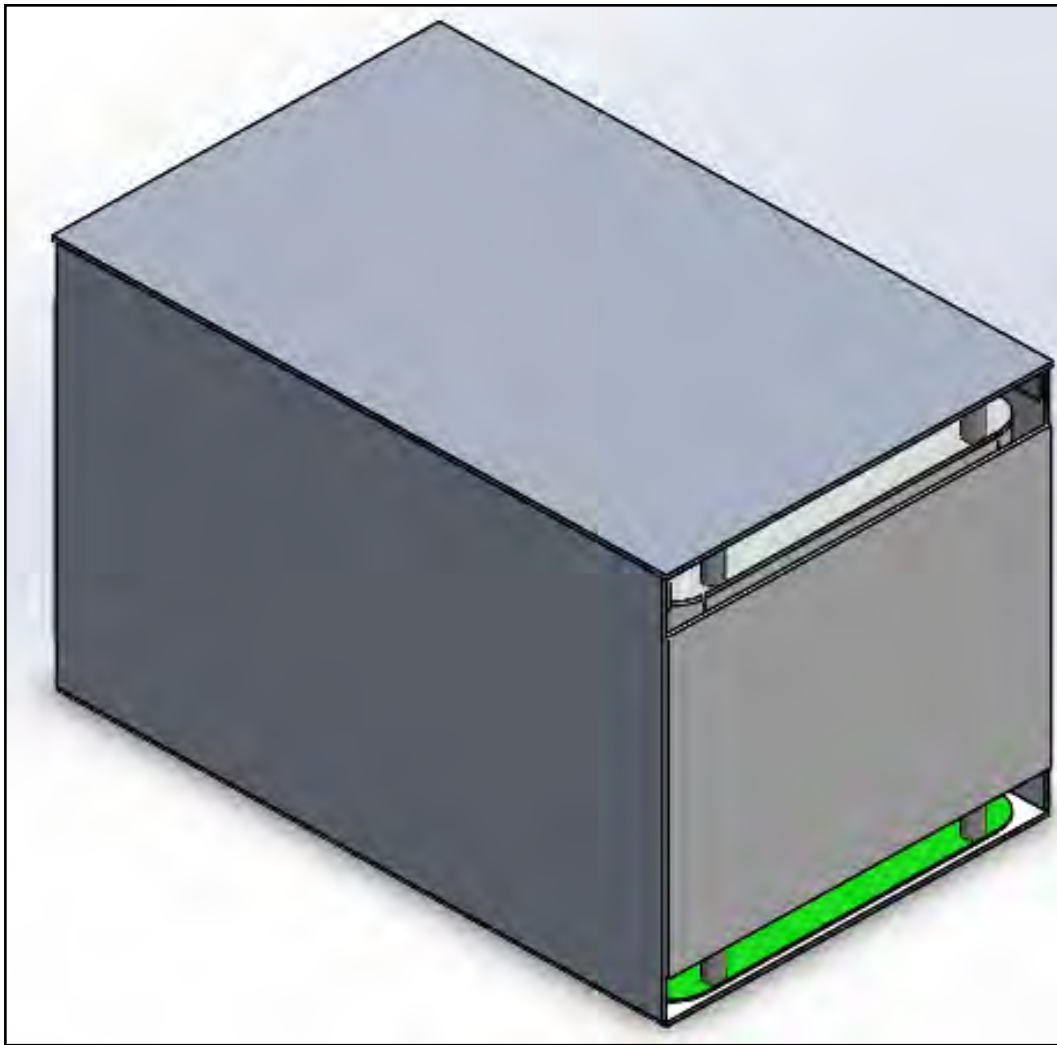
Figure 77. CAD of the Manifold Design

Figure 77 shows the manifold module design. To dissipate heat and direct hot gases, steel plates were mounted on the top and bottom of this module enclosure. The melting point of the steel is 1510°C or roughly twice the aluminum's, so the steel was utilized to handle all the direct blast of the hot gases. Standoffs between the cover and steel plate created a gap to let the gases easily flow out of the module.
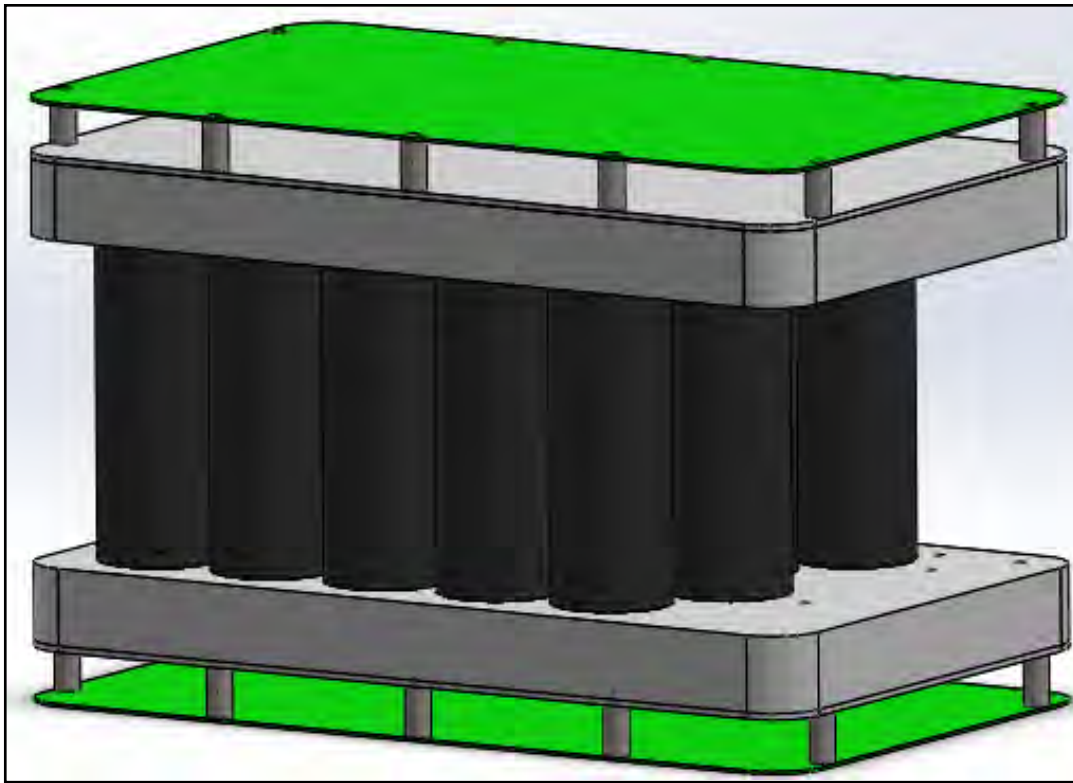
Figure 78. CAD of the Inside Manifold Design

Figure 78 shows the standoff and plate configuration inside the module enclosure.
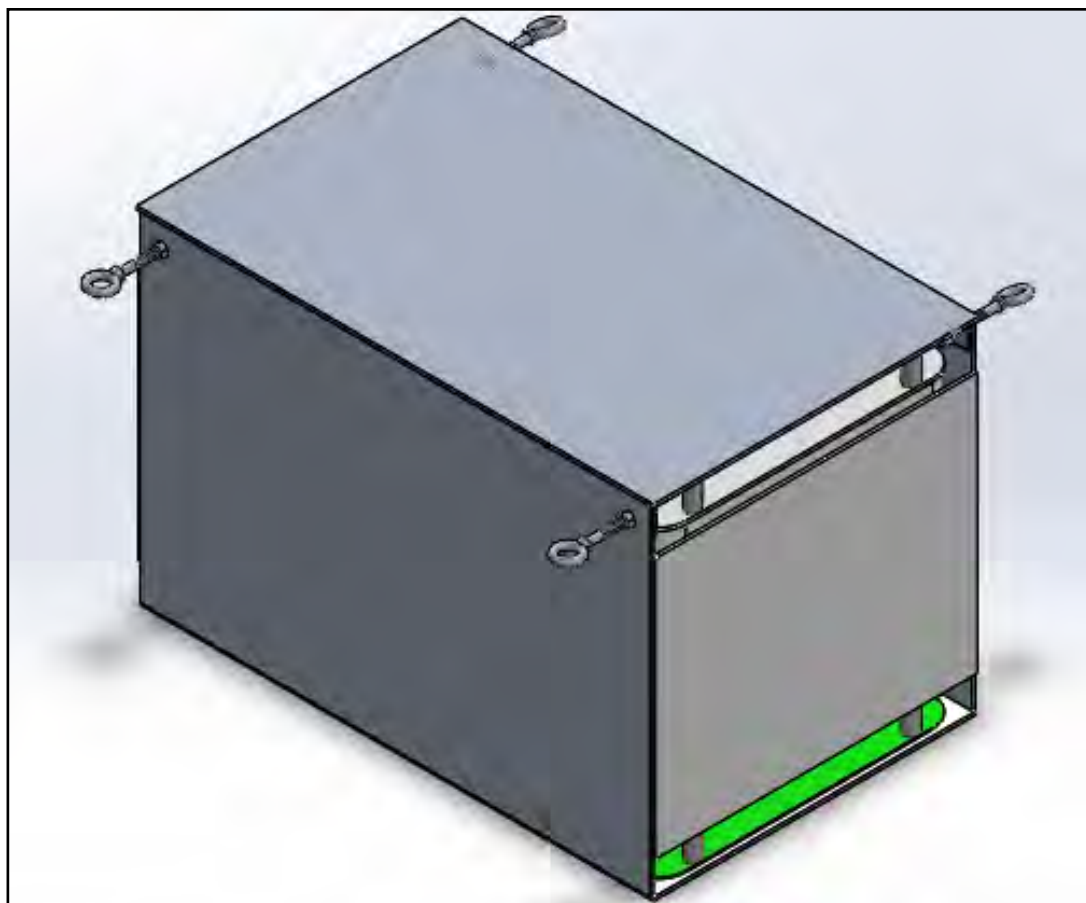
Figure 79. CAD of the Manifold Design with Eye Bolts

Figure 79 shows the complete assembly with eyebolts. These were used as anchors to stabilize the pack during testing.

CELL SEPARATOR DESIGN

The cell separator configuration was intended to study/prevent thermal propagation between cells. The idea was to create a separate environment for each battery in order to keep the heat and venting gases from the cell in their own isolated area to limit the heat transfer to adjacent cells. The separator configuration used only 10 cells to allow the necessary room for the separating materials. No mechanical resources were used to secure down the separator material; it was simply sandwiched between the two headers and secured via the threaded rods connecting the two headers together.
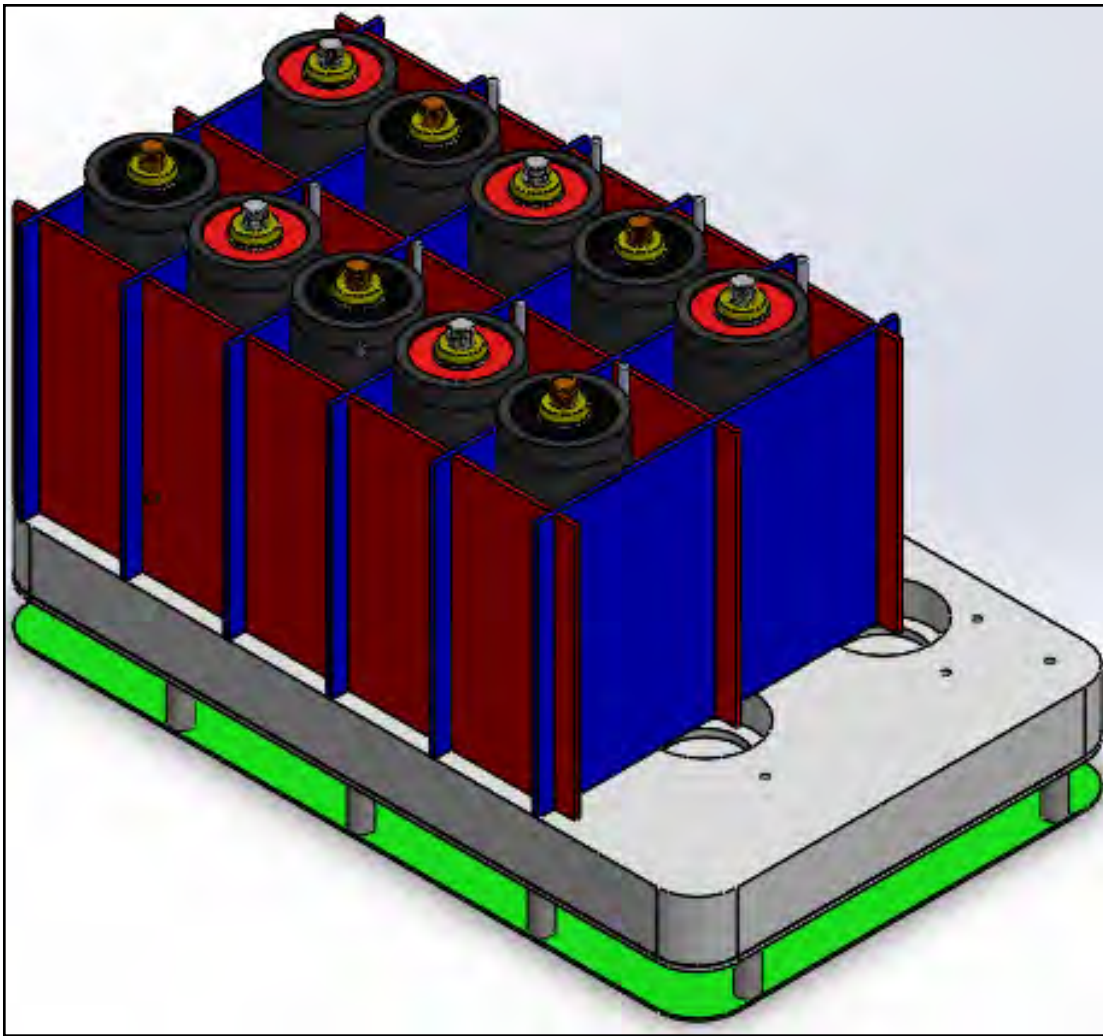
Figure 80. CAD of Separator Design without Top

Figure 80 shows the CAD of the separator design.

PRESSURE RELEASE / CHECK VALVE

When one or more cells start venting in a completely closed battery pack, the copious amount of gas released builds up pressure that could lead to an explosive scenario. To release pressure from the enclosure, this research team chooses to incorporate a check valve. The check valve is designed to open once a predetermined pressure is reached. A Matlab Simulink Module was created to simulate the increment of pressure as well as the check valve performance and to determine the proper check valve.

The pressure inside the module is based on the volume of free space inside the module and the volume of gases emitted during the venting of at least one cell. For these calculations, it is assumed that the internal exothermic reactions boil 100% of the electrolyte. Ideal gas laws are assumed. From the Material Safety Data Sheet (MSDS), the mass of electrolyte per cell is known. Through the gas analysis previously presented the gas composition and percentages per volume are known. It is assumed that immediately after a cell vented, all

the moles inside a cell were released as gas into the free space inside a module. A trigger structure therefore had to be created in order to simulate the venting process. It is assumed that the cell starts to vent at a tenth of a second. According to the experience gained through the previous tests it was known that venting durations last for about 5 seconds.

Simultaneously, moles of air are being added to the moles of the cell to get the total moles inside the enclosure. This value is then divided by the seconds that the cell is venting to get the rate of moles/s. Later, the rate of moles/s is multiplied by the output of the switch that will be either one if the clock is between a tenth and five seconds (because the cell is venting) or zero when the clock is out of this range. However, the moles that are being released by the check valve have to be subtracted to know the remaining moles in the enclosure that build up pressure. To simulate this increment of moles along the venting time, an integrator block is used. After the switch, the "moles_in_the_enclosure" variable is set as an output and graphed, as is the trigger through the scope block. Figure 81 shows the trigger and its blocks.
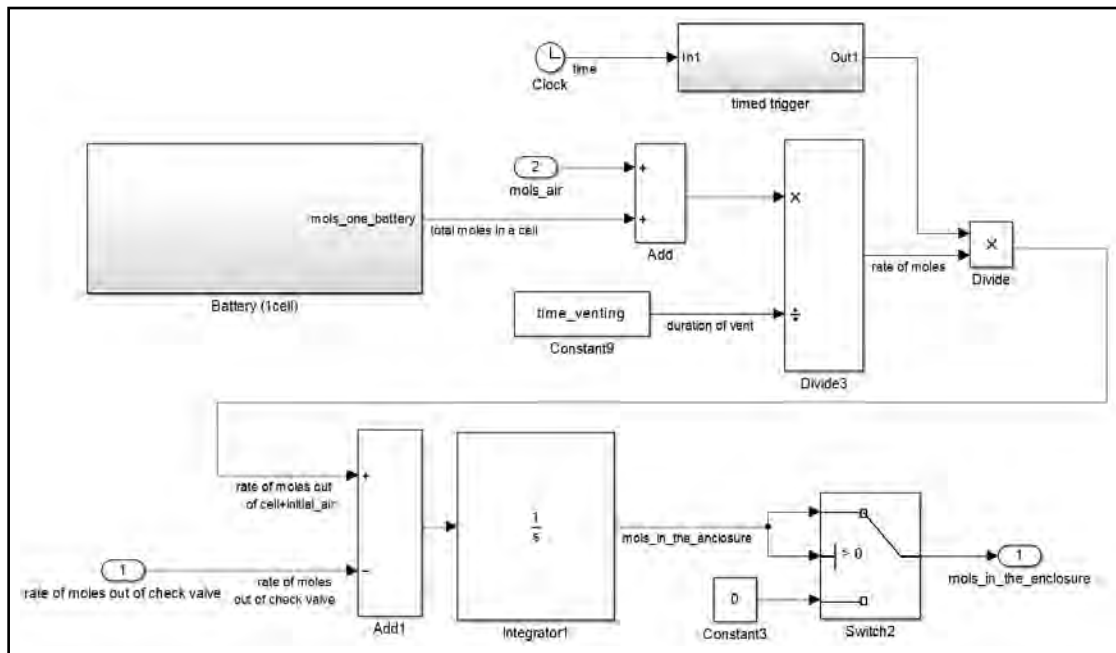
Figure 81. Trigger

Then the variable moles_in_the_enclosure acts as an input to the next subsystem responsible for calculating the pressure generated for these moles using the equation of ideal gases.

The ideal gas law is used which states:

PV=NRT

Where:

P: Pressure (atmospheres or atm)
V: Volume (liters)
N: Number of moles (constant, no unit)
R: Gas constant (0.08205736 L·atm·mole−1·K−1)
T: Temperature (Kelvin or K)
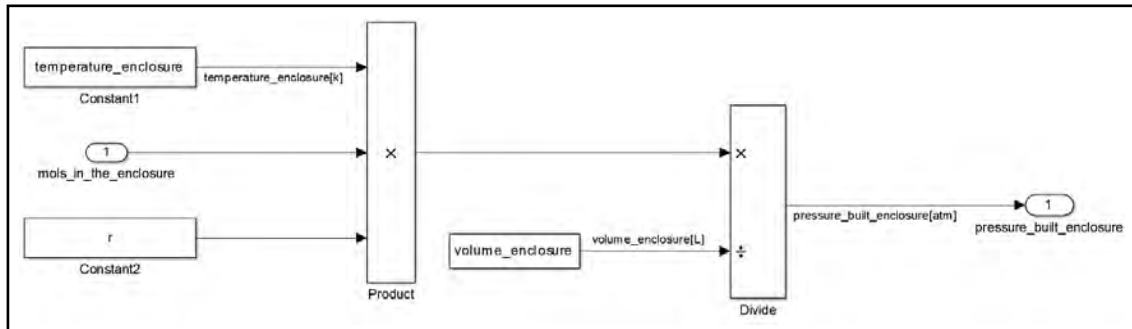
Figure 82. Enclosure Pressure Subsystem

Figure 82 shows the pressure calculation. Based on previous tests, the temperature inside the enclosure is assumed to be 650ºC. To get the volume, the volumes of the plastic parts and cell have to be subtracted from the total volume of the enclosure. Then the ideal gas law is applied to calculate the pressure that is used later as an input to simulate the check valve operation. Figure 83 shows the subsystem accountable for replicating the check valve operation and quantifying the flow rate.
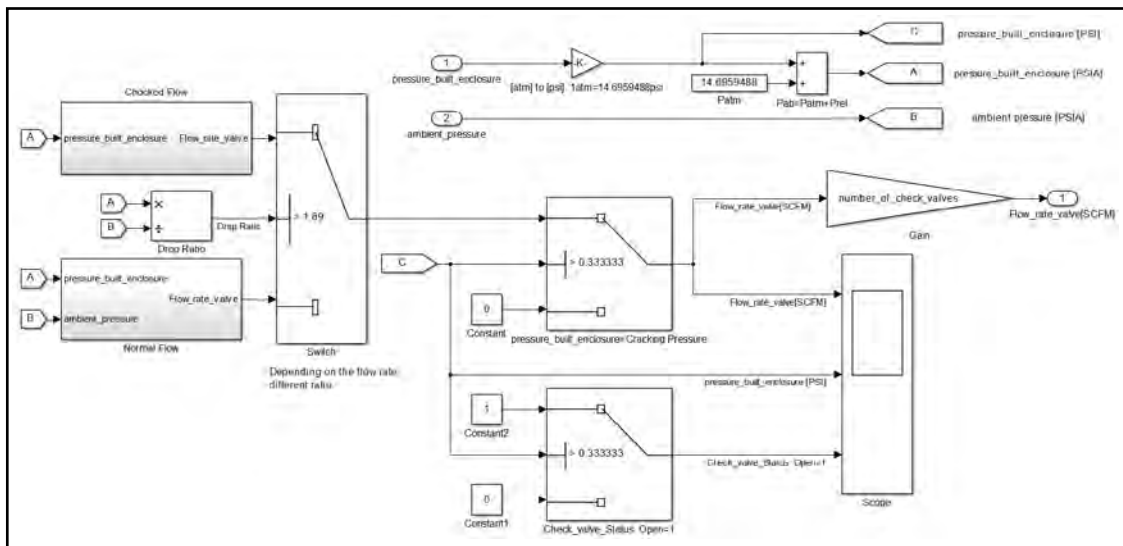
Figure 83. Check Valve Subsystem

The check valve flow rate changes depending on whether it is under normal flow or choked flow, which is governed by a certain value of the pressure drop ratio. Figure 84, obtained from Forberg web site,[17] shows equations to calculate each flow rate and the flow coefficient (Cv) of each case.

Normal Flow's Critical Pressure Drop Ratio: (Flow rate less than theoretical limit)	$$\frac{P_1}{P_2} < 1.89$$
Flow Rate (SCFM) (Normal Flow)	$$Q = 16.05 \times C_v \sqrt{\frac{(P_1{}^2 - P_2{}^2)}{T(°R) \times S_g}}$$
Flow Coefficient (Normal Flow)	$$C_v = Q \times (0.0623) \sqrt{\frac{T(°R) \times S_g}{(P_1{}^2 - P_2{}^2)}}$$
Choked Flow's Critical Pressure Drop Ratio: (Flow rate at theoretical limit)	$$\frac{P_1}{P_2} > 1.89$$
Flow Rate (SCFM) (Choked Flow)	$$Q = 13.63 \times C_v \times P_1 \sqrt{\frac{1}{T(°R) \times S_g}}$$
Flow Coefficient (Choked Flow)	$$C_v = \frac{Q \times (0.0734)}{P_1} \sqrt{T(°R) \times S_g}$$

Figure 84. Flow Rate Equations

Note: P_1 and P_2 are in units of PSIA.

Where:

P: Absolute pressure (Absolute Pounds per Square Inch or PSIA)
T: Temperature (degrees K)
Sg: Specific gravity (unit-less)
Cv: Flow coefficient

The specific values of the gases are tabulated, and since the substances that composed the gas as well as their percentage are known, the specific gravity can be calculated.

Given the pressure of the enclosure and the ambient pressure, the equations are implemented such that the output provides flow rate. A switch is then imposed to determine if the flow was normal or choked. If the pressure ratio was less than 1.89 the flow was normal; otherwise it was choked.

Another switch checked if the pressure in the enclosure was higher than the cracking pressure of the check valve. The cracking pressure is defined by the manufacturer and specifies the pressure at which the check valve is going to open. In this application, a very low cracking pressure was sought in order to start releasing the pressure as soon as possible. This value was then sent through a gain representing the number of check valves. This was used to model multiple check valves.

Finally, the output of this subsystem was the flow rate of the valve, which was fed back to the trigger subsystem. The simulation was run with a valve flow coefficient of 3.53. There are valves available with a higher Cv, but they are expensive. The results are shown below.
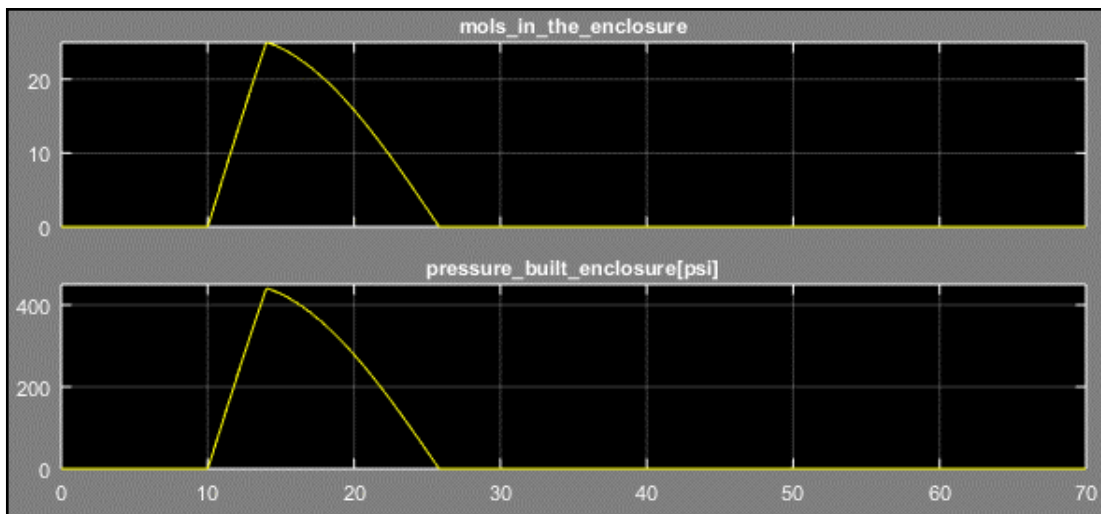
Figure 85. Simulation Results

Figure 85 shows simulation results. Note that the x-axis in both charts is time in units of seconds. The top chart shows the total number of moles released by the cell and the bottom the pressure of the enclosure in units of psi.

At first sight, it is clear that the peaks of both signals occur at the same time. Analyzing the value of pressure, it turns out that it is surprisingly high. According to these results, the box won't be able to withstand this much pressure and will end up exploding. To solve this problem, more check valves should be mounted or the use of check valves with higher flow rate should to be considered, or both. The check valves necessary may need to be very large in diameter to achieve the required flow rate.

This was just a simulation, and these results had to be verified. For this reason, the actual test was run to get real values and validate or disprove our assumptions and model.

SECURING THE MODULE

Due to the sheer amount of energy released by the whole module, it is unsafe to leave it unsecured during a destructive test. Prior single-cell testing proved to the research team that tie-downs to the ground were necessary to ensure the pack did not take off once cell venting occurred. Figure 86 shows the tie-down configuration.

Figure 86. Handle to Lift the Battery Pack up with the Forklift

The remainder of this section describes in detail the tests conducted at the module level and displays the data that was collected during each test.

SINGLE CELL OVERCHARGE IN A MODULE WITH ACETAL HEADERS

This was the first of three module-level tests performed. The test served as practice for the coming full-module tests and as a way to obtain information about the thermal response of the headers, the thermal runaway propagation between cells, and the performance of the pack design.

The test consisted of overcharging a single cell at 20 A with four bad cells on the corners of the acetal headers. The enclosure used was the manifold design, an aluminum enclosure with a 1/16" steel sheet mounted on the top and bottom. Openings on the side were included to release smoke and heat produced during venting.

Voltage, current and temperatures were gathered over a CAN communication network. The temperature sensors were distributed among the cells, headers, and covers. Below are their locations:

- Center of cell that is being overcharged

- Enclosure ambient

- Back right center of cell closest to overcharged cell

- Top right center of cell closest to overcharged cell

- Top right center of cell farthest away from overcharged cell

- Bottom right center of cell farthest away from overcharged cell

- Back left center of cell closest to overcharged cell

- Back left center of cell farthest away from overcharged cell

- Top left center of cell farthest away from overcharged cell

- Top left center of cell closest to overcharged cell

- Bottom header front

- Bottom header right

- Bottom header back

- Bottom header left

- Ambient

- Top cover center

- Top cover right

- Top cover back

- Top cover left

Unfortunately, the sensor on the top left center of the cell closest to the overcharged cell got damaged and the data was irrecoverable, so this sensor was not graphed.

To analyze the entire test and not miss any detail, the data will be presented progressively, starting with the information related to the cell that was being overcharged. The next figure shows the current, voltage, and temperature. The test plan for this event was to charge at a constant 20 A until the cell vented.

Figure 87 shows that the voltage increased following the same trend as the previous tests. According to the data graph, however, the cell went off at 9.2 V. This is technically impossible, so it means that something was wrong with the voltage sensor. Proof of that is the increase of voltage right after the cell vented, which is technically impossible since if the cell has vented once it is not going to vent again.

In reference to the temperature, the data show that the temperature increased as the cell was being overcharged; it hit the thermal runaway and then vented. As usual the cell temperature went up to about 700ºC. It then cooled down to 200ºC and then ramped back up due to the burning acetal headers.
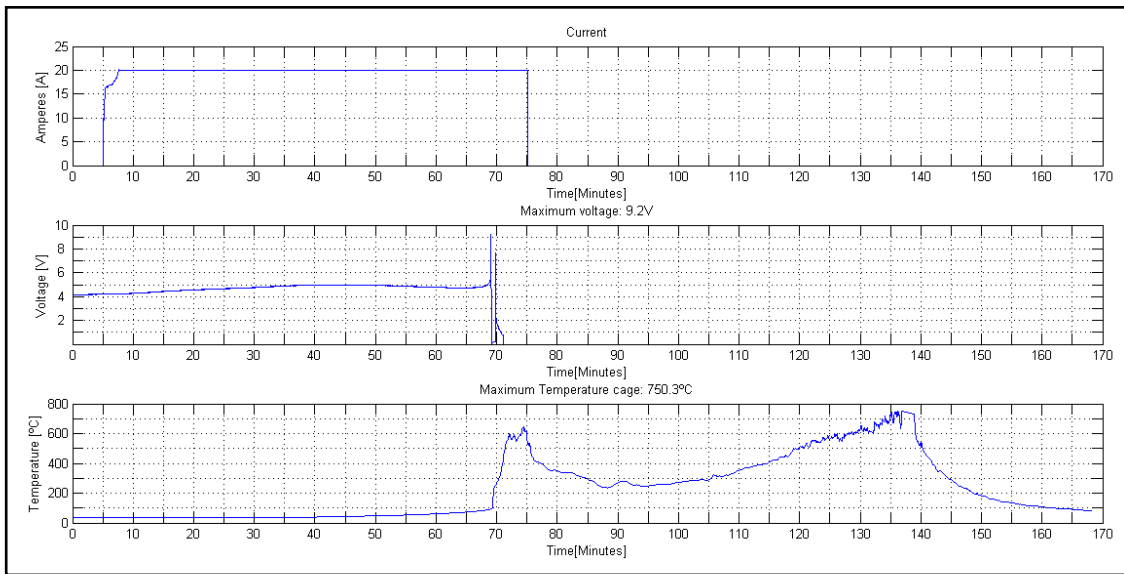
Figure 87. Data – Cell Overcharge

Some completely discharged cells (dummy cells) were used to mechanically complete the module and allow for proper alignment of the test cell relative to the module components. Each dummy cell had a couple of temperature sensors attached to indicate if the venting of the overcharged cell resulted in thermal propagation as well as to indicate differences of temperatures between the sensors farthest and closest from the overcharged cell. Instead of graphing all the sensors in the same graph, the cells will be treated individually. Each graph in Figure 88 represents the data of one dummy cell: the temperature sensors attached to it, the temperature of the overcharged cell, and the temperature of the ambient cage. The second graph just contains three signals because many sensors were damaged.
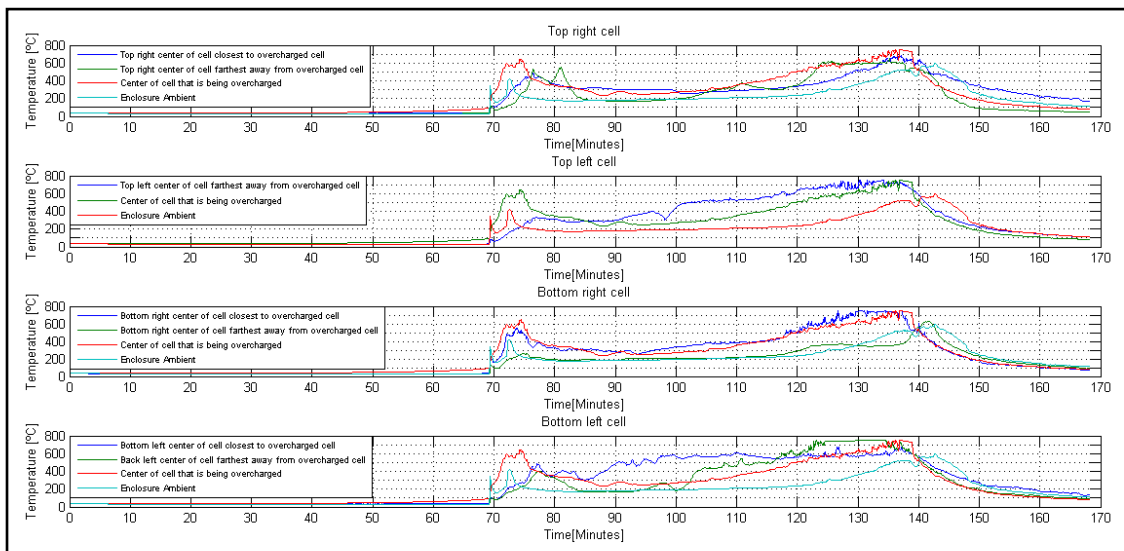
Figure 88. Data Dummy Cells

Each cell held two temperature sensors. The sensor closest to and/or in direct view of the overcharged cell was always the first to increase. Shortly after the venting event, both sensors of the same cell read very similar values. Eventually all four dummy cells also vented due to the excessive heat inside the enclosure.
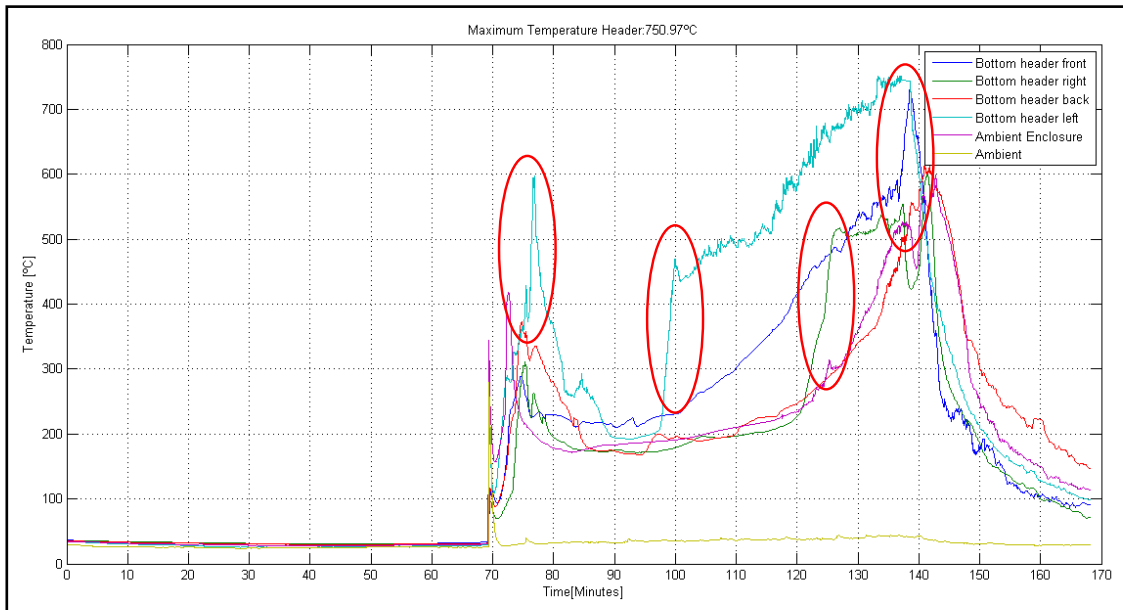
Figure 89. Bottom Header Temperatures

Figure 89 shows the bottom header temperature sensor readings. Analyzing the graph, it appears each sensor suddenly increased in temperature multiple times. This likely indicates when each dummy cell vented. It would therefore be convenient to treat each sensor individually; sensor data is shown in Figure 90.
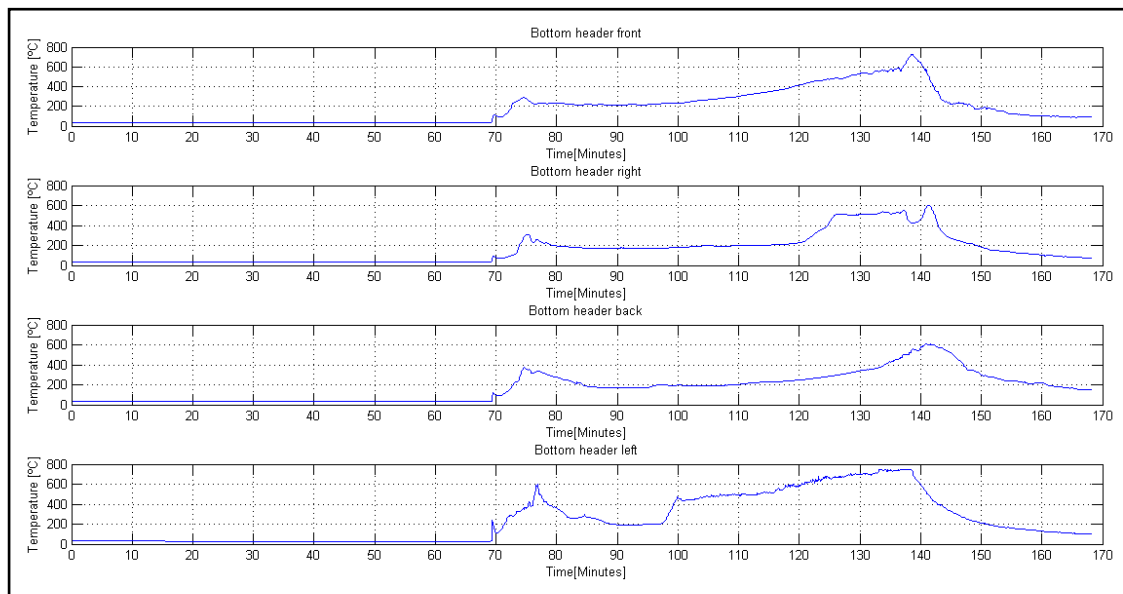
Figure 90. Bottom Header Temperatures (Treated Individually)

All the sensors recorded when the overcharged cell vented with a sudden increase of temperatures. Following the venting event one sensor cooled, then rapidly increased its reading, whereas the other sensors only continued to increase their temperature gradually. Then, about 2 hours and 20 minutes into the experiment, all sensors experienced another increase in temperature, probably due to another cell venting or internal fire. Also, probably because of proximity to the venting gases, the "bottom header left" sensor/cell shows a relatively higher peak temperature value during the initial thermal event. This could be a sign that the flow of hot gases/electrolyte was initially directed toward this sensor because of the unique and somewhat unpredictable failure of the cell casing due to this overcharge event.

To try to match the sudden increase of temperature with the cells venting, the next figure has four graphs that contain the data of each sensor of the header as well as the data of the two closest cells. The data of the cell always correspond to the closest sensor to the overcharged cell.
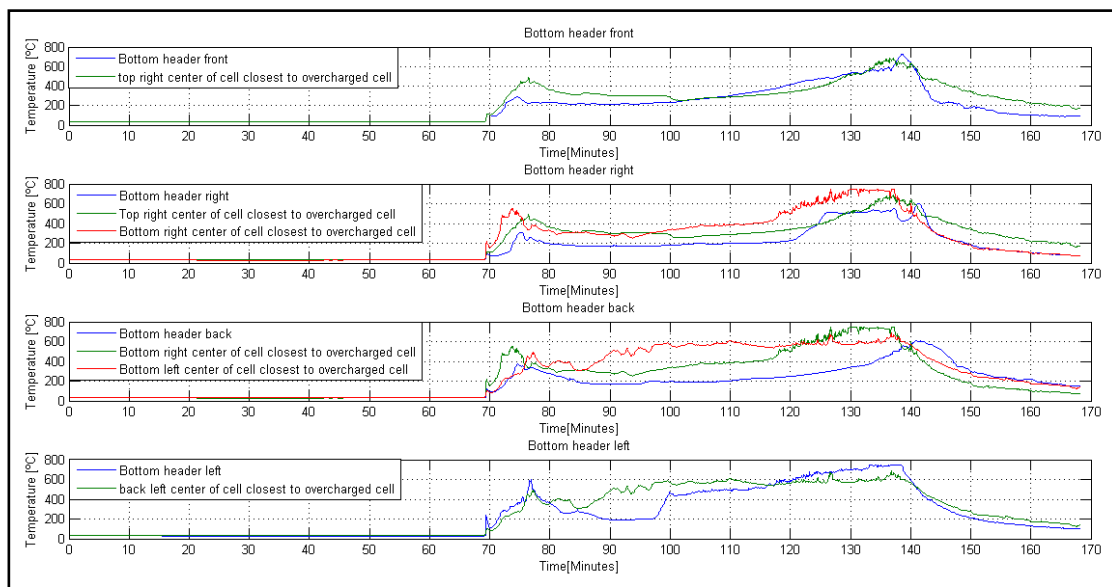
Figure 91. Bottom Header and the Closest Cell Temperatures

The data in Figure 91 does not clearly indicate when individual cells would have vented. Again, the highest temperatures were captured by the end of the test because of the plastic of the headers burning.

The cover is the final part left to analyze. The overcharged cell caused a rise in all the temperature sensors to around 300-400ºC.The majority of them kept going progressively up to around 700ºC, then shortly after started a cooling process. Nevertheless, the sensors on the back, center and right presented different responses. The first two sensors mentioned experienced a brutal increase of temperature right after the cell went off and then joined the other sensors. On the other hand, the one on the right always had lower values, although higher than the melting point of acetal (168ºC).
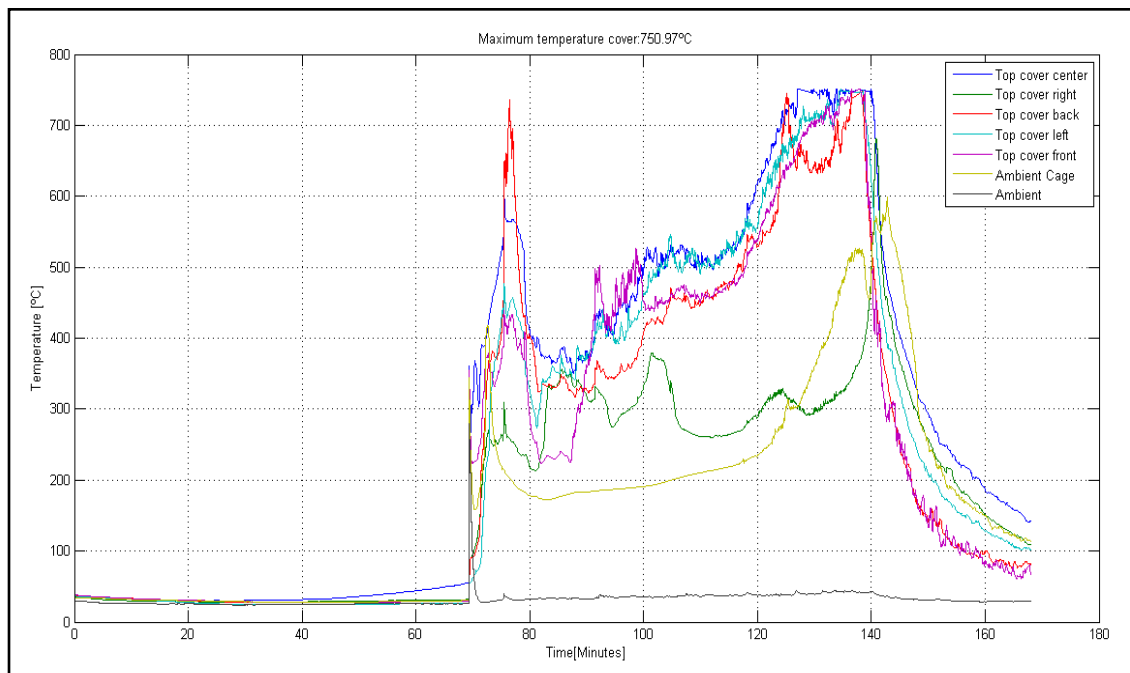
Figure 92. Cover Temperatures

Note that, based on the test data and notes from this test, it is clear that the "top cover right" sensor fell off during the test as it was much closer to ambient measurements than the temperature of the venting gases. Once everything cooled down to ambient temperature, the cleanup procedures started. The first surprise was that the front and back sides of the enclosure's Aluminum were melted as well as the sides as shown in Figure 93. The heat of the plastic headers burning likely caused it. On the other hand, the top and bottom steel plates successfully handled the direct impact and heat exposure of the cells venting gases.

Figure 93. Enclosure After the Test

All cells were investigated and confirmed to have vented given that all burst discs were opened. Inside the enclosure only metal parts remained. No plastic part remained. No clear sign was left that the box had ever contained any plastic.

OVERCHARGE OF 20 CELLS IN STEEL ENCLOSURE

In this test, the 20 cells were connected in series to obtain a high-voltage battery pack with a nominal voltage of 72 V. Our intention was to overcharge a single cell to avoid a really intense event where multiple cells would begin venting simultaneously. This scenario would be more consistent with a BMS charging failure of a single cell due to a flawed voltage reading. It would also show the effect of thermal propagation from one failed cell to the other cells at normal state of charge. The method chosen was to start charging at 20 A with all cells below 3.5 V except the one intended to vent, which was fully charged at the nominal cell voltage of 3.6 V. In this way, only one cell was actually being overcharged.

The manifold design enclosure was used, the design with the openings on the side. Adopting lessons learned from the previous single cell overcharge in a module, however, the aluminum enclosure was replaced with one entirely made out of steel.

The headers used were made out of acetal although it was already known that they would burn up eventually, so their function was only to hold the batteries initially.

With the amount of energy in the pack and the experience of the previous test, the event was expected to be very intense. Test setup had to provide maximum safety for the

researchers as well as avoid any potential hazard. The first step taken was to move the observation and instrumentation trailer 250 feet away from the concrete test pad. The trailer contained the chargers as well as the laptop that logged data. Data and power lines were extended to reach the new trailer location.

In addition, the concrete pad was surrounded by three Jersey barriers to block any flying debris, although one side facing an open field was left open for access during setup and cleanup. The pack was tied down using the cable system explained in the section Module-Level Testing.

The cell voltages, temperatures and current were recorded through CAN. Two slave modules and a BMS were needed to capture the voltages. Starting at the main negative, the terminals of each battery were connected to the slaves. One slave measures 10 cell voltages. Slaves are connected in an RS485 daisy chain to each other and to the BMS main board, which provides all the cell voltages and pack voltage to the CAN network.

Several thermo-scanners were deployed, each supporting up to 40 temperature sensors so that temperature distributions throughout the pack could be measured. All the sensors on the first thermo-scanner were attached to a surface of a cell starting from the most negative cell to the most positive. Sensors of the second thermo-scanner were distributed throughout the pack and enclosure as follows:

- Bottom header left

- Bottom header back

- Bottom header right

- Bottom header front

- Top cover left

- Top cover back

- Top cover right

- Top cover front

- Top of cover on center

- Top of steel enclosure

- Front of steel enclosure

- Left of steel enclosure

- Ambient inside pack

- Ambient

Figure 94 shows the battery pack at the start of testing, secured down and with all the data being logged prior to initiation of charge current. The current sensor was placed at the output of the charger in the instrumentation trailer on the power cables running out to the pack on the test pad.
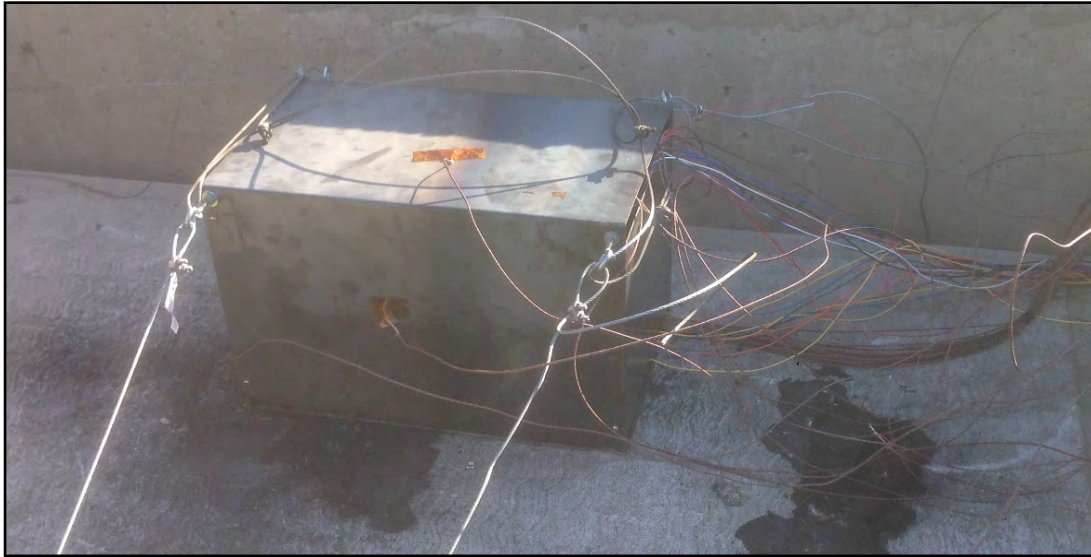
Figure 94.   Battery Pack prior to Testing

Figure 95 summarizes the data of a successful test.
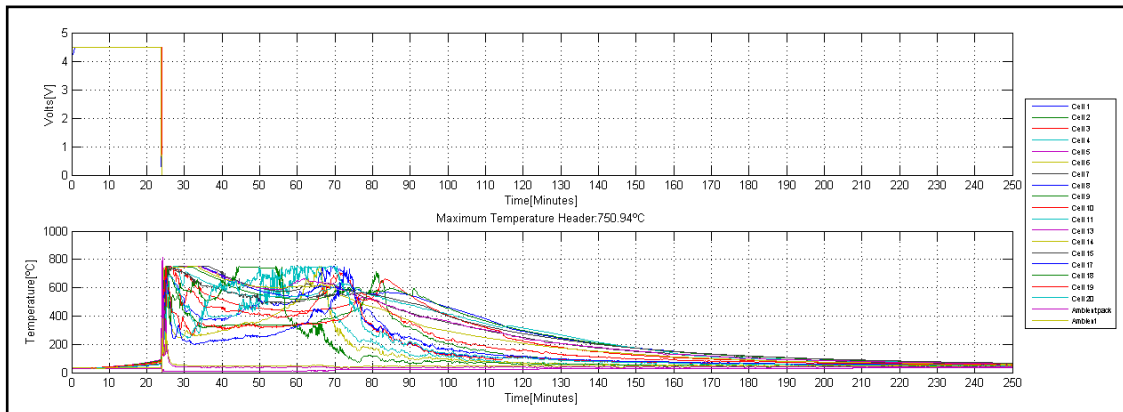
Figure 95.   Overcharge_20_cells_steel_enclosure – Data

Figure 95 shows the voltages and the temperatures of the cells. The voltage was used to make sure that temperatures climbed as soon as the voltages dropped. Neither graph can support determining which cell was the first to go off or the exact moment in which each cell vented.

Taking a look at the temperatures graph, the first surprising information is that the temperature was between 200ºC and 700º for almost one hour and then started cooling down over another hour.

Nonetheless, the sensor measuring pack internal temperature reached 300ºC just as the first cell vented; following this event it cooled down to ambient temperatures. This behavior is very odd, as the venting cells were releasing a lot of heat. Hence the intensity of the event: the smoke or flames most likely kicked the sensor out of the pack, and the sensor then started reading internal pack temperatures.

At the same time, the heat was also affecting the plastic parts of the battery pack. Figure 96 presents the data of the sensors spread on the bottom header. Of course, each plastic part of the pack caught fire and burned until it was gone.

Analyzing the data available, one sees that at first a couple of sensors went up to 1200ºC. That must be a consequence of multiple cells going off at the same exact moment. The other cells went up to more familiar values between 600ºC and 800ºC. After those peaks, the sensors registered very different values, and none of them followed the same trend. Some of them took more time to cool down, while some of them took less.
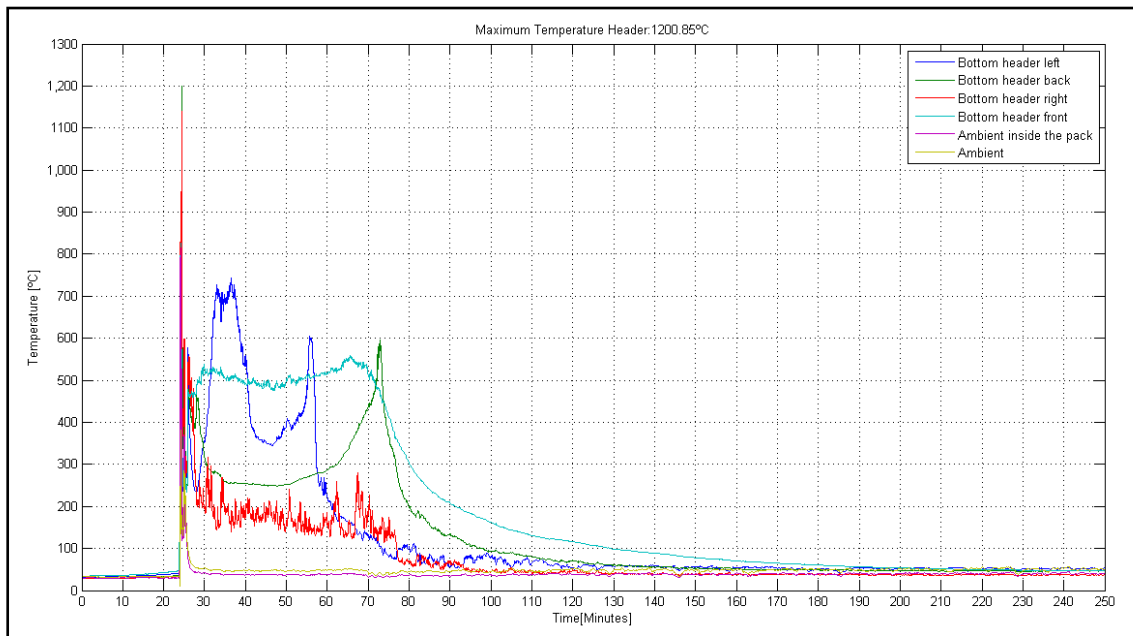
Figure 96. Bottom Header Temperatures

The covers, (see Figure 97 below) also reached 1200ºC, although the location did not match with the one on the header. The extreme heat damaged the sensor on the right and the one in the center. Of course, the covers also burned down.
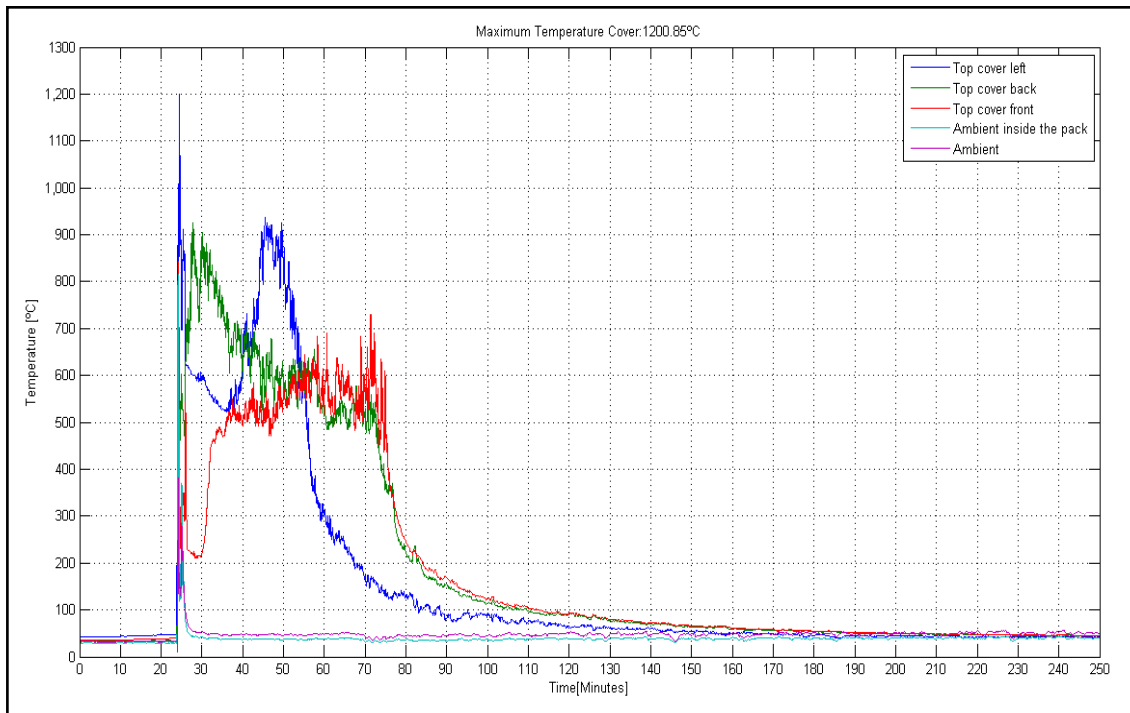
Figure 97. Cover Temperatures

Accordingly, as the next image shows, the metal parts for the enclosure, instead of getting to as high a temperature as the cover and headers, reached around 1000ºC. Remember that the enclosure was made out of steel, and its melting point was higher than the temperature captured by the sensors. Therefore, the enclosure should not present any signs of melting or any holes caused by the flames of the cell. Notice also that it cooled down so quickly because it was the outside layer of the pack, the one that received less heat and was in contact directly with the ambient temperature.
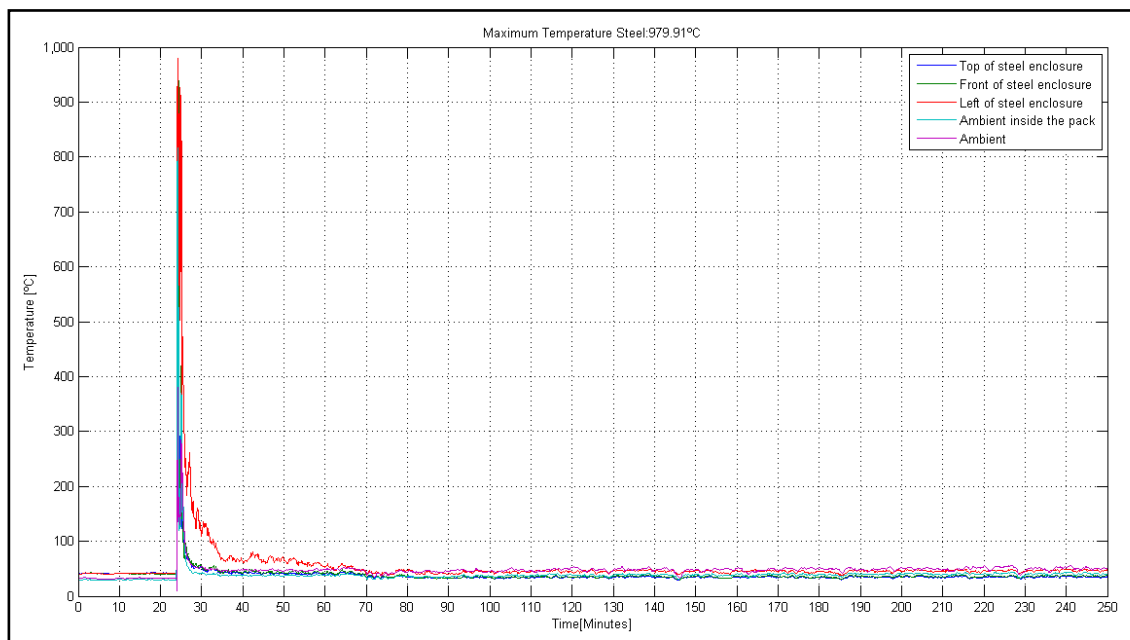
Figure 98. Steel Temperatures

After a reasonable time to let everything cool down, the pack was analyzed. The metal enclosure passed the test very successfully as it did not get melted anywhere. The only noticeable sign that it had been exposed to high temperatures was that each side bent a little and the steel got a different tonality.

Again, as expected according to the previous tests, the plastic parts did not make it and burned up.

All the cells, moreover, had their vents opened, meaning that all of them vented. Their voltages were analyzed and were null.

Figure 99 is a screen shot of video recorded during the event. The picture demonstrates the brutality of the flames coming out of the openings of the pack. It would not be unreasonable to think that some batteries vented at the same time due to the effect of the thermal runaway propagation.

Figure 99. Battery Pack Venting

The thermal propagation was also palpable, however, because multiple times, right after one cell had finish venting, another one started venting right away. The event is shown and explained through the next sequence of images in Figure 100.

Figure 100. Sequence of the Venting Process

On the top left of each picture is the exact second the image was taken counting from the first cell that vented. As has been mentioned before, the thermal propagation appeared several times and actually happened before the 30th second, but the shots were not as clear as these ones.

The first picture of the sequence shows the venting of at least one cell. It also shows how flames exit the openings. Venting occurred in the second picture as well; flames kept coming out because plastic parts were still burning, and cells were not venting at this point. The fire and high temperature forced another cell to vent as is shown in the last picture of the sequence.

The venting of the 20 cells lasted about one-and-half minutes, after which the pack kept burning for six more minutes.

Though it is not appreciable from the images, a huge dark cloud of smoke was generated. It was assumed to be very toxic, highlighting the importance of treating the smoke as a potential hazard as well as the necessity of evacuating it rapidly to keep it away from human beings.

The steel enclosure did a great job; it could handle those extreme temperatures without any problems. It did not melt and could be even reused for another test. Figure 101 shows the resulting steel module enclosure.

Figure 101. Resulting Steel Module Enclosure

Our approach was to test a one-cell overcharge in a module (with no other active cells and current passing through only one cell), then a full module overcharge (with current through all 20 cells at a relatively close state of charge). These tests are presented above. The research team overcharged a single cell in a module and 20 cells in a module. Given the nature of battery systems and the fact that they are never completely equal in state of charge and/or voltage, however, it is nearly impossible to have all cells reach the point of venting at the same time. What is more usual is what happened in this test. One cell reached a venting stage first and the additional heat released by this venting cell caused the other cells to vent. This all happened in a few seconds, so if they were all to vent due to an overcharge or to excessive heat released from a venting cell the result would the same: all cells venting in a few seconds, as is shown in the test results.

CHECK VALVE TEST

A sealed pack of 20 cells with only a check valve opening was overcharged at 20 A to determine the feasibility of controlling an enclosure venting event. A pressure sensor was also installed on this battery pack to support verification of previous modeling efforts and better understand the rise in pressure due to cell venting. For this setup a single module was installed into a sealed battery pack enclosure to replicate a full battery system.

Twenty cells were connected in series to obtain a high-voltage pack with a nominal voltage of 72 VDC. It is important to note that one of these cells was initially charged to a relatively higher SOC. This configuration was built to allow for the entire pack to experience an overcharge with the expectation that the high-SOC cell would be the first to vent and do so well before the other cells in the pack. The goal was to allow enough time to understand a single-cell event before the remaining cells vented.

Both the internal module and pack enclosure were made of low-carbon steel to ensure the longest possible test time and avoid holes burning and breaking the pack seal prematurely. All air gaps were sealed prior to testing. The check valve device was threaded to the lid through a weld-in-bung. Meanwhile the other end was threaded to a tube that worked as an exhaust manifold for venting cell gasses.

A relatively high flow rate check valve was selected based on simulation results.

The check valve did work, but unfortunately just for a short time. An increase in pressure built up, causing the lid to open. Also, the exhaust manifold including check valve broke free due to excessive vibration and force.

Results from this test were very interesting. First of all, it was quite remarkable that just one cell vented and there wasn't enough thermal propagation to cause runaway in any other cells. In fact, during the cleaning up process each voltage was measured and except for the cell that went off, the other ones held the SOC they had been charged to prior to a cell venting.

Flames produced during venting did not ignite the packaging material. Only the area immediately surrounding the cell that vented showed damage. The steel enclosure that surrounded the module did not experience any damage, and (besides the lid) neither did the external enclosure.

VII. CRASH TESTING

In contrast to the many standardized battery impact tests found in the literature, this pendulum-based crash test was designed to simulate the specific and common scenario of a light vehicle impacting the side of a transit bus, including the worst-case scenario of the vehicle impacting directly at the point where a battery pack was mounted outside the bus frame rail. The intention was to include realistic vehicle speeds, vehicle mass, bumper dimensions, and dynamics of bus chassis and tires as will be seen later in the section. LTI regularly performs full-scale crash tests of this type, but the cost of such a full-scale test was beyond the scope of this project. A pendulum impact serves as a close approximation.

The impact test required significant preparation, as everything had to go perfectly on the first try. The tasks were split up as follows: preparation of the truck to simulate a bus, preparation of the battery pack, and preparation of the test.

PREPARATION FOR THE TRUCK

To simulate a small to medium transit bus, an 18,400-lb. Gross Vehicle Weight Rating (GVWR) refrigerated box truck was selected from an inventory of available crash trucks at our test track. The particular truck shown in Figure 103 was used for on-campus delivery by the Penn State Creamery and was not in running condition, a fact that would not affect the goal of replicating the dynamics of the vehicle during an impact.

Figure 102. 18,400-lbs. GVWR Refrigerated Truck to Simulate Bus

The box was removed from the truck for safety reasons, because if the batteries burned the bed could also catch on fire. In addition, current buses do not use similar insulated materials for their side panels, so it was incompatible to test it. Using a torch, the box was cut off and lifted by two forklifts. The truck was then pulled from underneath the box. All liquids were removed, the tires were filled up with air, and the exhaust was cut off.

The bare truck chassis weighed in at 12,250 lbs. Several options were considered to add weight; the final choice was to mount two Jersey barriers at 4,750 lbs. each mounted on I beam sections welded to the frame as shown in Figure 104 and Figure 105. Heavy ratchet straps secured the Jersey barriers.

Figure 103. I Beam Sections Welded to Chassis Frame

Figure 104. Jersey Barriers Mounted onto Truck Chassis

At this point the truck weighed 17,750 lbs. After taking into account that the weight of the battery pack would be 100 lbs., an extra 550 lbs. of sand bags were distributed throughout the back of the truck until the GVWR of 18,400 lbs. was achieved. The truck was then moved to the pendulum test pad and was placed at the impact point.

PENDULUM

The College's track facilities include a 40-ft. tall impact pendulum tower and test pad. In this case, the impact mass would simulate an SUV crashing into the side of a transit bus. The empty impact pendulum weighed 1200 lbs. Because a typical SUV weighs between 3500 and 4500 lb., the pendulum was loaded with all twenty-eight available steel plates, each weighing 100 lbs., achieving a total mass of 4000 lbs.

A front bumper for a 2006 Suburban was shortened to avoid a collision with the truck cab and back wheels. It was attached to the impact mass with steel tubes of similar proportions to the original Suburban frame. Figure 106 shows that both square tubes were welded to a c-channel base, and extra tabs were added to support the bumper from the main square frame tube in a manner similar to the vehicle design.

Figure 105. Left, Top View of Bumper, Right Bottom View

The bumper was mounted on the impact mass and the truck aligned for direct impact on the battery module as shown in Figure 107.

Figure 106. Impact Mass Mounted Bumper and Battery Position

FREE SWING TEST

Goals of the free swing test were to insure the pendulum would impact the battery pack at a right angle, accurately, and at the desired velocity. Exact location of the truck tires was marked on the test pad with spray paint, and the truck was then moved off the test

pad. Radar was set up to measure impact mass velocity. The radar is composed of two components: a laptop with software that monitors the velocity and the sensor to measure velocity of the moving mass.

To determine exactly where the pendulum would impact the battery module, a sponge filled with yellow paint was attached to the bumper. A white cardboard target of the same dimensions as the battery pack was placed on the spot and height where the battery pack would be mounted on the truck, as shown in Figure 108. Additional targets were placed in the positions of the truck cab and wheels to insure pendulum clearances.

Figure 107. Pendulum Test Swing Setup

The final setup step was to attach a measuring tape to the bottom of the impact mass to determine static height and lifted height above the ground. The static height was found to be 26 inches. The lifted height for a target impact speed can be determined through equating the potential and kinetic energy equations. Three free swings were performed, lowest speed first, to test the releasing system and accuracy of pendulum swing. The pendulum was pulled up to a lifted height of 11.36 ft. and a velocity of 18.5 mph was measured as validated by the following energy equations which predict a speed of 18.44 mph.

Pendulum weight = 4000 lbs. = mg

Gravity g = 32.2 ft./s^2

Pendulum mass = 4000 lbs. / 32.2 ft./s^2 = 124.22 lb-s^2/ft.

Potential Energy = mgh= 4000 lbs. * 11.36 ft. = 45,453.3 lb. ft.

Kinetic Energy = mv^2/2 = PE

v = (2*PE/m)$^{1/2}$ = (2 * 45,453.3 / 124.22)$^{1/2}$ = 27.05 ft./s = 18.44 mph

As a second test, the impact mass was raised to the maximum practical total height (limited by lift cable tension) of 21 feet and 1 inch, and velocity measured was 25.0 mph. A third try validated that the velocity at 21 feet and 1 inch was again 25.0 mph. This speed is typical of vehicles impacting the side of buses in urban environments, especially at intersections.

The last free swing was also used to validate the accuracy of bumper impact location relative to the battery box position. In Figure 109, the yellow paint mark indicates that the bumper impacted the battery position (simulated by the gray tape) within two inches of the original alignment. The fact that the pendulum impacted lower than the static alignment is likely due to cable stretching under additional dynamic loading from swing velocity.

Figure 108. Impact Accuracy of Pendulum to Battery Position

BATTERY PACK PREPARATION

The intention of this test was to simulate a full-sized bus battery pack, but space limitations on the frame of the truck restricted the test to a single module with 20 cells. After making sure that all BMS and temperature data was logging properly, the investigators inserted the pack into a steel box that was subsequently housed within an external aluminum enclosure as shown in Figure 110. The aluminum enclosure was designed with flanges for mounting to the truck frame between the cab and rear wheels. A power connector was also attached to the pack to simulate a real pack as closely as possible.

Figure 109. Aluminum Enclosure with Frame Mounting Flanges

Figure 111 shows the battery module mounted to the truck frame between the cab and rear wheels. A thermocouple scanner was mounted to the truck frame, and a data acquisition box was placed on the ground as far away as cabling allowed.
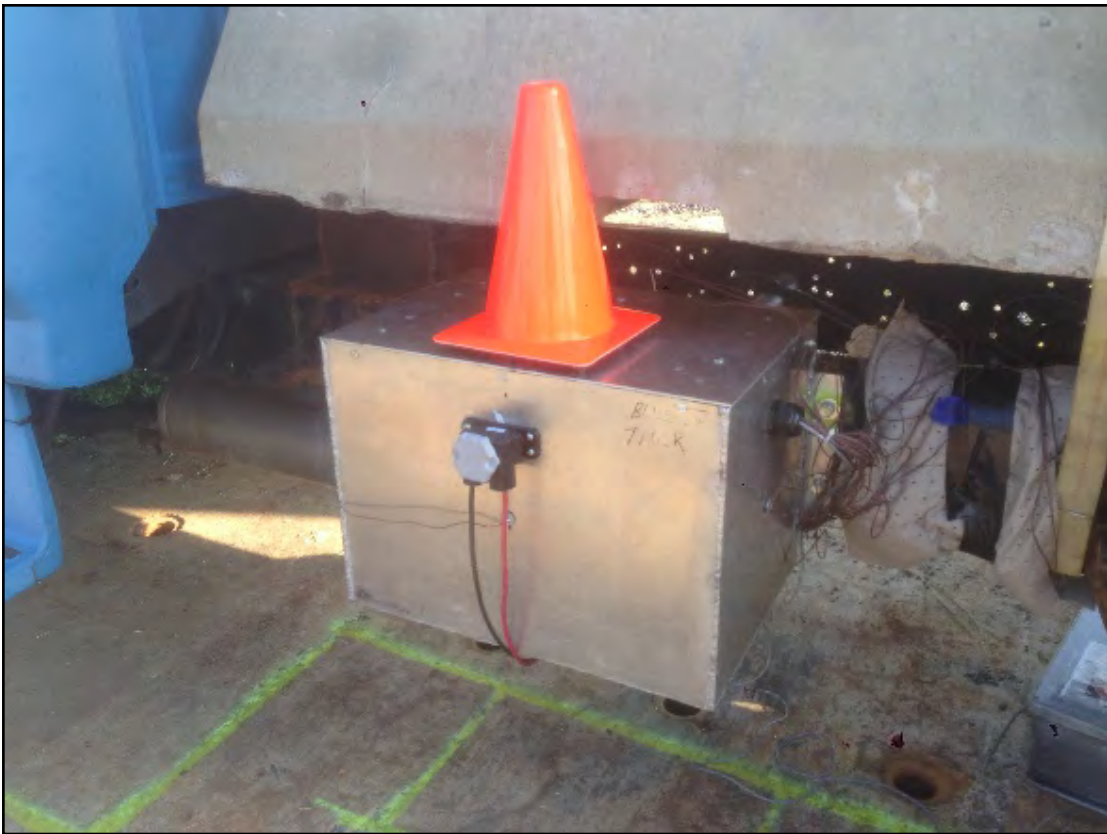
Figure 110. Battery Module Mounted on Frame with Data Acquisition

Figure 112 shows the positions of video and high-speed cameras placed to capture the crash event. The orange cone atop the pack is intended to serve as an inertial reference in the high-speed video. The pendulum can be seen suspended a few feet away from the battery module prior to lifting.

Figure 111. Camera Layout

IMPACT TEST RESULTS AND CONCLUSIONS

Test setup included camera placement and extension of the pendulum release tether to 200 feet. Local fire departments were invited to observe the test. The area was cleared of all personnel except one observer and the tow truck driver. The pendulum was pulled up to the 25 mph lifted height of 18.92 ft. Finally, the cameras were triggered, and the area was cleared of all personnel to a radius of 200 feet. A horn blast was given and the release mechanism was triggered to drop the pendulum. The pendulum impacted the box and truck, which was pushed back about one foot. No venting of cells was detected upon impact. As shown in Figure 113, local firefighters drilled on approaching the pack in full personal protective equipment (PPE) ready to apply water coolant, as would be their practice in response to an actual traffic accident involving an electrified transit bus. They also deployed an infrared camera to remotely detect hot spots on the pack, an indication of thermal runaway. No excessive heat was detected. Afterwards, the pack was left undisturbed for at least 24 hours.

Figure 112. Fire Fighters Approach Battery Pack after Impact

The BMS collected voltage and temperature data on all 20 cells within the module during the simulated crash test in anticipation of venting and thermal events. Since no venting occurred, the voltage data was unchanged, and only small perturbations in temperature occurred due to ambient conditions as shown in Figure 114. A slight temperature rise of 3°C was detected on all cells at the time of impact. This was probably due to mechanical energy and frictional work dissipated within the pack during the impact event. Cell 5 also demonstrated sensor bias and scaling which was unrelated to the crash event.
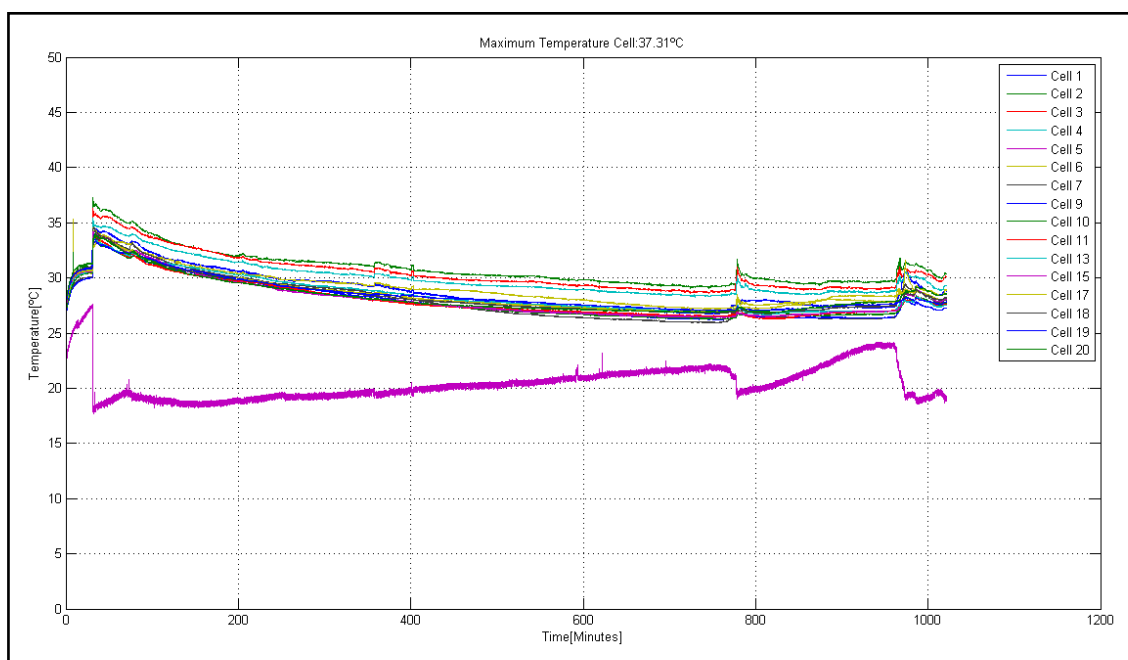
Figure 113. Individual Cell Temperatures during Simulated Crash Event

Upon inspection, it was noted that the center section of bumper deformed until the simulated SUV frame impacted the truck frame on either side of the battery module. The battery enclosure was significantly dented but not totally crushed, as shown in Figure 115. Some truck frame deformation was detected. The impact momentum transferred to the truck moved the front axle back 13 inches and the rear axle back 11 inches. Almost all the energy was transformed into deformation of the bumper and into movement of the truck.

Figure 114. Deformation of Bumper and Module Enclosure

Upon disassembly of the battery pack, it was observed that none of the battery cells were severely crushed or penetrated by any part of the pendulum. In this case, all four cells on the impact side of the pack showed some abrasion and slight denting on the outside casings, as shown in Figure 116. This impact represents a best-case scenario, however, with the bumper and vehicle dynamics absorbing much of the energy. This would not have been the case if a more rigid component of the impacting vehicle, such as the frame, had penetrated the pack. Here no thermal runaway occurred within 48 hours before disposal. These dents are severe enough, however, to have potentially resulted in either immediate or eventual internal shorting leading to thermal runaway. Delayed thermal runaway has

occurred in some high-profile cases. Individual cells retained their full voltage output. All cells from this pack were placed in a saltwater bath to safely discharge prior to disposal.

Figure 115. Dented Battery Cell

This test demonstrated that the simulated shock of a 25 mph SUV collision directly into a battery module mounted outside a bus frame might not necessarily result in a venting event. In this case, the bumper absorbed much of the energy by deformation, a significant energy portion was transferred into vehicle momentum, and the battery pack was not penetrated by any rigid vehicle components. The dual-wall steel-aluminum enclosure and header also provided substantial strength and protection against crushing. A different outcome would have been expected, however, if the collision had included battery pack penetration.

VIII. ENVIRONMENTAL IMPACTS

In the case where NCA batteries onboard a bus vent, it is important to understand the gases released, which may present an exposure risk to bus passengers and bystanders. A study of the gases venting from a cell is analyzed in this report, though it does not cover the gases generated from any of the selected packaging materials. Figure 4 showed the types and amounts of gases released during venting, most of which were common carbon oxides and hydrocarbons including methane (CH_4), methylene (CH_2), ethane (C_2H_6), propane (C_3H_8), butane (C_4H_{10}), hydrogen (H_2), and higher hydrocarbons C3 and C5. A validation test of gases released was run during one of our cell nail puncture tests. Sample gases were collected near the event through a tube leading to a gas collection bag.

The gas sample bag was processed at a Penn State laboratory using a GC-17A gas chromatograph manufactured by Shimadzu. The method used Flame Ionization Detection (FID), which is only effective at detecting hydrocarbons. The results are shown in Figure 118. Peaks were detected for several hydrocarbons including CH_4, CH_2, C_2H_6, C_3H_8, and C_4H_{10}. These gases (with the exception of CH_2) were also present in the more comprehensive gas analysis depicted previously and presented here again in Figure 119 with the commonly detected gases highlighted.
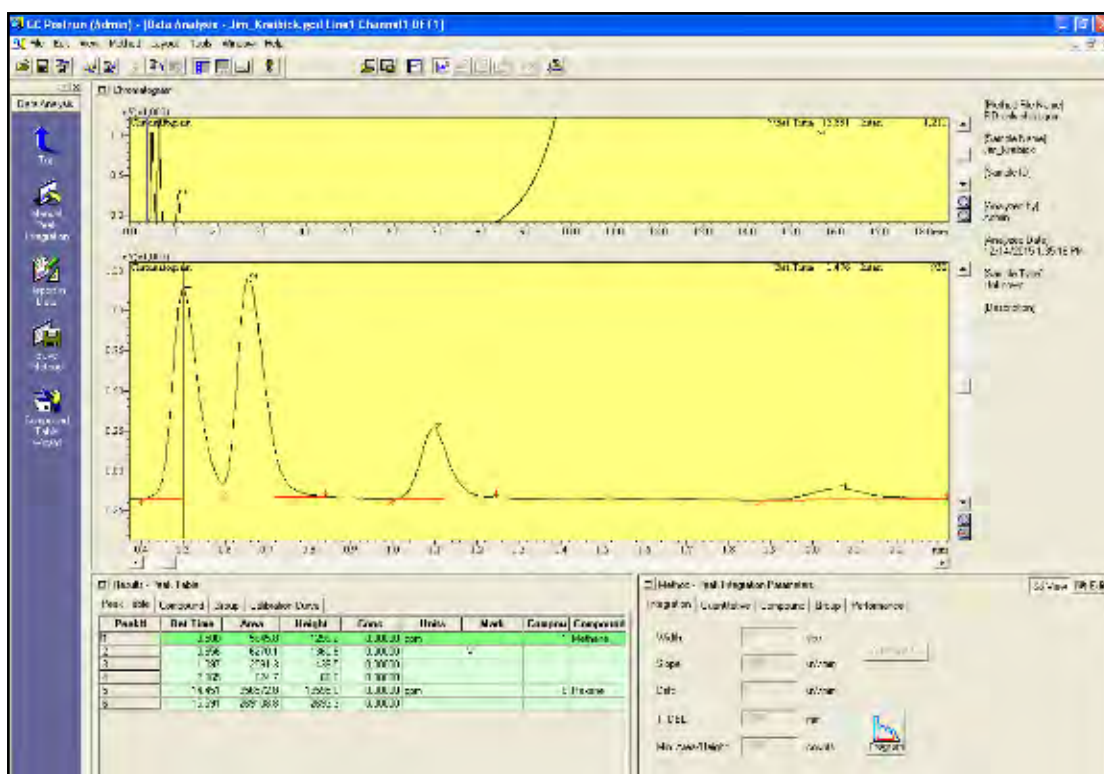
Figure 116. Gas Chromatography Results
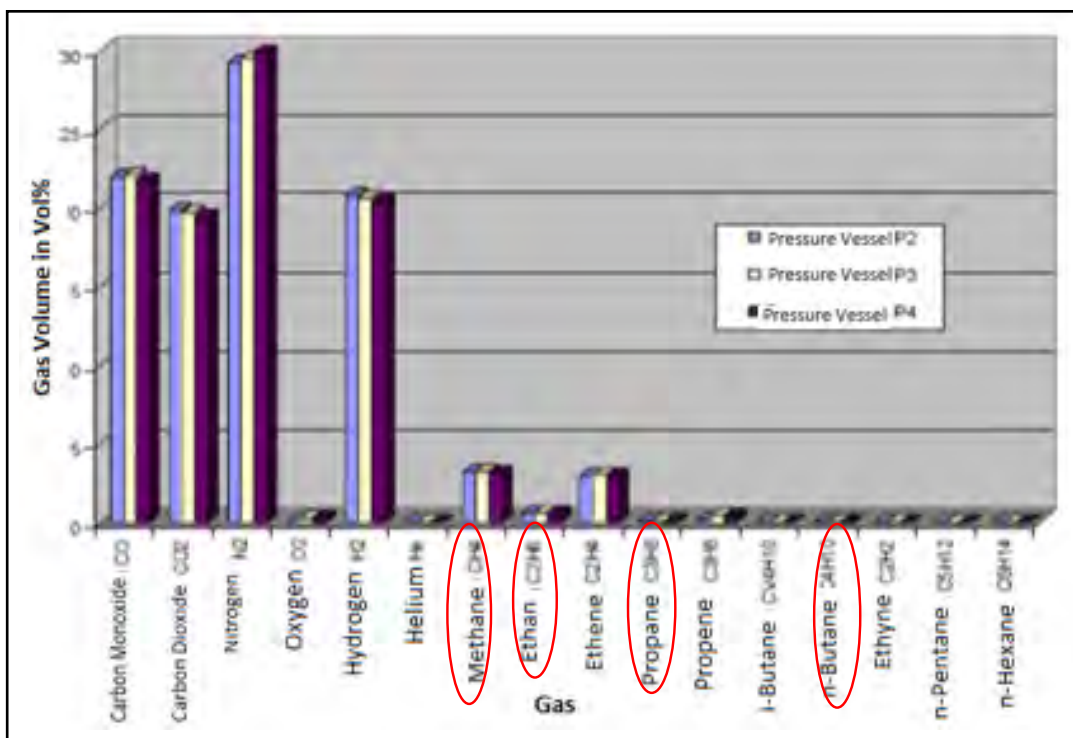
Figure 117. Molecules Present in Venting Gas

IX. CONCLUSION

When considering the use of an NCA battery system in a transit bus application, material and structural design is critical to keeping passengers safe. Common plastics such as acetal and PET have acceptable structural properties, but their swift and sustained combustibility under the high temperatures of a nearby thermal event poses a risk of rapid and severe events. Teflon is an affordable material and works well as a cell radiant heat separator because its melting point is high enough to withstand the heat generated by the large-format cells used in this testing. Pyrophobic phase-change material also performed well in our single-cell testing. Aluminum enclosures cannot withstand the temperatures of venting or sustained battery fires. Steel performs very well and can also provide additional strength to resist crush and puncture.

The research team found that the greatest safety concern when using such a high-energy chemistry is ensuring passenger safety when a cell's electrolyte boils and causes the ventilation of high-temperature toxic material. A cell-venting event can be triggered by a variety of scenarios with differing levels of likelihood. Though no system is perfect, a properly functioning and intelligent battery management system with voltage and temperature measurement should be able to avoid loading cells beyond their limits. As shown in this report, however, just one volt beyond the limit or a one-volt error can cause an overcharge event. Redundant voltage measurement is recommended and should be considered a high-risk, mandatory validation performed often by the battery management system. More noteworthy are the external temperature measurement results. Depending on how well a battery management system can track temperature or a model's internal temperature, a cell could vent before an external temperature sensor reads a value outside the nominal limitations. In conclusion, redundant voltage measurement and real-time internal temperature modeling or a virtual sensor should be mandatory to avoid cell-venting events.

Most interestingly, the team discovered that following a venting event the large-format cells tested immediately reached and remained at extremely high external skin temperatures for very long periods. If an event happens, it must be understood that danger can still be present for hours after the venting event. A fire may take place hours after the battery vents. Even worse, other cells can be heated and caused to vent due to the heat produced by the initial vented cell. Cooling is very important in crash/incident recovery and system design.

APPENDIX A – SPECIFICATION SHEETS

GAIA
Advanced Lithium Battery Systems

HP 602030 NCA
45 Ah/ 162 Wh
Lithium Ion Cell

Physical and mechanical characteristics	
Diameter	60 mm
Height	232 mm (203 mm without terminals)
Terminals	Positive terminal Al M12 L: 9 mm
	Negative terminal Cu M12 L: 9 mm
Weight	approx. 1500 g
Volume without terminals	0.57 l
Case material	Stainless Steel

Chemical characteristics	
Positive electrode	Lithium nickel cobalt oxide
Negative electrode	Graphite

Electrical characteristics*	
Nominal voltage	3.6 V
Nominal capacity at 0.2 C	45 Ah
Minimum capacity	42 Ah
AC Impedance (1 kHz)	≤ 0.4 mOhm
DC Resistance (ESR) (2 s pulse discharge @ 20 C/ 50% SOC)	≤ 1.2 mOhm
Specific energy at 0.2 C	108 Wh/kg
Energy density at 0.2 C	282 Wh/l
Specific power (2 s pulse discharge @ 27.8 C/ 100% SOC)	2080 W/kg
Power density (2 s pulse discharge @ 27.8 C/ 100% SOC)	5440 W/l

Operating conditions*	
Recommended charge method	Constant current - constant voltage
End of Charge	I ≤ C/100
Maximum charge voltage	4.2 V
Recommended charge current	up to 45 A (1 C)
Continuous charge current	up to 180 A (4 C)
Maximum pulse charge current (15 s) (Max. SOC 80 %, average current < 180 A)	270 A (6 C)
Recommended voltage limit for discharge	3 V
Lower voltage limit for discharge	2.7 V
Lower voltage limit for pulse discharge	2 V
Recommended discharge current	up to 90 A (2 C)
Maximum discharge current	up to 450 A (10 C)
Maximum pulse discharge current (2 s)	up to 1250 A (27.8 C)
Operating temperature	- 30°C to + 60°C
Recommended charge temperature	0°C to + 40°C
Storage and transport temperature	- 40°C to + 60°C
Cycle life at 20°C and 100% DOD	> 1000 cycles to 80% nominal capacity
(0.5 C charge; 0.5 C discharge)	> 2000 cycles to 60% nominal capacity

* Reference temperature 20°C

Doc: HP 602030 NCA – 2008-08

Data in this document are subject to change without notice and are not binding.

High Power

GAIA
Advanced Lithium Battery Systems

GAIA Akkumulatorenwerke GmbH
Montanlastr. 17
99734 Nordhausen, Germany
www.gaia-akku.com

LTC Lithium
Technology Corporation

Lithium Technology Corporation
5115 Campus Drive
Plymouth Meeting, PA 19462
www.lithiumtech.com

APPENDIX B – FMVSS STANDARDS

FMVSS 201U

Test Procedure
A Free Motion Headform (FMH) impactor hits the upper interior parts with a velocity of 24 km/h (A-, B-, C-pillar, roof etc.).

FMH Impactor Data
Mass of FMH impactor: 4.54 kg
Head form according to SAE J 921 and J 977 including triaxial acceleration sensor.

Protection Criteria
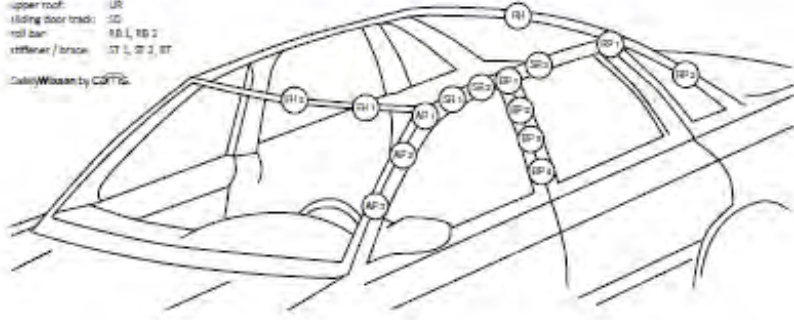
HIC Calculation

$$HIC = \sup_{t_1,t_2} \left\{ \left[\frac{1}{(t_2-t_1)} \int_{t_1}^{t_2} a\,dt \right]^{2,5} (t_2-t_1) \right\} \qquad t_2-t_1 < 36\ ms;\ a\ [g];\ t\ [s]$$

HIC value for FMH $HIC(d) = 0.75446\ HIC + 166.4$

HIC(d) must not exceed 1000.
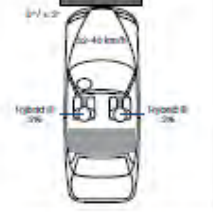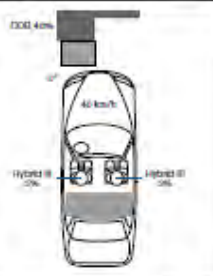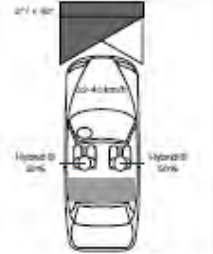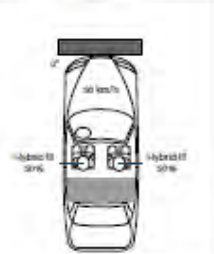
24 points defined for impact according Test Procedure TP-201 (each side, left and right)

other pillars: OP 1, OP 2
upper roof: UR
sliding door track: SD
roll bar: RB 1, RB 2
stiffener / brace: ST 1, ST 2, BT

Data/Wissen by COMPG.

FMVSS 208: Frontal Impact Requirements: In-Position

FMVSS 208: Frontal Impact Requirements: Out of Position

Front seat	Dummy	Test configuration
Driver side	Hybrid III 5 % female	chin on airbag module in steering wheel
		chin on top of steering wheel
Passenger side	CRABI 12m	in 23 defined CRS / positions
	Hybrid III 3 y/o	chest on instrument panel
		head on instrument panel
	Hybrid III 6 y/o	chest on instrument panel
		head on instrument panel

Roof Crush

FMVSS 216a — Docket No. NHTSA-2009-0093

Application:
Vehicles with a GVWR ≤ 4536 kg

Applied Force:
for vehicles with a GVWR ≤ 2722 kg:
$F = 3.0 \times GVWR \times 9.8 \, m/s^2$
for vehicles with a GVWR > 2722 kg:
$F = 1.5 \times GVWR \times 9.8 \, m/s^2$

Feed Rate: ≤ 13 mm/s

Double Sided Test

Requirements:
Platen displacement ≤ 127 mm
Load on headform located at head position of 50% male ≤ 222 N

Phase-In for GVWR ≤ 2722 kg:

Manufacturing Period	%*
01.09.2012-30.08.2013	25%
01.09.2013-30.08.2014	50%
01.09.2014-30.08.2015	75%
on or after 01.09.2015	100%

* in % of the production of the respective period or in % of the average production of the 3 previous years

Introduction for GVWR > 2722 kg: **01.09.2016**

IIHS — Testing Protocol Version II (Dec 2012)

Platen Displacement: 127 mm

Feed Rate: 5 mm/s

Single Side Test: Lab selects worst case

Assessment:
based on Strength-to-weight ratio (SWR) = F_{max} / m x g

SWR	Rating
≥ 4.00	Good
≥ 3.25 till <4.00	Acceptable
≥ 2.50 till <3.25	Marginal
< 2.50	Poor

A "Good" rating in the roof crush test is a requirement for the Top-Safety-Pick award.

FMVSS 226 - Ejection Mitigation

Requirements:

- At up to 4 impact test locations on each side window in the first 3 rows of seats the head excursion may not exceed 100 mm
- Tests at two impact velocities: 16 km/h and 20 km/h
- Head protection systems (e.g. curtain airbags) must be fired before the impact:
  - at 20 km/h with a time delay of 1.5 s prior to the impact
  - at 16 km/h with a time delay of 6 s prior to the impact
- Tests are done without glazing or with pre-damaged glazing
  - pre-damage: perforation in a 75 mm grid pattern
- Valid for vehicles with GVWR ≤ 4536 kg
- Phase-In: 2013 - 2017

max. 100 mm

v=16 km/h / 20 km/h

m=18 kg

Locating Targets:

Daylight Opening (DLO)

25 mm Offset

Primary-Target

Secondary-Target

Front Row Window

Rear Row Windows

A1 A3 A2 A4

B3 B4 B1 B2

1/3 1/3 1/3

1/3 1/3 1/3

Steps	Front Row Window	Rear Row Windows
1	Set Primary Target A1 in lower front corner	Set Primary Target B3 in upper front corner
2	Set Primary Target A4 in upper rear corner	Set Primary Target B2 in lower rear corner
3	Divide horizontal distance between A1 and A4 in thirds	Divide horizontal distance between B3 and B2 in thirds
4	Move A3 at the first third vertically upward	Move B1 at the first third vertically downward
5	Move A2 at the second third vertically downward	Move B4 at the second third vertically upward
6	Measure Distances D_h (horizontal) and D_v (vertical) of the target center points	
7	If D_h (A2 - A3) < 135 mm and D_v (A2 - A3) < 170 mm → Eliminate A3	If D_h (B1 - B4) < 135 mm and D_v (B1 - B4) < 170 mm → Eliminate B4
8	If D_h (A4 - A3) (or A2 if A3 was eliminated in step 7) < 135 mm and D_v (A4 - A3/2) < 170 mm → Eliminate A3/2	If D_h (B3 - B4) (or B1 if B4 was eliminated in step 7) < 135 mm and D_v (B3 - B4/1) < 170 mm → Eliminate B4/1
9	If D_h (A4 - A2) (or A3 if A2 was eliminated in step 8) < 135 mm and D_v (A4 - A2/3) < 170 mm → Eliminate A2/3	If D_h (B2 - B1) (or B4 if B1 was eliminated in step 8) < 135 mm and D_v (B2 - B1/4) < 170 mm → Eliminate B1/4
10	If D_h (A1 - A4) < 135 mm and D_v (A1 - A4) < 170 mm → Eliminate A4	If D_h (B3 - B2) < 135 mm and D_v (B3 - B2) < 170 mm → Eliminate B3
11	If only 2 targets remain: Measure absolute distance D the center points of the targets	
12	If D > 360 mm, set additional 3rd target on the center of the line connecting the targets	
13	If less than 4 targets remain, repeat steps 1-12 with the impactor rotated by 90 degrees. If this results in a higher number of targets use the rotated targets.	
14	If no target is found rotate the impactor in 5 degree steps, until it is possible to fit the impactor in the DLO-offset. Then place the center of the target as close to the geometric center of the DLO as possible.	

APPENDIX C – TABLES OF TEST SETUP AND RESULTS

ACETAL – OVERCHARGE				
Type of test	Overcharge			- Positive terminal
Nº of cells	1			- Negative terminal
Material	Acetal			- Top of the cell by positive terminal
Cell stand	Base	Acetal		- Top of the cell by negative terminal
	Cage	No	Temperature sensors location	- Top of the cell by center of the cell
	Separator	Acetal		- Front of the cell by positive terminal
	Housing	No		- Front of the cell by negative terminal
Charged at	20 A			
Data aquisition	- Voltage - Temperature - Current			
Equipment	- Voltage: Single board A/D - Temperature sensors: 18B20 - Current sensor: LEM CAB 300			

ACETAL – Nail Puncture				
Type of test	Nail Puncture			
Nº of cells	1			- Positive terminal
Material	Acetal			- Negative terminal
Cell stand	Base	Acetal		- Top of the cell by positive terminal
	Cage	No	Temperature sensors location	- Top of the cell by negative terminal
	Separator	Acetal		- Top of the cell by center of the cell
	Housing	No		- Steel sheet by positive terminal
Data aquisition	Voltage Temperature			- Aluminum sheet by negative terminal - Ambient
Equipment	Voltage: Single board A/D Temperature sensors: Thermocouple J type			- Base

ACETAL - OVERCHARGE AND MATERIAL TEST				
Type of test	Overcharge			
Nº of cells	1			- Positive terminal
Material	Acetal			- Negative terminal
Cell stand	Base	Acetal		- Top of the cell by positive terminal
	Cage	No	Temperature sensors location	- Top of the cell by negative terminal
	Separator	Acetal		- Top of the cell by center of the cell
	Housing	No		- Steel sheet by positive terminal
Charged at	20 A			- Aluminum sheet by negative terminal
Data aquisition	Voltage Temperature Current			- Ambient - Base
Equipment	Voltage: Single board A/D Temperature sensors: Thermocouple J type Current: LEM CAB300			

PYROPHOBIC - OVERCHARGE				
Type of test	Overcharge			- Positive terminal
Nº of cells	1			- Negative terminal
Material	Pyrophobic			- Top of the cell by positive terminal
Cell stand	Base	Aluminum		- Top of the cell by negative terminal
	Cage	Pyrophobic	Temperature sensors location	- Top of the cell by center of the cell
	Separator	Pyrophobic		- Outside wall by the positive terminal
	Housing	No		- Outside wall by the negative terminal
Charged at	20 A			- Top Wall
Data aquisition	Voltage			- Ambient
	Temperature			- Base
	Current			
Equipment	Voltage: Single board A/D Temperature sensors: Thermocouple J type Current: LEM CAB300			

PYROPHOBIC - NAIL PUNCTURE				
Type of test	Nail Puncture			- Positive terminal
Nº of cells	1			- Negative terminal
Material	Pyrophobic			- Top of the cell by positive terminal
Cell stand	Base	Aluminum		- Top of the cell by negative terminal
	Cage	Pyrophobic	Temperature sensors location	- Top of the cell by center of the cell
	Separator	Pyrophobic		- Outside wall by the positive terminal
	Housing	No		- Outside wall by the negative terminal
Data aquisition	Voltage			- Top Wall
	Temperature			- Ambient
Equipment	Voltage: Single board A/D Temperature sensors: Thermocouple J type Current: LEM CAB300			- Base

PYROPHOBIC - OVERCHARGE WITH HOUSING				
Type of test	Nail Puncture			- Positive terminal
Nº of cells	1			- Negative terminal
Material	Pyrophobic			- Top of the cell by positive terminal
Cell stand	Base	Aluminum		- Top of the cell by negative terminal
	Cage	Pyrophobic		- Top of the cell by center of the cell
	Separator	Pyrophobic	Temperature sensors location	- Outside wall by positive terminal
	Housing	Aluminum		- Outside wall by negative terminal
Data aquisition	Voltage			- Top Wall
	Temperature			- Front Wall
	Current			- Between Pyrophobic cage and Aluminum Housing
Equipment	Voltage: Single board A/D Temperature sensors: Thermocouple J type Current: LEM CAB300			- Ambient inside Pyrophobic cage
				- Ambient

PET - OVERCHARGE				
Type of test		Overcharge		- Positive terminal - Negative terminal - Top of the cell by positive terminal - Top of the cell by negative terminal - Top of the cell by center of the cell - Outside wall by the negative terminal - Front Wall - Cage Ambient - Ambient - Base
Nº of cells		1		
Material		PET		
Cell stand	Base	PET	Temperature sensors location	
	Cage	PET		
	Separator	PET		
	Housing	No		
Charged at		20A		
Data aquisition		Voltage Temperature Current		
Equipment	Voltage: Single board A/D Temperature sensors: Thermocouple J type Current: LEMCAB300			

PET -NAIL PUNCTURE				
Type of test		Nail Puncture		- Positive terminal - Negative terminal - Top of the cell by positive terminal - Top of the cell by negative terminal - Top of the cell by center of the cell - Outside wall by the positive terminal - Front Wall - Cage Ambient - Ambient - Base
Nº of cells		1		
Material		PET		
Cell stand	Base	PET	Temperature sensors location	
	Cage	PET		
	Separator	PET		
	Housing	No		
Data aquisition		Voltage Temperature		
Equipment	Voltage: Single board A/D Temperature sensors: Thermocouple J type			

TEFLON - OVERCHARGE				
Type of test		Overcharge		- Positive terminal - Negative terminal - Top of the cell by positive terminal - Top of the cell by negative terminal - Top of the cell by center of the cell - Outside wall by the negative terminal - Front Wall - Cage Ambient - Ambient - Base
Nº of cells		1		
Material		Teflon		
Cell stand	Base	Teflon	Temperature sensors location	
	Cage	Teflon		
	Separator	Teflon		
	Housing	No		
Charged at		20A		
Data aquisition		Voltage Temperature Current		
Equipment	Voltage: Single board A/D Temperature sensors: Thermocouple J type Current: LEMCAB300			

TEFLON - NAIL PUNCTURE				
Type of test	Nail Puncture			- Positive terminal
Nº of cells	1			- Negative terminal
Material	Teflon			- Top of the cell by positive terminal
Cell stand	Base	Teflon		- Top of the cell by negative terminal
	Cage	Teflon	Temperature	- Top of the cell by center of the cell
	Separator	Teflon	sensors	- Outside wall by the positive terminal
	Housing	No	location	- Front Wall
Data aquisition	Voltage Temperature			- Cage Ambient
				- Ambient
Equipment	Voltage: Single board A/D Temperature sensors: Thermocouple J type Current: LEM CAB300			- Base

NAIL TIP TEMPERATRUE MEASUREMENT			
Type of test	Nail Puncture		- Positive terminal
Nº of cells	1		- Negative terminal
Material			- Top of the cell by positive terminal
Cell stand	Metal Bands		- Top of the cell by negative terminal
		Temperature	- Top of the cell by center of the cell
		sensors	- Inside the nail
		location	- Inside the nail
Data aquisition	Voltage Temperature		- Inside the nail
			- Inside the nail
Equipment	Voltage: Single board A/D Temperature sensors: Thermocouple K type		- Inside the nail
			- Inside the nail
			- Ambient

SINGLE CELL OVERCHARGE IN A MODULE WITH ACETAL HEADERS				
Type of test	Overcharge		- Center of cell that is being overcharged	- Bottom header left
Total nº of cells	5		- Ambient inside the enclosure	- Ambient
Nº of cells overcharged	1		- Back right center of cell closest to	- Top cover center
Pack made out of	Acetal		- Top right center of cell closest to	- Top cover right
Module Enclosure	Aluminum with steel plates. Enclosure with openings	Temperature	- Top right center of cell farthest away	- Top cover back
		sensors	- Bottom right center of cell farthest away	- Top cover left
Charged at	20 A	location	- Back left center of cell closest to	
Data aquisition	Voltage Temperature Current		- Back left center of cell farthest away	
			- Top left center of cell farthest away from	
			- Top left center of cell closest to	
Equipment	Voltage: Single board A/D Temperature sensors: Thermocouple J type Current: LEM CAB300		- Bottom header front	
			- Bottom header right	
			- Bottom header back	

OVERCHARGE OF 20 CELLS IN STEEL ENCLOSURE				
Type of test	Overcharge		- Bottom header left	- Ambient
Total nº of cells	20		- Bottom header back	
Nº of cells overcharged	20		- Bottom header right	
Pack made out of	Acetal		- Bottom header front	
Module Enclosure	Steel. Enclosure with openings		- Top cover left	
		Temperature	- Top cover back	
Charged at	20 A	sensors	- Top cover right	
Data aquisition	Voltage Temperature Current	location	- Top cover front	
			- Top of cover on center	
			- Top steel enclsoure	
Equipment	Voltage: Production Batter Management Temperature sensors: Thermocouple J type Current: LEM CAB 300		- Front of steel enclosure	
			- Left of steel enclosure	
			- Ambient inside pack	

CHECK VALVE TEST			
Type of test	Overcharge	Temperature sensors location	- Bottom header left
Total nº of cells	20		- Bottom header back
Nº of cells overcharged	20		- Bottom header right
Pack made out of	Acetal		- Bottom header front
Module Enclosure	Steel. Enclosure with openings		- Top cover left
Pack Enclosure	Aluminum. Closed Enclosure		- Top cover back
Charged at	20 A		- Top cover right
Data aquisition	Voltage Temperature Current Pressure		- Top cover front - Top of cover on center - Top steel enclsoure - Front of steel enclosure
Equipment	Voltage: Single board A/D Temperature sensors: Thermocouple J type Current: LEM CAB 300 Pressure sensor: Honeywell MLH150PGB06A		- Left of steel enclosure - Ambient inside pack - Ambient

CRASH TESTING				
Type of test	Crash	Temperature sensors location	- Cell 1	- Cell 13
Total nº of cells	20		- Cell 2	-Cell 14
Nº of cells crashed	20		- Cell 3	- Cell 15
Pack made out of	Acetal		- Cell 4	- Cell 16
Module Enclosure	Steel. Enclosure with openings		- Cell 5	- Cell 17
Pack Enclosure	Aluminum. Closed enclosure		- Cell 6	- Cell 18
Data aquisition	Voltage Temperature		- Cell 7 - Cell 8 - Cell 9	- Cell 19
Equipment	Voltage: Production Battery Management Temperature sensors: Thermocouple J type		- Cell 10 - Cell 11 - Cell 12	

Mineta National Transit Research Consortium

Single Cell Test Results											
Pastic parts made out of	Acetal			Pyrophobic			PET		PTFE(Teflon)		No plastic
Parts made of plastic	Base			Cage & Base							None
Module Housing Material											
Enclosure Housing Material						Aluminum					
Test	Overcharge	Nail Puncture	Overcharge and Material Test	Overcharge	Nail Puncture	Overcharge w/ metal Housing	Overcharge	Nail Puncture	Overcharge	Nail Puncture	Nail Tip Temperatrue
Name	Acetal-Overcharge	Acetal-Nail Puncture	Acetal-Overcharge and Material Test	Pyrophobic Overcharge	Pyrophobic Nail Puncture	Pyrophobic Overcharge w/ metal Housing	PET - Overcharge	PET- Nail Puncture	PTFE - Overcharge	PTFE- Nail Puncture	Nail Tip Temperatrue Measurement
Max Temperatures ºC — Positive terminal	Temperatures sensors used were not capable of capturing the highest temperatures of the test.	Temperatures sensors used were not capable of capturing the highest temperatures of the test.	685.47	369.13		429.00	582.88	603.72	293.16	414.97	37.59
- Negative terminal			685.59	316.13	544.91	512.03	747.19	641.44	748.56	343.28	97.09
- Top of the cell by positive terminal			603.53	740.41	296.09	440.25	Got Damaged	553.44	604.75	422.94	70.06
- Top of the cell by negative terminal			644.13	227.16	275.41	486.38	750.69	711.03	342.41	361.75	188.84
- Top of the cell by center of the cell			649.97	269.81	403.09	566.13	730.00	630.84	361.31	386.81	86.25
- Aluminum sheet by positive terminal			745.94								
- Steel sheet by negative terminal			577.09								
- Base			347.97	101.66	19.97		378.53	116.09	667.47	52.03	
- Outside wall by positive terminal				133.50	59.41	525.72		620.69	748.47	Got damaged	
- Outside wall by negative terminal				163.03	162.84	305.03	698.38		717.44		
- Top Wall				75.25	129.34	540.72			Got Damaged		
- Front Wall						406.28	572.03	265.84		102.28	
- Between Pyrophobic cage and Aluminum Housing						29.97					
- Cage Ambient						555.19	741.41	665.22		437.31	
- Top Housing						129.88					
- Nail Temperature											602.19

Module Tests Results						
			Pack Module Level			
Pastic parts made out of			Acetal			
Parts made of plastic			Battery pack: headers, covers			
Module Housing Material			Aluminum	Steel	Steel	Steel
Enclosure Housing Material					Aluminum	Aluminum
Test			Overcharge			Crash Testing
Name			Single Cell Overcharge in a module with Acetal headers	Overcharge of 20 cells in steel enclosure	Check Valve Test	Crash Testing
Max Temperatures ºC	- Center of cell that is being overcharged	Cell 12	750.34	67.91		Damaged
	- Top right center of cell closest to overcharged cell	Cell 1	604.28	750.94		34.66
	- Top right center of cell farthest away from overcharged cell		750.94			
	- Bottom right center of cell closest to overcharged cell	Cell 19	598.66	739.78		33.91
	- Bottom right center of cell farthest away from overcharged cell		612.44			
	- Bottom left center of cell closest to overcharged cell	Cell 15	683.91	749.78		34.19
	- Bottom left center of cell farthest away from overcharged cell		750.97			
	- Top left center of cell farthest away from overcharged cell	Cell 5	646.72	561.25		27.59
	- Top left center of cell closest to overcharged cell		279.78			
	Cell 2			710.91		37.31
	Cell 3			749.91		36.34
	Cell 4			750.91		35.41
	Cell 6			750.78		35.31
	Cell 7			750.72		34.63
	Cell 8			750.63		34.66
	Cell 9			750.72		33.34
	Cell 10			750.09		34.19
	Cell 11			749.25		33.78
	Cell 13			750.06		33.88
	Cell 14			750.56		34.13
	Cell 16			76.44		Damaged
	Cell 17			745.22		33.94
	Cell 18			749.34		33.72
	Cell 20			750.69		34.13
	- Ambient inside the enclosure		731.81	815.91		
	- Bottom header front		731.81	826.60		
	- Bottom header right		604.28	1140.35		
	- Bottom header back		612.44	1200.85		
	- Bottom header left		750.97	775.91		
	- Top cover center		750.97	1117.48		
	- Top cover right		682.22	839.48		
	- Top cover back		748.22	925.04		
	- Top cover left		750.53	1200.85		
	- Top cover front		750.56	842.91		
	- Top of steel enclosure			855.23		
	- Front of steel enclosure			938.73		
	- Left of steel enclosure			979.91		

ACRONYMS AND ABBREVIATIONS

A/Ah	Ampere/Ampere-Hour
AC	Alternating Current
APTA	American Public Transit Association
atm	Atmospheres
BATTERY	Battery Application Technology Testing and Energy Research Laboratory
BMS	Battery Management System
BRTC	Bus Research and Testing Center
C	Centigrade
CAD	Computer Aided Design
CAN	Controller Area Network
CFD	Computational Fluid Dynamics
CH2	methylene
CH4	methane
C2H6	ethane
C3H8	propane
C4H10	butane
CNC	Computer Numerical Control
C Rate	Battery Hourly Power Rate
DC	Direct Current
DFMEA	Design Failure Mode and Effect Analysis
DOT	Department of transportation
DP	Dual Polarization
DST	Dynamic Stress Test
ECE	Economic Commission for Europe
EIS	Electrochemical Impedance Spectroscopy
EOL	End of Life
ESR	Effective Series Resistance
ESS	Energy Storage System
EV	Electric Vehicle
FEA	Finite Element Analysis
FMVSS	Federal Motor Vehicle Safety Standards
FID	Flame Ionization Detection
FMVSS	Federal Motor Vehicle Safety Standards
GVWR	Gross Vehicle Weight Rating
HEV	Hybrid Electric Vehicles
HLDI	Highway Loss Data Institute
H2	hydrogen
Hz	Hertz, a unit of frequency

IIHS	Insurance Institute for Highway Safety
K	Kelvin
kW/kWh	kilowatt/kilowatt-hour
LFP	Lithium Ion Phosphate
LTI	Thomas D. Larson Pennsylvania Transportation Institute
LTO	Lithium Titanate Oxide
MNTRC	Mineta National Transit Research Consortium
mph	Miles Per Hour
MSDS	Material Safety Data Sheet
mV	Microvolt
NCA	Lithium Nickel Cobalt Aluminum Oxide
NCAP	New Car Assessment Program
NFPA	National Fire Protective Association
NHTSA	National Highway Traffic Safety Administration
OCV	Open Circuit Voltage
PET	Polyethylene Terephthalate
POM	Polyoxymethylene (commercially known as acetal)
PCB	Printed Circuit Board
PPE	Personal Protective Equipment
PTFE	Polytetrafluoroethylene (commercially known as Teflon)
PHEV	Plug-In Hybrid Electric Vehicle
PSIA	Absolute Pounds Per Square Inch (Absolute Pressure)
RTD	Resistance Temperature Detectors
RC	Resistor-Capacitor
SAE	Society of Automotive Engineers
SBC	Single Board Computer
SBPG	Standard Bus Procurement Guidelines
SOC	State of Charge
SUV	Sport Utility Vehicle
UNECE	United Nations Economic Commission for Europe
TIG	Tungsten Inert Gas
VAC	Variable Alternating Current
V	Volt
VAC	Volts Alternating Current
VDC	Volts Direct Current

ENDNOTES

1. Arora, Ashish, Noshirwan K. Medora, Thomas Livernois, and Jan Swart, "Safety of Lithium Ion Batteries for Hybrid Electric Vehicles," in Electric and Hybrid Vehicles. Power Sources, Models, Sustainability, Infrastructure and the Market, edited by G. Pistoia, 464-490 (Amsterdam: Elsevier, 2010).

2. NHTSA, "Traffic Safety Facts Annual Report 2013," (2015), https://crashstats.nhtsa.dot.gov/#/DocumentTypeList/12 (accessed September 27, 2015).

3. National Highway Traffic Safety Administration, (n.d.). Retrieved from Federal Motor Vehicle Safety Standards and Regulations, http://www.nhtsa.gov/cars/rules/import/FMVSS/

4. Gerardo Olivares, Vikas Yadav. "Injury Mechanisms to Mass Transit Bus Passengers during Frontal, Side and Rear Impact Crash Scenarios," (n.d.), http://www-nrd.nhtsa.dot.gov/pdf/esv/esv21/09-0427.pdf (accessed December 7, 2015).

5. Carhs Empower Engineers, "Safety Companion 2016," (2016), https://www.carhs.de/en/companion-poster/product/safetycompanion-2016pdf.html (accessed December 4, 2015).

6. United Nations Economic Commission for Europe, "Spectrum Of Road Safety Activities," (2012), https://www.unece.org/fileadmin/DAM/trans/roadsafe/publications/Spectrum_of_Road_Safety_Activites.pdf (accessed April 8, 2014).

7. SafetyWissen, "UnitedStatesNewCarAssessmentProgram," https://www.safetywissen.com/#/object/B10/B10.nw37346182s1mokz8mq64428r5m0on63470973228/?_k=88xugz (accessed December 3, 2015).

8. IIHS ,"About the Institutes," http://www.iihs.org/iihs/about-us/hldi (accessed December 3, 2016).

9. New York State Department of Transpiration, "Bus & Passenger Vehicle Regulations: Title 17 Official Compilation of Codes, Rules and Regulations of the State of New York, Parts 720, 721, 722, and 723," (July 18, 1999), https://www.dot.ny.gov/divisions/operating/osss/bus-repository/busregs1.pdf (accessed April 16, 2014).

10. Code of Federal Regulations (CFR) Annual Edition, US Government Publishing Office (GPO), (2016),http://www.ecfr.gov/cgibin/textidx?SID=66b4d9b929a5faec813ec0fa6bf5c6b4&mc=true&node=se49.6.571_1301&rgn=div8, Figure 2.(accessed April 8, 2014).

11. American Public Transportation Association, "Standard Bus Procurement Guidelines RFP 2013," (May, 2013) https://www.google.es/url?sa=t&rct=j&q=&esrc=s&source=web&cd=1&cad=rja&uact=8&ved=0ahUKEwjNquXF99LOAhWTyRoKHV9CBXQQFggoMAA&url=http%3A%2F%2Fwww.apta.com%2Fresources%2Fstandards%2FDocu

ments%2FAPTA%2520Bus%2520Procurement%2520Guidelines.docx&usg=AFQjC
NHzi3MXJhPJ2UyULPuXaMyjSA5V5g (accessed April 20, 2014).

12. National Fire Protection Association, "Tactical Considerations for Extinguishing Fires in Hybrid and Electric Vehicles," (December 9, 2014), https://www.youtube.com/watch?v=mtCk3srID_w (accessed April 28, 2014).

13. Power Vehicle Innovation, "Our Expertise," http://www.pvi.fr/energie-embarquee-batteries,042.html?lang=en (accessed September 27, 2015).

14. Life of Guangzhou, "Guangzhou's Frist Electric Bus Line Opens," http://www.lifeofguangzhou.com/node_981/node_989/node_997/node_1007/2010/11/19/12901 4852382496.shtml (accessed October 4, 2015).

15. NFPA, "Lithium-Ion Batteries Hazard and Use Assessment," July 2011, http://www.nfpa.org/news-and-research/fire-statistics-and-reports/research-reports/hazardous-materials/other-hazards/lithium-ion-batteries-hazard-and-use-assessment (accessed April 22, 2014).

16. Wech, Lothar, Richard Richter, Rainer Justen, and Rodolfo Schöneburg, "Crash Safety Aspects of HV Batteries for Vehicles," National Highway Traffic Safety Administration (NHTSA) (n.d.), http://www-nrd.nhtsa.dot.gov/pdf/esv/esv22/22ESV-000302.pdf (accessed June 3, 2015).

17. Arora, Ashish, Noshirwan K. Medora, Thomas Livernois, and Jan Swart, "Safety of Lithium Ion Batteries for Hybrid Electric Vehicles," in Electric and Hybrid Vehicles. Power Sources, Models, Sustainability, Infrastructure and the Market, edited by G. Pistoia, 464-490 (Amsterdam: Elsevier, 2010).

18. Forberg, "Support/Documentation. Valve Flow Calculations and Sizing Guidelines," http://www.forberg.com/pdf/techSup/Home_Tech%20Support_Valve%20Flow_calc_and_sizing.pdf (accessed June 3, 2015).

BIBLIOGRAPHY

American Public Transportation Association. "Standard Bus Procurement Guidelines RFP 2013." May 2013. http://www.apta.com/resources/reportsandpublications/ Pages/BusParatransit.aspx (accessed April 20, 2014).

Arora, Ashish, Noshirwan K. Medora, Thomas Livernois, and Jan Swart. In "Safety of Lithium Ion Batteries for Hybrid Electric Vehicles." *Electric and Hybrid Vehicles. Power Sources, Models, Sustainability, Infrastructure and the Market*, edited by G. Pistoia, 464-490. Amsterdam: Elsevier, 2010.

Carhs Empower Engineers. "Safety Companion 2016." 2016. https://www.carhs.de/en/ companion-poster/product/safetycompanion 2016-pdf.html (accessed December 4, 2015).

Chu, Jennifer. "Crash-testing Lithium-ion Batteries." *MIT News*. June 4, 2013. http:// news.mit.edu/2013/crash-testing-lithium-ion-batteries-0604 (accessed April 2, 2014).

Code of Federal Regulations (CFR) Annual Edition. US Government Publishing Office (GPO). 2016. http://www.ecfr.gov/cgi-bin/text-idx?SID=66b4d9b929a5faec813ec0f a6bf5c6b4&mc=true&node=se49.6.571_1301&rgn=div8 (accessed April 8, 2014).

Forberg. "Support/Documentation Valve Flow Calculations and Sizing Guidelines." (n.d.) http://www.forberg.com/pdf/techSup/Home_Tech%20Support_Valve%20Flow_ calc_and_sizing.pdf (accessed June 3, 2015).

IIHS. "About the Institutes." http://www.iihs.org/iihs/about-us/hldi (accessed December 5, 2016).

National Fire Protection Association. "Tactical Considerations for Extinguishing Fires in Hybrid and Electric Vehicles." December 9, 2014. https://www.youtube.com/ watch?v=mtCk3srID_w (accessed April 28, 2014).

National Fire Protection Association. 2015. *Emergency Field Guide*, Volume 4.

National Highway Traffic Safety Administration. (n.d.). Retrieved from Federal Motor Vehicle Safety Standards and Regulations. http://www.nhtsa.gov/cars/rules/ import/FMVSS/ (accessed April 28, 2014).

New York State Department of Transportation. "Bus & Passenger Vehicle Regulations: Title 17 Official Compilation of Codes, Rules and Regulations of the State of New York, Parts 720, 721, 722, and 723." July 18, 1999. https://www.dot.ny.gov/ divisions/operating/osss/bus-repository/busregs1.pdf (accessed April 16, 2014).

NFPA. "Lithium Ion Batteries Hazard and Use Assessment." July 2011. http://www.nfpa. org/news-and-research/fire-statistics-and-reports/research-reports/hazardous-materials/other-hazards/lithium-ion-batteries-hazard-and-use-assessment (accessed April 22, 2014).

NHTSA. "Traffic Safety Facts Annual Report 2013." 2015. https://crashstats.nhtsa.dot. gov/#/DocumentTypeList/12 (accessed September 27, 2015).

Olivares, Gerardo and Vikas Yadav. Injury Mechanisms to Mass Transit Bus Passengers During Frontal, Side and Rear Impact Crash Scenarios. (n.d.) http://www-nrd. nhtsa.dot.gov/pdf/esv/esv21/09-0427.pdf (accessed December 7, 2015).

Power Vehicle Innovation. "Our Expertise." http://www.pvi.fr/energie-embarquee-batteries,042.html?lang=en (accessed September 27, 2015).

Safety Wissen. "United States New Car Assessment Program." ttps://www.safetywissen. com/#/object/B10/B10.nw37346182s1mokz8mq64428r5m0on63470973228/?_ k=88xugz (accessed December 3, 2015).

The San Diego Union – Tribune. "New electric School Bus." http://www.sandiegounion tribune.com/photos/2014/mar/19/1269201/ (accessed October 4, 2015).

United Nations Economic Commission for Europe. "Spectrum Of Road Safety Activities." 2012. https://www.unece.org/fileadmin/DAM/trans/roadsafe/publications/ Spectrum_of_Road_Safety_Activites.pdf (accessed December 2015).

Wech, Lothar, Richard Richter, Rainer Justen, and Rodolfo Schöneburg. "Crash Safety Aspects of HV Batteries for Vehicles." National Highway Traffic Safety Administration (NHTSA) (n.d.). http://www-nrd.nhtsa.dot.gov/pdf/esv/esv22/22ES V-000302.pdf (accessed April 23 2014).

ABOUT THE AUTHORS

TIMOTHY CLEARY, MS

Timothy Cleary is the director of the Battery Application Technology Testing & Energy Research Laboratory (BATTERY) at the Larson Institute at Penn State. He earned his B.Sc. and M.S. degrees in mechanical engineering from Penn State. He is involved in the U.S.DOE-sponsored Advanced Vehicle competitions serving as team leader for the 2007-2008 competition and currently an assistant faculty advisor to the current PSU team. In 2009-2010 he was a vehicle systems and simulation contracted engineer supporting U.S. DOE research in the area of plug-in hybrid electric vehicles. In 2010-2011 he gained Top Secret security clearance and assisted the U.S. Army's Seeker Effects Laboratory in performing infrared countermeasure testing. Currently he concentrates his research in battery system development and application testing for advance chemistry automotive batteries ranging from starter to full electric buses.

MARC SERRA BOSCH

Marc is an international student from Barcelona who was in an exchange program for his master's degree in Investigation. He graduated in Mechanical Engineering at Institut Químic de Sarrià (IQS), and his interests are mostly focused on different aspects of the vehicle industry, such as the implementation of alternative energies, active vehicle safety systems, and vehicle testing.

JAMES A. KREIBICK

James A. Kreibick earned his BS in Electrical Engineering from Penn State. His studies focused on control systems and power systems. During his time at Penn State he was involved in the Penn State Advanced Vehicle team that participated in the EcoCar2 competition sponsored by General Motors and the Argonne National Laboratory. He also spent three years working on battery research with the Pennsylvania Transportation Institute that included two funded research projects from MNTRC and Norfolk Southern Corporation. These projects ranged from battery testing and hardware in the loop testing to battery modeling. He intends to join industry related to energy storage and power transmission.

DR. JOEL ANSTROM, PH.D.

Dr. Joel R. Anstrom is Director of the Hybrid and Hydrogen Vehicle Research Laboratory and the DOE Graduate Automotive Technology Education Program at the Thomas D. Larson Pennsylvania Transportation Institute at Penn State University. He is responsible for developing and managing transportation research projects that advance hybrid electric and fuel cell vehicles, hydrogen fueling infrastructure, and high-power in-vehicle energy storage. His research focus is modeling and demonstration of electric, hybrid electric, and fuel cell vehicles for efficiency and dynamic handling.

Dr. Anstrom earned B.S. and Ph.D. degrees in Mechanical Engineering from Penn State University and a Master's degree in Manufacturing Systems Engineering from the University of Texas at Austin.

PEER REVIEW

San José State University, of the California State University system, and the MTI Board of Trustees have agreed upon a peer review process required for all research published by MNTRC. The purpose of the review process is to ensure that the results presented are based upon a professionally acceptable research protocol.

Research projects begin with the approval of a scope of work by the sponsoring entities, with in-process reviews by the MTI Research Director and the Research Associated Policy Oversight Committee (RAPOC). Review of the draft research product is conducted by the Research Committee of the Board of Trustees and may include invited critiques from other professionals in the subject field. The review is based on the professional propriety of the research methodology.